TOWARDS THE DEVELOPMENT OF A STANDARD TEST PROTOCOL:
APPLICATION OF THE MMLS3 FOR EVALUATING THE PERFORMANCE OF SURFACING SEALS

by
Mohammad Shafee Abrahams

Thesis presented in fulfilment of the requirements for the degree of Master of Science (Engineering) in the Faculty of Engineering at Stellenbosch University

Supervisor: Professor K J Jenkins
Co-supervisor: C Rudman

December 2015

__Declaration__

By submitting this thesis electronically, I declare that the entirety of the work contained therein is my own, original work, that I am the sole author thereof (save to the extent explicitly otherwise stated), that reproduction and publication thereof by Stellenbosch University will not infringe any third party rights and that I have not previously in its entirety or in part submitted it for obtaining any qualification.

Date: ………………………………………………………………….

ABSTRACT

For a road to perform optimally, both functionally and structurally; a durable, waterproof, skid-resistant, all-weather and dust-free surfacing is required to provide the road user with an acceptable level of service. Surfacing seals serve to protect the structural layers of the pavement from the abrasive forces of traffic and from the detrimental effects of the environment especially moisture.

Surfacing seal design, in South Africa, and many parts of the world is governed mainly by empirical rules and experience guided practices. There is thus a need for a performance related seal design method, with a more scientific foundation.

This study aims to address this challenge by investigating the failure mechanisms of seals with the aim of simulating its manifestation using an accelerated pavement tester, the Model Mobile Load Simulator (MMLS3). Based on this investigation, seal stone embedment was identified as the target failure mechanism. Key seal variables were identified which are thought to directly influence the embedment of the stones in a seal. This research project was then centred around this failure mechanism and an experimental seal testing setup was developed along with an analysis procedure to measure and quantify the embedment of the stones in a seal.

Based on the literature study the factors influencing the performance of seals were identified along with the capabilities of the MMLS3 for application on seals. The following key seal design parameters were identified and selected for comparison:

- Tack coat binder type
- Aggregate spread rate configuration
- Aggregate size

A seal construction method was developed along with a software aided embedment calculation method for use with the Laser Texture Meter (LTM). This integral part of this study allowed for the processing of large amounts of data obtained from the LTM and subsequent analysis of the processed data.

Based on the analysis of the data it was established that more than 70% of the total embedment observed over 100 000 load cycles occurred during the initial embedment period i.e. the first 10 000 load cycles. The statistical analysis also provided an idea as to the level of influence of the variables on the embedment measured. The following was noted:

- Aggregate configuration showed the lowest influence
- Binder type showed an intermediate influence

- Aggregate size showed the highest influence

This study shows that with an effective testing setup and an efficient analysis procedure, the application of the MMLS3 can successfully be used for evaluating the performance of surfacing seals. Through further research and refinement the development of an effective accelerated seal testing protocol would be possible. Such a protocol should able to quantify and analyse the performance of seals.

The major recommendations for the improvement of similar research include:

- The inclusion of more testing variables allowing a greater comparative scope.
- The use of more precise laser measurement technology with capabilities extending beyond the LTM used in this study.
- The establishment of performance index parameters to quantify and rank the variables investigated from which an acceptable protocol can be developed.

OPSOMMING

Vir 'n pad om optimaal te presteer , beide funksioneel en struktureel ; 'n duursame , waterdigte , slip bestand, alweerstand en stof-vry oppervlak is nodig om die padgebruiker te voorsien met 'n aanvaarbare vlak van diens. Oppervlakseël dien om die strukturele lae van die plaveisel te beskerm teen die skuur kragte van die verkeer en die nadelige gevolge van die omgewing

Oppervlakseël ontwerp, in Suid-Afrika , en baie dele van die wêreld word hoofsaaklik beheer deur empiriese reëls en ervaring geleide praktyke . Daar is dus 'n behoefte aan 'n prestasie -verwante oppervlakseëlontwerpmetode, met 'n meer wetenskaplike grondslag .

Hierdie studie het ten doel om hierdie uitdaging aan te spreek deur die ondersoek na die mislukking meganismes van oppervlakseël met die doel van sy manifestasie simuleer met behulp van 'n versnelde plaveisel toetser, die Model Mobile Lassimulator (MMLS3) . Op grond van hierdie ondersoek, is oppervlakseëlklip ingebedheid geïdentifiseer as die teiken mislukking meganisme. Sleutel oppervlakseël veranderlikes was geïdentifiseer wat gedink is, is die direkte ïnvloed op die ingebedheid van die klippe in 'n oppervlakseël. Hierdie navorsingsprojek is toe gesentreer rondom hierdie mislukking meganisme en 'n eksperimentele Oppervlakseël toets opstel, ontwikkel saam met 'n ontleding prosedure te meet en te kwantifiseer in die ingebedheid van die klippe in 'n oppervlakseël.

Gebaseer op die literatuurstudie, die faktore wat die prestasie van oppervlakseël was geïdentifiseer saam met die vermoëns van die MMLS3 vir toepassing op oppervlakseëls. Die volgende sleutel oppervlakseël ontwerp parameters is geïdentifiseer en gekies vir vergelyking :

- Seëlbindmiddel tipe

- Oppervlakseëlklip verspreiding koers opset

- Oppervlakseëlklip grootte

ʼn Oppervlakseël konstruksie metode was ontwikkel saam met 'n sagteware aangehelpte ingebedheid berekening metode met die gebruik van die Laser Tekstuur Meter (LTM). Die integrale deel van hierdie studie is toegelaat vir die verwerking van groot hoeveelhede data verkry is uit die LTM en daaropvolgende ontleding van die verwerkte data.

Gebaseer op die ontleding van die data is vasgestel dat meer as 70 % van die totale ingebedheid waargeneem,

van die 100 000 vrag siklusse wat plaasgevind het tydens die aanvanklike ingebedheid tydperk dws die eerste 10 000 vrag siklusse. Die statistiese analise ook voorsien 'n idee as die vlak van die invloed van die veranderlikes op die ingebedheid gemeet . Die volgende is opgemerk :

- Oppervlakseëlklip opset het die laagste invloed

- Seëlbindmiddel tipe het 'n intermediêre invloed

- Oppervlakseëlklip grootte het die hoogste invloed

Hierdie studie toon dat met 'n effektiewe toets opstel en 'n doeltreffende ontleding prosedure , die toepassing van die MMLS3 kan suksesvol gebruik word vir die evaluering van die prestasie van oppervlakseëls. Deur verdere navorsing en verfyning van die ontwikkeling van 'n doeltreffende versnelde oppervlakseël toets protokol moontlik sou wees. So 'n protokol moet in staat wees om te kwantifiseer en die prestasie van oppervlakseël te ontleed.

Die groot aanbevelings vir die verbetering van soortgelyke navorsing sluit in:

- Die insluiting van meer toets veranderlikes sodat 'n groter vergelykende omvang.

- Die gebruik van meer akkurate lasermetingtegnologie met vermoëns om buite die LTM gebruik in hierdie studie, uit te brei.

- Die vestiging van prestasie-indeks parameters om te kwantifiseer en die veranderlikes te gradeer wat ondersoek was, waaruit 'n aanvaarbare protokol ontwikkel kan word.

ACKNOWLEDGEMENTS

I would firstly like to thank my Creator, for blessing me with the ability to complete this study.

Bismillah hir-Rahman nir-Rahim

"In The Name of God, The Most Beneficent, The Ever Merciful."

TOWARDS THE DEVELOPMENT OF A STANDARD TEST PROTOCOL:
APPLICATION OF THE MMLS3 FOR EVALUATING THE PERFORMANCE OF SURFACING SEALS

By

Mohammad Shafee Abrahams

TABLE OF CONTENTS

LIST OF FIGURES

LIST OF TABLES

LIST OF PLATES

Plates are used to show diagrammatic or photographic processes and are usually a collection of images or diagrams

LIST OF APPENDICES

LIST OF ABBREVIATIONS

ALD - Average Least Dimension

APT - Accelerated Pavement Tester

Ball Pen- Ball Penetration

CAT 65 - Cationic Spray Grade Emulsion with 65% net bitumen content

DPG1 - Draft Protocol Guideline 1

ELV - Equivalent Light Vehicles

LTM - Laser Texture Meter

MDD - Maximum Dry Density

MLS - Mobile Load Simulation

MMLS - Model Mobile Load Simulator

OMC - Optimum Moisture Content

PEN 70/100 - Penetration Grade 70/100 Bitumen

pr.SE-1 - Precoated Aggregate with Polymer Modified Bitumen

(SBS Modified)

SABITA - South African Bitumen Association

SAPEM - South African Pavement Engineering Manual

SBR - Styrene Butadien Rubber

SBS - Styrene Butadien Styrene

SC-E1 - SBR Modified Bitumen Emulsion

sh-sh - Shoulder to Shoulder

TMH - Technical methods for highways

TRH - Technical Recommendations for Highways

1. <u>INTRODUCTION</u>

1.1 Background

For a road to perform optimally, both functionally and structurally; a durable, waterproof, skid-resistant, all-weather and dust-free surfacing is required to provide the road user with an acceptable level of service. Seals serve to protect the structural layers of the pavement from the abrasive forces of traffic and from the detrimental effects of the environment. In South Africa, bituminous seals and slurries are commonly used for new construction. They are also used for resealing of existing roads due to the fact that they are relatively inexpensive and have proven to be successful on highways, rural roads, and urban streets, under dynamic traffic conditions of varying load magnitudes (TRH3, 2007).

Although seals have been used extensively over decades, there are still many uncertainties and variability. Most of the design specifications are based on many years of experience as well as visual assessments of in-service seals. There is a need for a performance related seal design method, with a more scientific foundation. In order to develop such a design method, a testing procedure that can effectively simulate in-service conditions must be developed. Unlike other structural pavement layers, seals cannot be easily replicated in a laboratory, so the challenge is to construct a seal in a test bed and evaluate it using a realistic loading system.

Mobile load simulation (MLS) technology has been used effectively by engineers to simulate in service conditions for at least the past twenty years. Since the development of the first Mobile Load Simulator in the early 1990's by Professor Fred Hugo and his team, and subsequent feedback and refinement, has led to the proposal and building of a scaled down (1/3) version of the full scale MLS. This version, known as the Model Mobile Load Simulator 3 (MMLS3) was found to be more practical at simulating in-service conditions than the initial MLS1 (being 1/10 scale) while being more feasible than its full scale counterpart. Various road authorities and research facilities around the world acquired their own MMLS machines and started running accelerated testing on road pavements. (Kemp, 2006)

MMLS testing being done in South Africa, along with the data acquired from other researchers and engineers using the MMLS in other parts of the world, has led to a draft testing protocol being successfully developed for evaluating permanent deformation and moisture susceptibility of asphalt mixes. Although it is not an International Standard Test Protocol, it provides valuable guidelines for rutting and stripping and is thus included as a test method in the *South African Asphalt Pavement Design Manual (2013)* and in the evaluation of asphalt mixes for Agrément Certification.

Additionally, the protocol requests feedback from practitioners which would aid researchers in making adjustments and revisions to the document. This type of interactive sharing of information is vital when striving toward an International Standard Test Protocol.

Dr T. Milne, a researcher and pavement engineering practitioner, mentions that his experiences in the field indicate strongly that a seal placed under conditions of high ambient temperatures and heavy traffic, with both modified and straight run binders, could perform other than expected. Under certain circumstances, these seals would be more susceptible to bleeding and loss of adhesion (Milne, 2004). Since the function of a seal is to provide skid resistance as well as protection to the structural layers of the pavement, bleeding and chiploss (through lack of adhesion) would affect riding quality and could lead to the rapid deterioration of the pavement by allowing water ingress. It is possible that current laboratory test methods as well as tests used in practice (such as the ball penetration test) do not effectively simulate the behaviour of the various materials in a seal. Since the design of the seal is based largely on these test results, the battle could already be lost at the design phase. Accurately testing and modelling the seal and its components in the laboratory could provide confidence and reliable data for analysis by the designer, leading to an improved seal design.

1.2 Project Definition, Aims and Objectives

The primary aim of this project is to develop a standard test protocol by which key seal variables and their performance can be measured. The development of such a protocol requires a significant amount of data to be gathered from a wide range of tests for a range of variables. The data would then be analysed to establish draft guidelines for seal evaluation, as has been done for evaluating asphalt using the MMLS.

The completion of a final protocol will require a significantly larger data set and is beyond the scope of this study. Instead, the aim will be reached using the following primary objectives:

(a) Investigate the failure mechanisms of surfacing seals.

Using this knowledge, the failure mechanisms requiring improved testing can be identified. This, along with the capabilities and limitations of the MMLS device should provide insight as which aspects of seal failure should be targeted in this study.

(b) Through the identification of critical performance parameters, setting up an experimental design to be executed with the aim of establishing an acceptable test protocol.

(c) Develop an experimental seal testing setup, along with an effective analysis procedure to quantify and analyse the targeted failure mechanism.

A secondary objective would include investigating a number of variables influencing the performance seals,

This study, following the work of Dr Terence Milne, would then form part of the first contribution toward developing a standard test protocol for MMLS testing on seals.

1.3 Thesis Outline

Chapter 1 provides a brief introduction of the proposed study, defining the project and objectives and touches briefly on the origin and need for this type of research. *Chapter 2* consists of an intensive literature study focussing on various key aspects related directly to this study. The history of surfacing seals is discussed briefly. *Chapter 3* elaborates on the materials involved in seal construction in detail, providing an overview of the origin and use of the materials in road construction. *Chapter 4* provides an outline of the equipment used in this study along with a discussion regarding the test methods followed when using the apparatus. This chapter expands further on the MMLS3 and provides details as to the technical aspects surrounding the operation and calibration of the machine. *Chapter 5* details the research methodology followed in this study. This chapter includes the experimental design, test setup and procedure and the theoretical analysis. The test setup is divided into various phases based on the process by which it was developed providing a detailed procedure which can be followed to execute the experiment. In addition, the data processing algorithm is explained and rationalised. *Chapter 6* discusses the consolidated results obtained from the testing phase along with an interpretation thereof. The report is then concluded in *Chapter 7* along with recommendations for future research*.*

2. <u>LITERATURE STUDY</u>

2.1 Introduction

This chapter will discuss various aspects relating directly to the subject matter of this study. The key elements included in this literature study will provide a broad idea as to the past and current research involving seals and their performance. The mechanisms by which seal failures occur will then be discussed with the aim of isolating the failure mechanism best suited to be targeted using an accelerated pavement testing apparatus. The history of the accelerated pavement tester used in this study is then deliberated along with a discussion regarding previous research and methodologies applicable to the device. Performance variables are then highlighted from an accelerated testing standpoint. This chapter will thus provide the setting for this research paper and the chapters that follow will be articulated using the aspects that follow as the foundation.

2.2 Seals: Globally and in SA

The popularity of surfacing seals in the early to mid-1900's were due mainly to the fact that they were relatively cheap, easy to place and maintain, and if properly constructed, durable. During the early years of seal utilisation, no formal design method was available. The successful implementation of the seal was dependent on the experience of the construction team. The low traffic volumes that were common during those times ensured that the seal was placed under minimal load during their serviceable lifetime. Through the decades, traffic loads on roads increased dramatically. Developed countries (such as the USA etc.) then resorted to asphalt surfacing, while the (then) developing countries like New Zealand, Australia and South Africa still maintained the use of seals for economic reasons. The first viable seal design method was implemented in New Zealand, by Hanson in the 1930's. Hanson's method used the Average Least Dimension (ALD) of the surfacing stone as a fundamental parameter in determining the volume of the aggregate mat, voids and related binder application rate. The growth in traffic after the Second World War exposed the flaws of Hanson's design methodology. Bleeding, and other failures occurred which could have been due to a lack of understanding of the materials being used, environmental effects, construction methods or a combination of these. Since then, several regional Roads Authorities implemented their own design methods, such as the McLeod method (based partially on the Hanson's work), Kearby method, Ausroads sprayed seal design method to name but a few (Milne, 2004).

In South Africa, it is estimated that approximately 80% of the road network is sealed with either an initial surfacing or as a reseal (SAPEM, 2014). It is thus clear that road surfacing seals make up a significant portion of South Africa's road construction and maintenance activities. Research towards improving the seal design method as well as seal testing procedures could potentially be of great

benefit to the engineering community and society at large. The design procedure used in South Africa is described in the *Technical Recommendations for Highways 3: Design and Construction of Surfacing Seals (TRH 3)*. Its design process is based on a number of primary input parameters such as traffic volume, preferred texture depth, surface hardness and the average least dimension of the stone used. Once the initial results are obtained using these primary inputs, practical adjustments can be made for differences in climate, gradients, existing texture, application temperatures, preferred aggregate spread rate and the use of modified binders. This method may be seen as a hybrid of the United Kingdom and Australian design methodologies, strongly influenced by extensive South African seal experience (Greyling, 2012).

2.3 Seals

2.3.1 Function of seals in a pavement structure

The *TRH3 (2007)* as well as the *SAPEM (2014)* summarises the function of surfacing seals as follows:

- Provides a waterproof cover to the underlying pavement structure

- Provides a safe, all-weather, dust-free riding surface for traffic with adequate skid resistance.

- Provides protection to the underlying layers from the abrasive forces of traffic as well as the environment.

It is worth noting that surfacing seals are generally thin, and are not designed for load distribution. The seal itself should however be able to withstand the horizontal and vertical stresses induced by traffic.

2.3.2 Basic Structure

Figure 1 below shows a typical structure of a single seal.
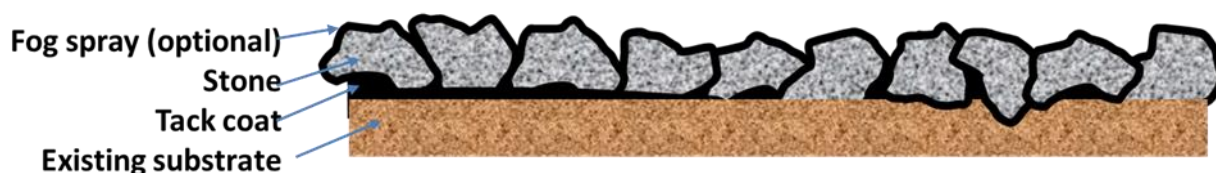
Figure 1: Single Seal (adapted from TRH3, 2007)

Various types of seals are used. The above example is one of the simplest seals that are constructed in SA. Seals generally consist of three basic elements that should work synergistically for the seal to perform effectively; the aggregate (stone), the bituminous binder (tack coat and fog/cover spray) and the substrate on which the seal is constructed.

The following summarises the basic seal construction practice as highlighted in the *TRH3*:

"In its simplest form a chip and spray seal consists of a coat of bituminous binder sprayed onto the road surface which is then covered with a layer of aggregate (stone or sand). The aggregate cover is applied immediately after the binder has been sprayed and then rolled to ensure close contact and thus good adhesion between the aggregate and the binder film. Rolling initiates the process of orientating the particles into a mosaic pattern and working the binder into the voids between the aggregate particles. The process is completed by the action of traffic, so that finally a dense and relatively impermeable pavement surfacing is obtained."(TRH3, 2007)

This method is used in various combinations to construct single seals, double seals, Cape seals, slurry seals to name a few. A detailed description of the components of a seal will be discussed in a later chapter.

2.3.3 Factors influencing seal performance

The performance of a seal is influenced by various factors and combinations thereof. The *TRH3*
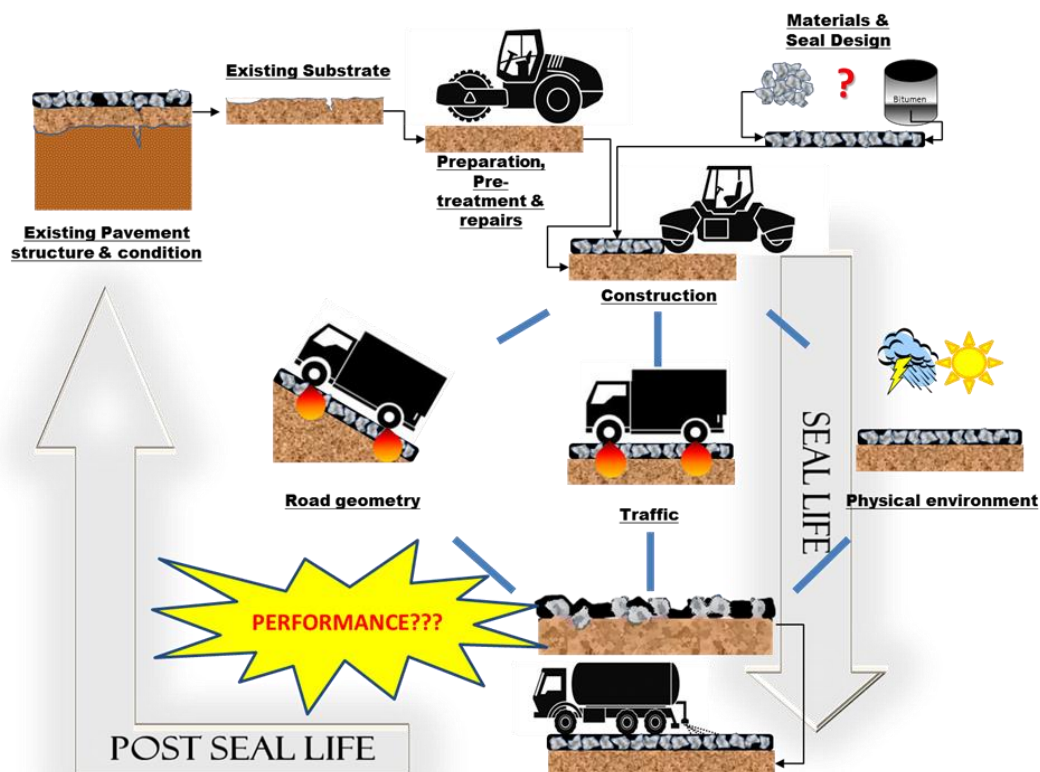
Figure 2: Factors influencing the performance of seals

6

(2007) describes these factors and makes mention of the fact that the failure of a seal to fulfil its functions as mentioned previously would indicate the end of the seals serviceable life. The performance of the seal is thus related to the effective serviceable life as well as the degree to which the required functions are fulfilled.

Figure 2 graphically displays the factors directly influencing the performance of seals. Each factor is then discussed from a performance perspective, along with a brief description of their influence as supported by previous researchers.

(a) Pavement structure and condition
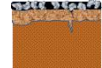
A seals performance is governed to a large extent by the structural capacity of the underlying pavement layers. Traffic loading is carried by these underlying layers, while the seal acts mainly as a wearing course resisting the abrasive effects of the moving wheel loads and it seals the pavement to prevent water from reaching the structural layers.

For new construction, the base type, materials and degree of compaction will affect the performance of the seal. The ability of the base course to resist the penetration (embedment) of seal stones allows for voids, which could lower the risk of fattiness, bleeding and their associated danger of lowered skid resistance (Milne, 2004). The flexural properties of a pavement structure also influence the seal. Rigid seals, low temperatures and binder oxidation will accelerate the development of surface cracks and ravelling. Reflective cracking is related to the magnitude and frequency of the movement between crack walls due to repeated traffic loading, chemical reactions that cause shrinkage, temperature changes and moisture changes. The greater the crack activity within the pavement structure, the quicker these cracks will reflect to the surface. A cracked seal will allow water ingress, fuelling the deterioration cycle of the pavement (Milne, 2004).

(b) Existing substrate

The surface and its materials upon which the seal will be constructed will influence the performance of the seal. The condition of the substrate is quantified through visual inspection and measurements of surface texture depth and unevenness, permeability, and the hardness. The hardness of the existing surface affects the extent to which the applied stones become embedded into the base surface during the seals service life (Read and Whiteoak, 2003). This aspect should therefore be carefully investigated when determining the most appropriate seal type, aggregate type and size, binder type and quantity and the necessary pre-treatment measures.

(c) Preparation, pre-treatment, and repairs before construction

Surface preparation is required to ensure a clean dense surface on which to construct the seal. Failure to do so could result in aggregate loss and embedment of the seal stones during construction or during the service life of the seal. Well before the construction of the seal, pre-treatment and repairs should be done. *Pre-treatment* is necessary if the surface texture varies, is uneven, dry or porous. *Repairs* should be done on any potholes or other defects in the existing pavement. Doing this in advance will ensure the effective evaporation of volatiles in the repair binder, before sealing over it.
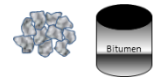
(d) Materials

As mentioned previously, the performance of a seal is dependent on the ability of the various elements within the seal to act synergistically. Each element and their properties could therefore affect the performance of the seal. The effect of the substrate has been discussed. Attention will now be given to the influence of the aggregate and binder on seal performance.

- **Aggregate**

The TRH3 summarises the four main functions of the aggregate in a seal:

- it provides resistance to the abrasive forces of moving wheel loads and transfers the load to the underlying structure;

- it provides a skid-resistant surface;

- it provides a structure to accommodate the elastic, impermeable bituminous binder while providing sufficient voids to prevent flushing, and

- it protects the binder from the sun's harmful ultra-violet rays

The following aggregate related factors affect the performance of seals:

Shape: The aggregate shape influences the way it will interlock in a constructed layer which, in turn, influences the stability of the seal. The more angular the aggregate, the better the interlock since there are more points of contact. The shape can also be described in terms of its degree of flatness and elongation. Van Niekerk describes the flakiness ratio and elongation ratio is used to quantify the shape of the particle using *Figure 3*.
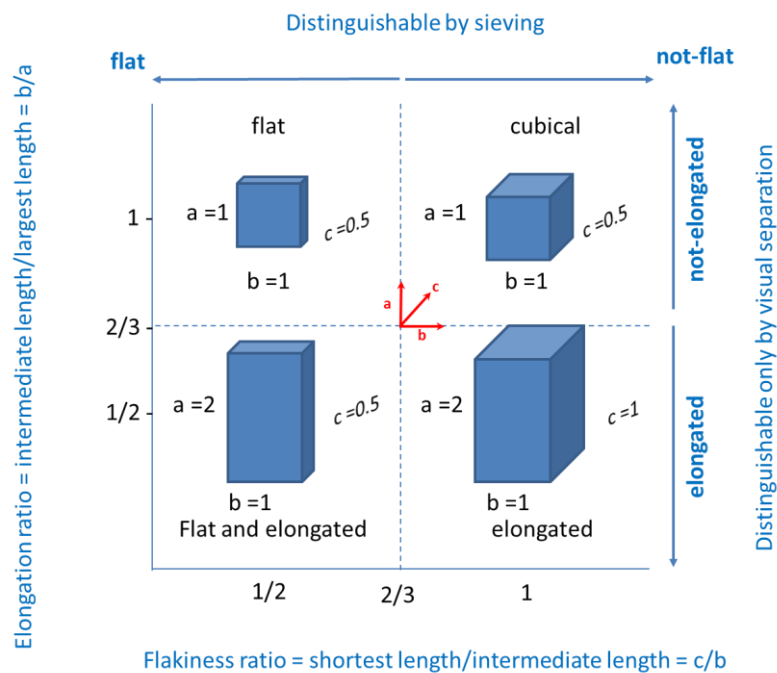
Figure 3: Flatness, elongation and cubicity of particles adapted from van Niekerk (2002)

Type, size and grading: The size and grading influence the voids of the matrix and in turn the amount of binder it can accommodate. Uniformly graded stone develop good interlock which increases friction and skid resistance. With large single-sized aggregates more voids are available than with small single sized aggregates. Larger aggregates therefore require more binder, resulting in a more impermeable, longer lasting seal.

Strength, durability and wearing characteristics: the aggregate should be hard enough to resist excessive breaking and crushing during construction as well as during the service life of the seal. Additionally, the mineral composition of the aggregate should be analysed to determine if it will be sufficiently resistant to weathering and polishing.

Skid resistance, one of the primary functions of a seal, is largely governed by these aggregate related factors. Panagouli et al (1997) reports that the size, shape, angularity and mineralogy of the aggregates will influence the degree of macro and microtexture developed at the surface of the seal during the service life. Polishing is the loss of microtexture (and therefore skid resistance) at the surface by smoothing the edges of coarse aggregates under the abrasive forces of traffic. The presence of macrotexture facilitates the surface drainage by providing drainage paths for the water to evacuate the area of contact between the tyre and seal surface (Kane et al, 2013).

Spread rate of aggregate: The aggregate protects the subgrade against damage and should be applied to lie shoulder to shoulder, in a single layer and in a tightly knit pattern. If the spread rate is to low it will lead to excessive ultra-violet damage to the binder and in turn

ravelling of the seal. If the spread rate is too high, the excess aggregate will be forced into the mat, leading to whip-off of the bonded aggregate.

Adhesion characteristics, cleanliness and dust content: Literature indicates that moisture as well as high amounts of dust negatively affect adhesion; causing 'spot flushing' .This results from the formation of water vapour blisters due to the increase in surface area owing to the high dust content (Herrington et al, 2012). Precoating of aggregates can improve and alleviate adhesion problems associated with excess dust and moisture.

Porosity and absorption: Porous aggregates absorb mainly the lighter fractions of the binder. Excess absorption of these light fractions may cause the binder to become brittle. This is undesirable for seals and will decrease the serviceable lifespan. This aspect should be kept in mind, particularly when analysing the binder type to be used.

- **Binder**

The performance of a seal is highly dependent on the formation of a significant adhesive bond between the aggregate, binder and the road surface upon which the seal is constructed. In addition, the durability and flexibility of the binder under varying climatic conditions also has an impact on the seals performance and service life.

Robertson (1991) speculates that bitumen is comprised of an internal multi-molecular matrix consisting of polar molecules dispersed in less-polar to non-polar phase. This implies that the bitumen is a material that has elastic properties as a result of the network formed by the polar molecules, and viscous properties due to the ability of the network to flow under prolonged stress. Bitumen is thus a visco-elastic material, with its viscous and elastic behaviour varying with composition.

The bitumen binder should be carefully selected to provide the initial viscosity required to flow and effectively coat the aggregate. As the binder cools, sufficient adhesive and cohesive strength should develop. This would prevent the dislodging of aggregates from the binder when the road is opened to traffic. The binder should be able to resist softening under high temperatures during its service life to retain the aggregate while under the forces of traffic. The binder should also remain flexible at low temperatures. Failure to do so would lead to reflection cracking, and eventually moisture ingress into the base.

The following binder related factors affect the performance of seals:

Binder type and properties: Penetration grade, cut-back, emulsions and modified binders all behave differently and different properties under certain conditions. Their selection should be made accordingly as it will certainly have an effect on the performance of the seal.

Binder grade: The correct binder grade for expected climatic, pavement and traffic conditions, both under construction and long term, must be selected to ensure optimal seal performance. Each grade of binder is characterized by its own temperature/viscosity relationship. It has an optimum range over which the bitumen can be sprayed, stored, mixed or pumped. It is essential that the viscosity be kept within the range for spray application in order to obtain optimum application and it is important for a binder to have sufficient viscosity to not soften up during operational temperatures in the road (Greyling, 2012).

Application Rate: the application rate that would yield the best seal performance should be based on the size and shape of the stone, the volume of voids in the compacted stone layer, traffic, gradients and the condition of the underlying surface. The optimal amount of binder would keep the stone adhesively in place, while maintaining sufficient voids to avoid bleeding. *Table 1* below is extracted from TRH3 (2007) and indicates the minimum amount of net cold binder required for the tack coat.

Table 1: Minimum amount of net cold binder required for tack coat (TRH3, 2007)

Aggregate size	9.5 mm	13.2 mm	19.0 mm
Only construction traffic	0.5 ℓ/m^2	0.7 ℓ/m^2	1.0 ℓ/m^2

The application rate can be monitored and adjusted to compensate for other factors which may be beyond the control of the designer. Lowering the application rate in areas where the base surface is softer could compensate for the loss of voids through embedment, preventing or minimising bleeding and loss of texture depth (Read and Whiteoak, 2003).

Viscosity at application: the uniformity in the application is dependent on the viscosity (which varies with temperature) at the time of application. If the temperature is too low, streaking will occur, while if it's too hot, degradation of the binder occurs.

(e) <u>Seal Design</u>

There should be allowance made during the design process, for different situations that may occur on a specific road section. The pre-design investigation is used to determine uniform sections and

numerous other factors which could affect seal performance. Designs can then be amended during the construction phase to incorporate changed conditions or the development of new information.

Pavement design is the process undertaken to select and regulate the aspects of the pavement structure. This implies that the designer specifies the type of structure, the materials to be used within that structure along with the corresponding materials layer thickness. The basic objective of the pavement design is to combine materials of sufficient strength in a layered system to maintain an adequate functional and structural service level over the entire design period, subject to the applicable traffic demand and particular environment (SAPEM, 2014).

Similarly, seal design is the process of combining materials (aggregate and bitumen) in various ways to provide an adequate wearing course to protect the underlying pavement structure as well as provide the required skid resistance.

The pavement design as well as the seal design will influence the long term performance of the seal.

The following factors are therefore, to a large extent, linked to the design aspect.

(f) Construction and supervision

Poor seal performance can often be caused by poor construction practices, inadequate supervision or by not paying enough attention to detail. The correct and uniform application of binder and aggregate are necessary along with properly calibrated equipment and plant to ensure maximum seal performance. The initial traffic speed should be limited to 60 km/h for a period of time, allowing the adhesive bond between the binder and aggregate to sufficiently develop. The construction of seals generally consist of three major steps: spraying the tack coat, spreading the aggregate and compaction of the aggregate through rolling. Kim and Lee (2006) noted that this three step construction procedure should occur uninterrupted to ensure the best seal

Figure 4: Roller compaction in seal construction (van Zyl, 2015)

performance. It is then further mentioned that having a sufficient number of rollers is essential to provide adequate initial rolling. *Figure 4* alongside depicts this critical step. The purpose of this initial compaction is to attain a desired predetermined embedment depth. Many seal design methods including the one used in SA makes use of the initial embedment depth, or the corresponding texture depth, as an input parameter in the design process. The desired initial embedment is achieved using roller compaction. The roller re-orientates and redistributes the seal stones while

12

also providing the sufficient compactive force required to seat the stones into the binder and base below it. This concept will be discussed further in a subsequent section.

(g) Road Geometry

Several aspects of the roads geometry may adversely affect the performance of a seal. This may not be a direct influence, but the roads geometry could dictate the speed of the vehicles traversing the road (gradients and intersections), the flow path of surface water and the concentration of wheel loads. Each of these having their own performance related issues. The *Shell Bitumen Handbook* highlights that sections of the road comprising of sharp bends induce increased traffic stresses on surface dressings. It is also mentioned that the gradient could impact the rate of binder application. This is due to the fact that on the ascent side of the road, traffic loading will be present for longer than on the descent side (Read and Whiteoak, 2003).

(h) Traffic

The traffic conditions imposed on the pavement structure will directly influence the performance of the seal during its service life. Although the influence of traffic is interrelated with other factors, the following traffic parameters are considered to be important:

- Volume (especially heavy vehicles)

- Loading (heavy/light vehicles, dual/ super-single wheel configurations)

- Tyre pressures

- Vehicle type and characteristics

- Speed

- Traffic distribution and occurrence

Milne (2004) notes that the volume of traffic along with the other factors as highlighted in the TRH3 will influence the seals performance directly as well as indirectly. High axle loads cause the stone to embed into the base course, this causes a reduction in voids promoting bleeding and flushing and the associated loss in skid resistance. He then further mentions that there is a minimum required volume of traffic to maintain the flexibility of the visco-elastic binder.

(i) Physical environment

The following factors relating to the physical environment can contribute to the seal's performance as indicated in the TRH3 (2007):

- ***Climatic conditions*** – the correct binder type and grade should be selected to accommodate the varying temperature conditions, UV radiation levels, and humidity conditions of the site environment.

- ***Drainage systems*** – roads in urban areas are often used to carry storm water. High flow speeds along with soil particles and detergents in suspension contribute to the erosion of the seal. Single seals, thin sand seals and slurry seals are particularly vulnerable to this and should be avoided on steep gradients with urban-type drainage.

- ***Mechanical damage*** – Damage sustained by the surface due to traffic, construction equipment or any other type of mechanical distress should be repaired as rapidly as possible. Failure to do so could result in water ingress, ravelling, potholing and other types of pavement and surfacing defects.

- ***Dust and sand*** – Dust and windblown sand cause poor adhesion development between the aggregate and the binder, and between the binder and the base. This inversely affects the short and long term performance of the seal.

- ***Fuel spillage and organic material*** – Fuel spillage occurs mainly at intersections, steep gradients and on roads to fuel depots and stations. These spillages cause the binder to soften potentially resulting in failure. Animal droppings, detergents and salt water also contain acid and have a similar effect softening the binder causing seals to fail.

(j) <u>Maintenance</u>

Various maintenance practices could prolong the seal's serviceable life. Some of these include the use of diluted emulsion to rejuvenate the binder, applying fine slurry seals to areas where ravelling has occurred or patching of small areas where delamination from the previous surfacing has occurred.

2.4 Failure mechanisms of seals

The work by Robertson et al (1991) and Milne (2004) shed some light on the failure mechanisms of seals. Their work describes clearly that the composition of the bituminous binder used plays a large role in this, at a molecular structural level. The composition of the bitumen, along with the traffic loading imposed on the seal, climatic conditions and construction practices all play their part in contributing to the development of these failure mechanisms. For the purpose of this study, the failure mechanisms will be divided into two categories based on the time taken for the failure mechanism to manifest.

Figure 5 provides a graphic overview of the failure mechanisms that will be discussed in this section.
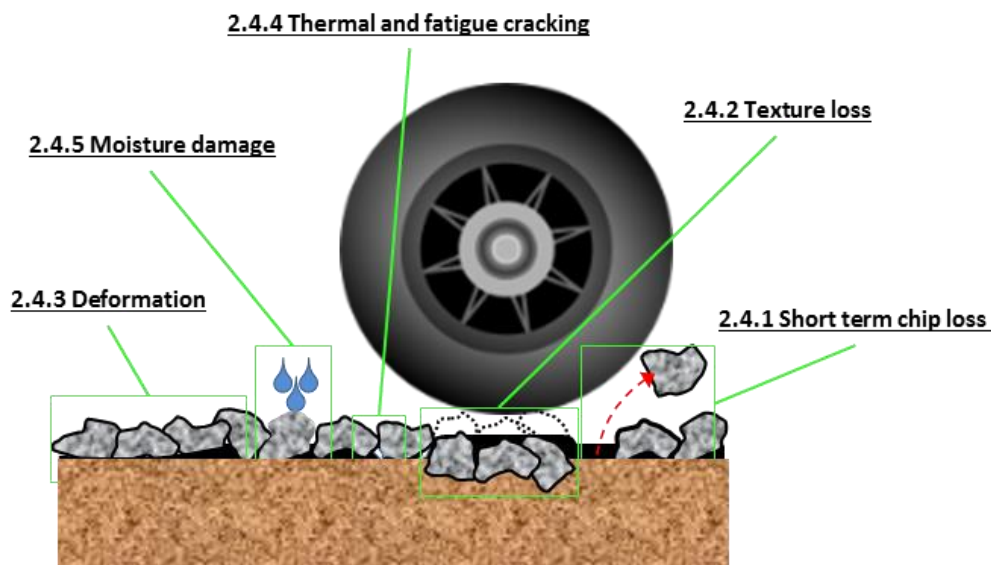
Figure 5: Overview of the failure mechanisms of seals as discussed in this section

2.4.1 Short term chip loss

When a chip seal loses its aggregate then flushing, bleeding, or both, will occur. Chip loss problems frequently occur when a chip seal is placed outside the established construction season i.e. the approved calendar period for chip seal construction, either early or late. Chip loss problems tend to
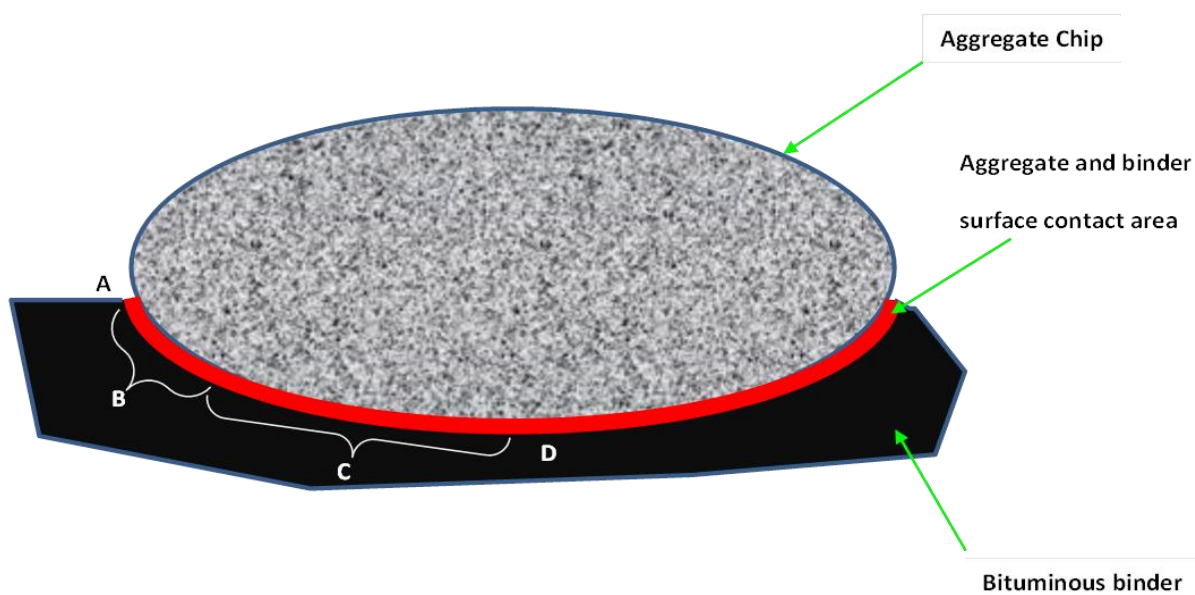
Figure 6: Conceptual aggregate chip and bitumen interface

manifest when abnormally cool or cold temperatures (or rain and snow) occur during or after

placement of a chip seal before the aggregate and binder bond has had a chance to fully develop (Lawson, Senadheera, 2009). Very early chip loss may also be due to low net cold binder application rates, slow breaking in the case of emulsions or poor wetting in the case of cutback bitumen. The use of cationic rapid setting emulsions with a high binder content should overcome problems due to slow breaking of the emulsion while the use of adhesion agents or precoating should assist in wetting when using cutbacks (Read and Whiteoak, 2003).

Figure 6 shows the conceptual idea of an aggregate chip and bituminous binder. The bond between the stone and the binder generally would strengthen from point A (in the figure) across toward point D. It is speculated that this is most likely due to the fact that the cutbacks evaporate at a higher rate when it is closer and has a more direct path to the surface. That being said, if the road is opened to traffic too early or if there were abnormally cold temperatures during the time the seal was left to set, it could be that, for example, surface B has set and fully bonded, but surface C has not and has not yet established a significant enough bond. When the road is then opened to traffic, the load and friction of the tyres on the road could easily dislodge partially unbounded chips from their binder. This type of failure is known as chip loss.

2.4.2 Texture Loss

The texture of a road surface governs the amount of skid resistance generated between the tyre and the road surface. This surface property is one of the most important with regards to safety (Kane, 2013). The texture depth is also an important design parameter used to determine the application rates of the binder. *Figure 8* that follows has been extracted from the TRH3 (2007) and graphically depicts the design principles used to determine the application rate of the binder.
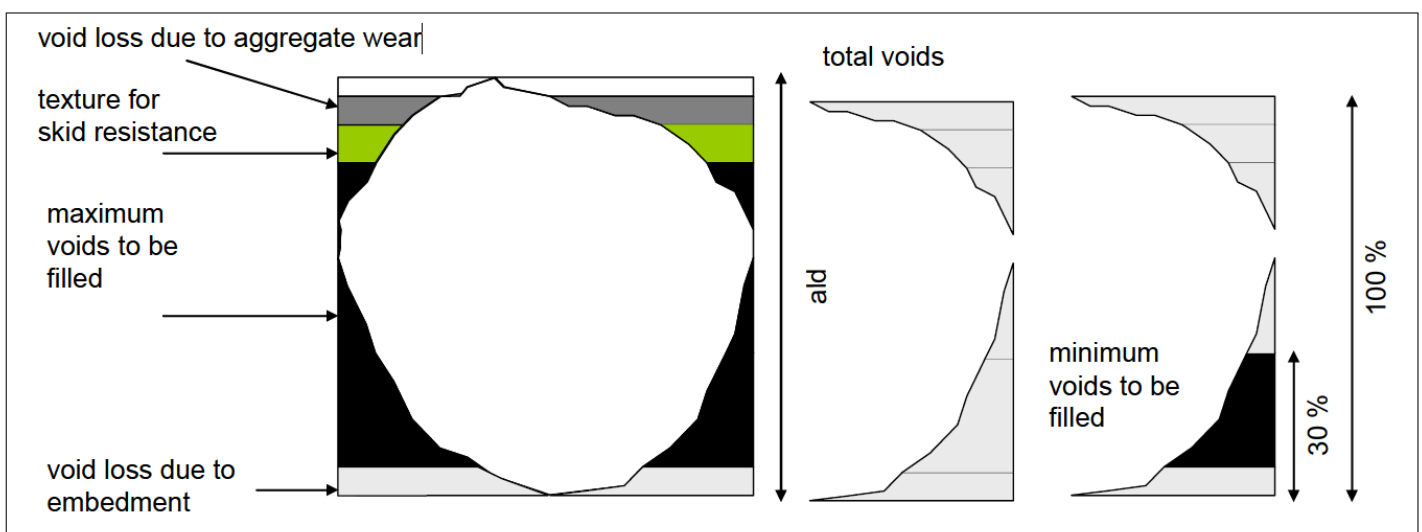
Figure 7: Principles applied for design of the binder application rate (TRH,2007)

From the diagram above, it becomes clear that the texture of a road surface is affected directly by the voids available at any given time during the seal life. The available voids essentially govern the amount of free space present for the flow binder within the seal. If the voids are unable to accommodate the volume of binder, the binder will move towards the surface. This is known as bleeding or flushing of the binder and is a primary cause of texture loss (Herrington et al, 2012).

The texture loss is, therefore, primarily dependant on the rate of void loss that occurs during the construction and service life of the seal and void loss manifests through the following mechanisms:

- Void loss due to the initial embedment and orientation of the seal aggregates during the roller compaction of newly constructed seals.
- Void loss due to long term embedment and aggregate wear during the service life of the seal.
- Embedment is defined as the loss of voids (and therefore texture depth due to flushing) in a seal due to the aggregate particles becoming embedded in the surface upon which the seal is constructed (as shown in *Figure 9*). Although some degree of embedment is required to ensure durability and performance during its service life (Woodward, ND), Milne identifies that the amount of embedment desired or expected is still not able to be predicted in practice (Milne, 2004). Read and Whiteoak (2003) highlight the factors which affect embedment the most:
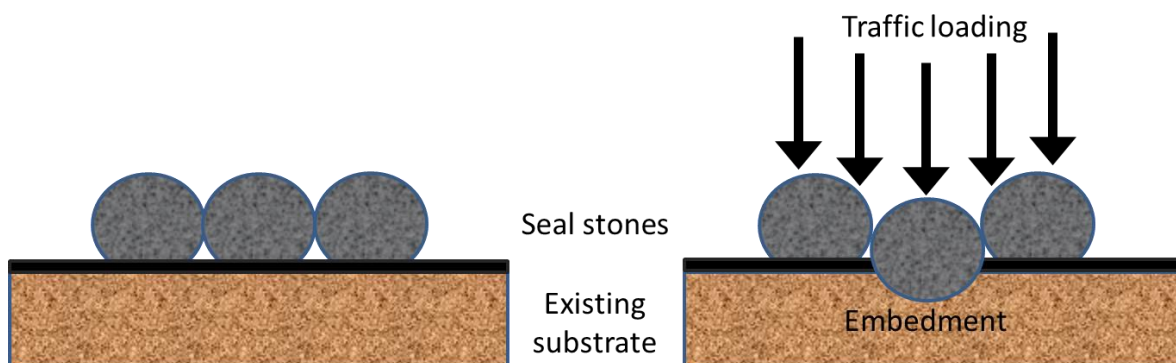
Figure 8: Conceptual idea of embedment

- The hardness of the surface upon which the seal is constructed.

A test method known as the ball penetration test was developed. This test quantifies the hardness of the existing surface, allowing the engineer to predict the expected embedment, and the corresponding reduction in voids in the seal (Milne, 2004). This test will be discussed in greater detail in a later section but it is worth mentioning that the ball penetration test uses a single sized metal ball with a single Marshall Hammer blow as the representative force. The test

can provide a basic idea as to the hardness of the surface but the degree of embedment would still be based on additional factors like aggregate shape, orientation spread rate etc. None of which are captured in the ball penetration test.

- Roller compaction

The effective rolling and compaction of the stones would establish an initial degree of embedment and stone reorientation. The TRH3 (2007) mentions that the initial embedment that can be expected during the construction of a seal is approximately equal to half of the embedment potential determined using the Ball Penetration Test. The roller also serves to orientate the stones such that their average least dimension (ALD) is perpendicular to the surface beneath the seal. This particle reorientation plays an important role in establishing the required degree of particle interlock and therefore also the resulting void content.

These first two aspects address the embedment and void loss during the construction of seals. The subsequent aspects address the embedment and void loss during the service life of the seal and would be considered the more important aspects relevant to this study.

- Intensity and type of traffic

Literature has shown that the volume and intensity of traffic has a marked influence on the performance of a seal (TRH3) and also on embedment (Milne, 2007; Cilliers, 2006; Read & Whiteoak 2004). The most influential type of traffic would be heavy vehicles, and thus APT devices generally only simulate this type of traffic. The MMLS3 trafficking is thus also based on heavy vehicle simulation. Since traffic in practice is an uncontrollable factor, designs are based on traffic surveys and forecasts to predict the traffic conditions the seal would need to endure during its serviceable life. The MMLS3 is therefore deemed an appropriate APT device for simulating traffic for texture loss purposes.

- The choice of aggregate size

In *The Shell Bitumen Handbook* Read and Whiteoak (2003) elaborates on this point noting that the use of stones that are too small will result in early embedment of the stones into the surface causing a rapid loss of texture depth and, in extreme cases, 'fatting up' of the binder. This is highly undesirable, and will certainly affect surface skid resistance. On the other hand, the use of stones which are too large may result in the immediate failure of the surface seal due to stripping of the binder from the aggregate under traffic loading. Excessive surface texture and an increase in noise generation can also be attributed to the

use of large aggregates. Higher stone sizes in a seal would result in a higher void content. Consequently, the available room for particle reorientation under traffic loading would increase.

- Aggregate characteristics

The mineralogical composition of the aggregate particle affects the stones ability to resist polishing and wear under the dynamic forces of traffic. Literature (Kane et al, 2013) has found that there are mechanisms of aggregate polishing or wear. The first is known as general polishing which tends to smooth off the coarse aggregate edges. This type of polishing usually occurs with single mineral aggregates which also have a relatively low hardness. The second is known as differential polishing. This type of polishing tends to create additional roughness on the stone surface. This is type of polishing is only possible with multi-mineral aggregates where the polished soft minerals are abraded easily while the harder minerals are less susceptible to polishing and abrasion. This results in the harder minerals being left behind causing peaks in the valleys of polished softer minerals. A method was developed in the 1950's to predict and forecast the capacity of an aggregate to resist polishing and has since been standardised. This test is known as the Polished Stone Value (PSV) test. It has however been shown that this test can only be used as a ranking tool for a given set of laboratory testing conditions. The ability of the PSV test to predict the complex development of skid resistance of surfacings is extremely limited.

The geometric characteristics of an aggregate could also influence the degree of embedment. These include the aggregate particle shape, angularity and flakiness index and they are built on the concepts highlighted by van Niekerk (2002) in *Figure 3*. These properties describe the physical nature of each particle at their surface. This in turn would affect their behaviour in terms of distributing forces placed on them during construction as well as through their service life. The TMH 1 describes the flakiness index as follows:

"The Flakiness Index of a coarse aggregate is the mass

Table 2: Slot dimensions for the different aggregate fractions (TMH1, 1986)

Size of fraction passing (mm)	Minimum length of slot (mm)	Width of slot (mm)
75	150	37.5
63	126	31.5
53	106	26.5
37.5	75	18.75
26.5	53	13.25
19	38	9.5
13.2	26.4	6.6
9.5	19	4.75
6.7	13.4	3.35

of particles in that aggregate, expressed as a percentage of the total mass of that aggregate which will pass the slot or slots of specified width for the appropriate size fraction as given in Table 2. The width of the slot is half that of the sieve openings through which each of the fractions passes" (TMH1, 1986).

The flakiness index thus provides an idea as to the average shape of each stone particle. With a higher flakiness index indicating that a larger percentage of aggregates are flaky *Figure 9*(a) or flat, while a lower flakiness index suggests that the particles are wider relative to their largest dimension, or non-flaky *Figure 9(*b). This concept is illustrated alongside. As can be seen, the flakiness index does not differentiate between angular and spherical particles, but still provides some
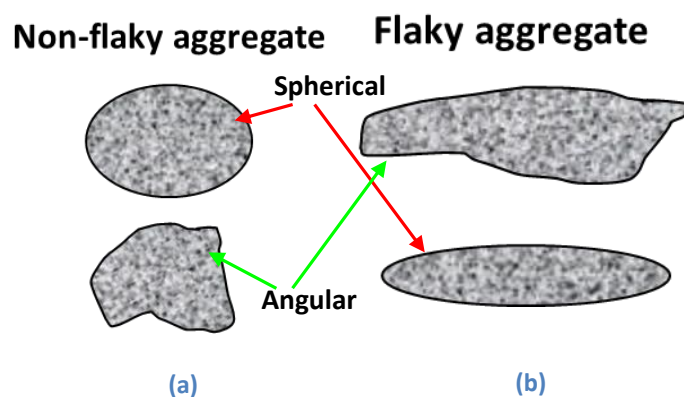
Figure 9: Non-flaky aggregate vs. Flaky (flat) aggregate

insight as to the overall shape of the particles relative to their mass. Another property relating to the flakiness of a particle is the average least dimension (ALD). Aggregates are graded commercially according to the percentages that pass through a specified set of sieves. Thus, seal stones are stockpiled and then obtained according to their 'average maximum dimension' because they were sieved by passing them through a particular fraction size. This would in effect mean that the flakiness of the particles is not controlled. For example relatively large flaky aggregate may pass a 13.2 mm sieve if the particle is orientated such that the shortest dimension is perpendicular to the sieve opening. This would then see the large flaky aggregate passing a 13.2 mm sieve despite its relatively large size. In order to gain a better perspective as to the aggregate shape or flakiness, the ALD can be determined. The *TMH1* describes the ALD as follows:

"The least dimension of an aggregate particle is the smallest perpendicular distance between two parallel plates through which the particle will just pass. The average least dimension is the overall average of the least dimension for a number of particles."

These two properties, together, provide a good idea of the average shape of the particles in an aggregate sample. They are important properties in seal design since they describe the average thickness of the seal mat that will result, while also affecting the void content and binder application rate. These properties also affect embedment, though perhaps not as much as the type and intensity of the traffic loads or the hardness of the surface upon which the seal is constructed. They affect the

transfer of forces on a smaller scale, and in combination with the traffic intensity and the existing surface hardness, they could possibly have a significant effect on the rate of embedment.

Graphically *Figure 10* alongside depicts the conceptual stress distributions on a cubical particle *Figure 10(a)* as well as a flaky (or flat) particle *Figure 10(b)*. The stresses transferred through a flaky aggregate particle allows for a more equal stress distribution while the stresses transferred through an angular particle would result in a larger amount of stress concentrations. These stress concentrations have a higher chance of shearing the surface below the seal stone, while the flaky particles distribute

(a)   **(b)**
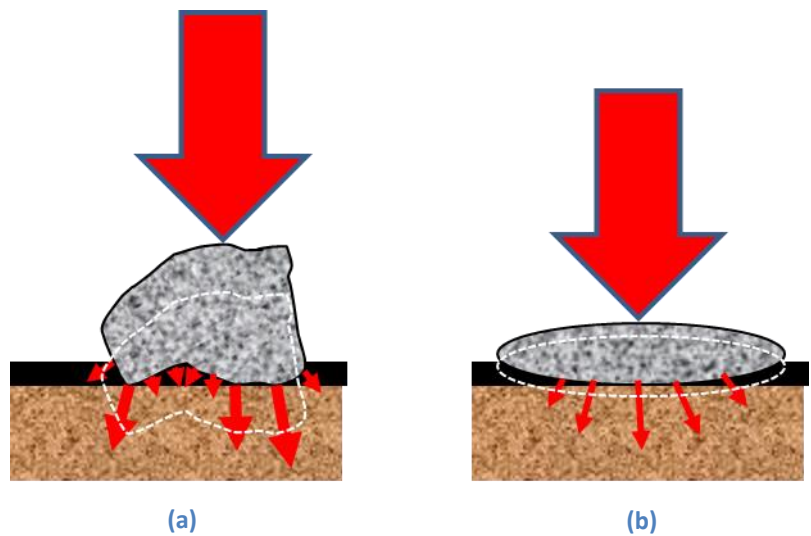
Figure 10: Influence of aggregate shape on stress distribution

the forces across its larger contact area, decreasing the number of points with large stress concentrations. Cubical particles as shown in *Figure 10(a)* would therefore be expected to embed into the substrate much easier than the flaky particles as shown in *Figure 10(b)*.

The use of modified binders could be beneficial when embedment issues are expected. Hoffman et al (2007) investigated the use of bitumen rubber in chip and spray seals. He noted that modified binders, especially non-homogeneous bitumen rubber binders, are stiffer than conventional binders. Since the stones in the seal are bound together with a stiffer binder, the load distribution characteristics of the seal will be improved. Despite the fact that seals are not specifically designed for load bearing, the transfer of loads to the underlying layers is an important function of the seal. The stiff binder will ensure that the seal acts as a rigid, uniform load on top of the base, preventing individual stones from punching into the base surface.

Embedment is the primary failure mechanism that will be investigated in this study and will be discussed further in a later chapter.

2.4.3 Deformation

It is reported that bitumen with a large proportion of molecules in the dispersed phase would characteristically not be very elastic and would not be sensitive to oxidation (Robertson, 1991). Binders of this nature would not be expected to harden well, and would deform easily, notably

under high temperatures. These types of binders lack the right proportion of large molecules to contribute to elasticity. The dispersing phase is made up of non-associated molecules, which organise themselves and harden at low temperatures. Thus, bitumen with a large proportion of non-associated material would have a high elastic modulus at high temperatures, reducing its potential for deformation. Bitumen with a higher proportion of large molecules would exhibit more elastic behaviour, even at low temperatures, making it less brittle, reducing its cracking potential. Although deformation in a road is largely related to structural issues and defects, the binder's composition and its relationship to seal performance is still evident. Deformation of the seal itself could occur through the rotating of seal stones, affecting the texture depth, available voids for the binder to flow, possibly causing bleeding.

2.4.4 Thermal and fatigue cracking

Reflective cracking is a common seal failure mode and is mainly due to failure within the structural layers of the pavement. Cracking can however be localised at the surface and are generally fatigue cracks, thermal cracks or cracks associated with their compound effects.

If the molecular structure of the binder becomes too rigid, the ability of the seal to deform elastically will be reduced. Brittle behaviour could cause the fracture of the binder if the loads placed upon it exceed its strength. This type of molecular arrangement is associated with low temperature conditions. The constant dynamic loading conditions associated with traffic would eventually cause the binder to fatigue and crack. The combination of these effects could therefore also accelerate the cracking process. Temperature fluctuations would cause the repeated rearrangement of molecules within the binder; this cyclic reorganization could result in shrinkage, and initiate cracking (Milne, 2004).

2.4.5 Moisture damage

Moisture damage contributes significantly to the premature deterioration of pavement structures. A generalised definition of the term damage is the degree of loss of functionality of a system. In this context, moisture damage on road surfaces is broadly defined as the degradation of mechanical properties of the material due to the presence of moisture in a liquid or vapour state. This loss of functionality is due to the loss of the adhesive bond between the aggregate and the binder (Caro et al, 2008).

Various mechanisms of moisture damage failure could occur under different conditions. A few terms describing these can be found in literature, they are listed below along with a basic idea of their manifestations (Caro et al, 2008):

- o *Stripping* - the process that results in the physical separation of the asphalt binder and aggregate due to the loss of adhesion at the interface of these materials in the presence of water or water vapour.

- o *Ravelling* - a distress manifestation that is identified by the dislodgement of aggregate particles in the mixture from the surface.

- o *Hydraulic scour* - a process that occurs on a saturated surface by which the pavement material is eroded due to the dynamic action of tyres in the presence of water.

The polar nature of water means that molecules within the bitumen could bond adhesively with water molecules. This is highly undesirable. The capacity of the bitumen to absorb water varies with composition. Aged or oxidised bitumen, due to polarity considerations, are more susceptible to moisture damage than fresh bitumen. Since older/aged bitumen is generally harder than fresh bitumen, it seemingly counters the effects of moisture related damage. The overall behaviour varies with bitumen composition (Milne, 2004).

2.5 Model Mobile Load Simulator (MMLS): Background and Developmental History

The Model Load Simulator (MLS) concept was initially founded on a chain of events starting in 1988. The Texas Highway Department considered developing a strategy for full-scale accelerated pavement testing. At the time, only two kinds of mobile accelerated testing machines were in use; the Heavy Vehicle Simulator (HVS) and the Accelerated Loading Facility (ALF). The HVS was developed in South Africa in the 1960's and the ALF had been used in Australia and in the United States from about the mid 1980's. Towards the end of the 1980's, Professor Fred Hugo, leader of the Texas project, returned to South Africa, and began working on a unique closed loop system. As part of the feasibility study on the implementation of accelerated pavement testing in Texas, a 1 to 10-scale model of the mobile load simulator was proposed and built by Hugo's team. This scale model was presented to the Texas Steering Committee in 1990. It was decided that a full-scale version of the MLS was to be developed, and was named the Texas Mobile Load Simulator (TxMLS) (Kemp, 2006).

Not long after the model for the MLS was completed, it was decided to upgrade this model to a fully operational laboratory mobile simulator (MMLS1), the first of which was used as a demonstration model in by the Department of Civil Engineering of Stellenbosch University. This machine was later sold to the University of Texas where it was used for testing and served also as an introduction to the TxMLS, while a second unit was used by Stellenbosch University for research purposes. Following this, MLS units were sold to the University of Arizona as well as to the Indonesian Government research organisation through a Japanese sponsorship (Kemp, 2006).

After some time, users of the MLS1 suggested that a more feasible model for the laboratories be developed, since the 1 to 10-scale modelling of a pavement was being challenged. The scaling of materials and pavement layers were questioned. This subsequently led to the development of the MMLS3, a new model mobile load simulator, based on a third scale modelling of the original concept and used a single wheel of a dual tyre. The first MMLS3 prototype was completed in 1997 and sold to the US. Units were then sold to various universities in Europe and America as well as to the Institute of Transport Technology (ITT) in Stellenbosch (Kemp, 2006). The MMLS3 comprises of four bogies with one 1/3 scale tyre per bogie (Kim and Lee, 2006). The pneumatic tyres are approximately 300 mm in diameter and 80 mm wide. The schematics of the MMLS3 are shown in *Figure 11.*

In 2008 a document was published as part of the development toward an international standard test protocol titled ***DPG1 – Method for evaluation of permanent deformation and susceptibility to moisture damage of bituminous road paving mixtures using the Model Mobile Load Simulator***

24

*(MMLS3).*Feedback from MMLS3 users was requested so that adjustments and improvements to the protocol could be made. The protocol is however restricted to use on asphalt surfacings and asphalt road base mixtures.
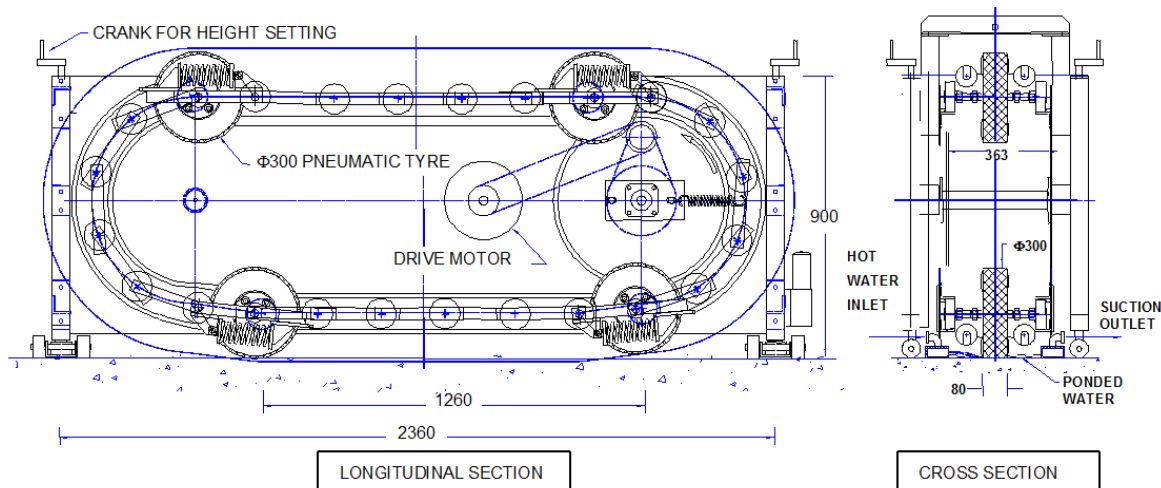
Figure 11: Schematic longitudinal and cross sectional diagrams of the MMLS3

2.6 Previous research on seals using the MMLS

Current road surfacing seal design practice is highly dependent on experience and empirical analysis. The application of bitumen and aggregate is primarily based on a volumetric approach. Milne (2004) conducted an intensive study toward the development of a performance based seal design method. Milne's research assessed the South African seal design philosophy, investigating design areas where review or updating is required to accommodate the changing bitumen types and sources as well as the change in traffic loading conditions. He examines the seal performance criteria (as shown in *Figure 12*), developing a matrix of influences on seal performance. Using this, the need for a seal design method based on mechanistic material properties is proposed. A prototype example of such a numerical model
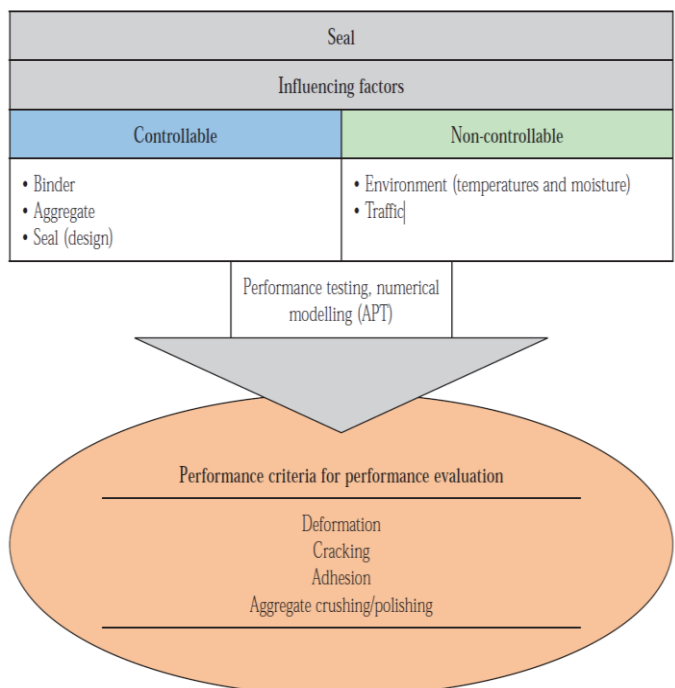
Figure 12: Interaction of influencing factors and identification of performance criteria (Milne, 2004)

25

using the finite element method is then presented.
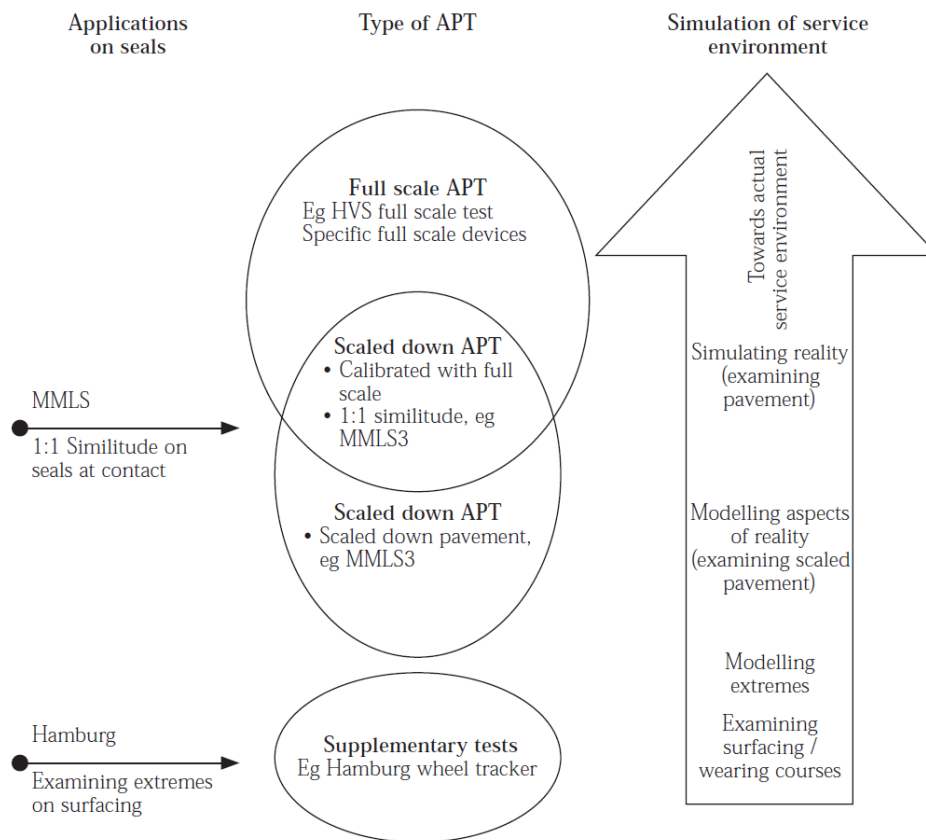
Figure 13: Types of pavement and surface accelerated performance test regimes (Milne, 2004)

To evaluate and verify the data provided by the prototype numerical model, and to further contribute to the development of a performance based seal design method, performance tests were developed using the Model Mobile Load Simulator (MMLS) testing device based on the test regimes shown in *Figure 13*. These performance tests were focused on the most basic seal type, the single seal. This enabled the primary seal constituents to be assessed in their most basic form of seal aggregate and binder. Various binder types were analysed – Penetration grade bitumen, SBS, SBR, EVA modified binders as well as bitumen rubber. Each was used to construct single seals, which were then tested using the MMLS and three different temperature regimes. Using the methodology for the assessment of in-service seal behaviour, the performance of the seals is reported in *Table 3*. The results indicate that each binder type has its unique contribution towards seal performance and Milne notes that the MMLS3 APT apparatus successfully enables comparative evaluation of the performance of each different binder type. The binders are then ranked based on their performance

under the various temperature regimes (*Table 4).* To complement the MMLS results additional comparative performance testing was conducted to assess the effects of aging and moisture.

Milne concluded that the current seal design method required further development to aid designers in the prediction of the effects of:

• Varying axle loads, tyre pressures and design speeds.

• Varying characteristics of the different binders (and their corresponding temperature-viscosity relationships, adhesion, and visco-elastic behaviour)

• He also noted that the major areas for suggested improvement in the current seal design methods towards a performance based seal design method are:

• Inclusion of variable traffic load and environmental characteristics, including temperature and moisture influences.

• Inclusion of mechanistic material characteristics into the design methodology.

Table 3: Summary of seal performance (Milne, 2004)

Summary: seal performance		Scale 100 maximum: worst / 0 minimum: best		
Binder	Overall perform-ance	Test regime		
		10 °C (cold)	Ambient	50 °C (elevated)
Binder modified 80/100 pen grade with:				
3 % SBR	0–22	19	17-22	0-6
3 % SBS	0–28	28	0-16	6–15
3 % EVA	11–28	17	11-28	11
20% bitumen rubber BR • TOSAS • COLAS	14–39 11–56	17	14–35 11-33	25–39 17–56
80/100 penetration grade	22–56	22	31	56

Table 4: Binder performance ranking (Milne 2004)

Binder ranking* Ranking (1 best, 5 worst), (BR consolidated)					
Regime	1	2	3	4	5
Cold	20 % BR	3 % EVA	3 % SBR	80/100	3 % SBS
Ambient	3 % SBS	3 % SBR	3 % EVA	20 % BR	80/100
Elevated	3 % SBR	3 % EVA	3 % SBS	20 % BR	80/100
Overall	3 % SBR	3 % SBS	3 % EVA	20 % BR	80/100

80/100 pen grade bitumen modified as shown

This performance testing procedure has assisted in identifying the critical parameters a seal designer should consider during the design phase of a seal project. Milne's research will play an important role in the structure and direction of this research project. He has effectively laid the foundation upon which further research in this field can be built.

2.7 Key features of the Asphalt Protocol relevant to this research project

The Draft Protocol Guideline 1 (DPG 1) covers the procedure for evaluating the permanent deformation performance and susceptibility to moisture damage of asphalt using simulated traffic loading with the 1/3 scale Model Mobile Load Simulator (MMLS3) under controlled environmental conditions. The protocol is applicable to asphalt surfacings and asphalt road base mixtures containing penetration grade bitumen and modified binders. The protocol does not consider asphalt mixes with emulsion and foamed bitumen, even though accelerated testing using the MMLS has been done on such materials (DPG1, 2008).

The DPG1 also clearly highlights that the test results obtained should always be considered in the context of construction characteristics as well as actual traffic and environmental conditions to which the material is subjected during its lifecycle (DPG1, 2008). This is an important point for designers using the MMLS testing system to be aware of. The materials, traffic conditions and environmental conditions in the laboratory should be representative of the conditions that the material will be placed under in the field.

The focus, when the research aim is toward a test protocol, is ensuring that the test method has adequate repeatability. Details regarding the testing procedure should be clearly outlined and all parameters should be effectively described. The DPG1 does so, describing the procedure for evaluating permanent deformation (rutting) and moisture susceptibility of asphalt using the MMLS3 in the laboratory as well as in the field. It provides information and guidelines with regard to the instrumentation and calibration of the MMLS3. The appendices also details the influence factors involved when targeting rutting performance, proposed guidelines for determining test specifications and performance benchmarks and quantitative analytical evaluation of rutting performance.

The following are key concepts from the DPG1 could be relevant in the experimental design when testing seal performance using the MMLS3.

2.7.1 Type of test setup

Laboratory: test bed on cores and compacted specimens

Cylindrical asphalt specimens can be prepared in the laboratory using gyratory compaction. Similar samples can be cored from in service pavements and tested in the test bed. The specimen thickness may be between 30 mm and 90 mm (± 2 mm). The moulds in the test bed require the cylindrical samples to be machined by sawing and trimming with a planning blade to a tolerance of ± 0.5 mm with two parallel edges of the specimen 112 mm apart. The specimens are then placed snugly, side by side with the sawed down edges perpendicular to the direction of trafficking. The samples can then be tightened with the clamps and screws in the test bed (DPG1, 2008). This concept is illustrated graphically in Figure 14 alongside.
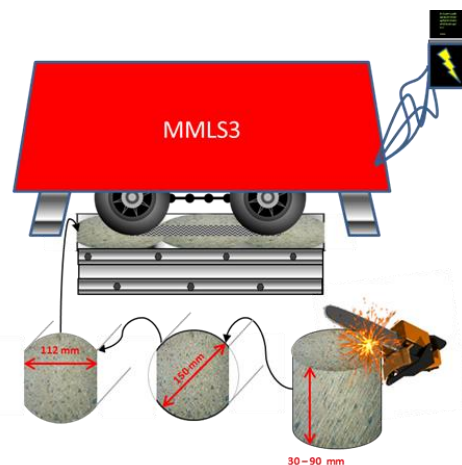
Figure 14: Conceptual representation of MMLS3 tests on cores and compacted specimens

Laboratory: Constructed slabs

Slabs can be constructed in the laboratory using roller compaction. The constructed layer system can then be placed under traffic loading for the desired number of load cycles as shown conceptually in *Figure 15*. Performance (rutting) can then be monitored throughout the service life. The advantage of using the slab method is the elimination of the specimen thickness limitation present when using the cylindrical samples in the test bed. The support structure can now also be constructed and its effect on the surface performance can be observed. The DPG 1 does not provide a detailed walkthrough of this test setup, it may be beneficial to this

Figure 15: Conceptual representation of MMLS3 tests on constructed slabs

project because an important failure mechanism for seals is the embedment of the aggregate. Since this failure mechanism is largely dependent on the supporting base layer, in order to monitor embedment and its effect on performance in seals, the base layer needs to be effectively modelled into the test setup. This method shows more promise than its predecessor for laboratory performance testing on seals. Further ideas to support or discourage this are necessary before a fitting test setup can be identified.

Field: On-site testing

The MMLS3 as its name suggests is a mobile laboratory tester and can thus be transported to the site and test pavement systems in-situ as shown conceptually in *Figure 16* alongside. This is a key advantage which provides the opportunity to run tests eliminating variables such as in service temperature fluctuations and wet trafficking along with many other environmental parameters which could prove difficult to model in a controlled testing environment. Lab and field results can then also be collected on similar mixes to establish if a good correlation exists between lab test results in service test results under MMLS trafficking.
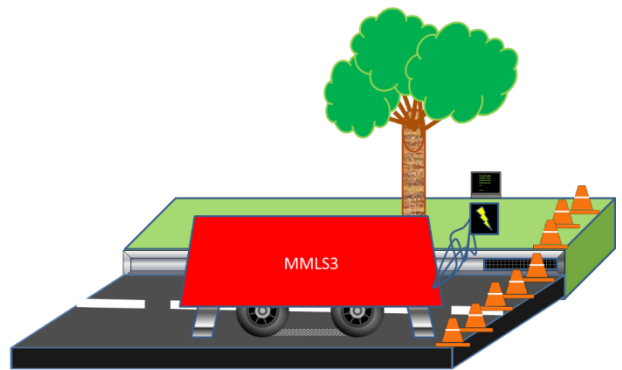
Figure 16: Conceptual representation of MMLS3 tests on-site

2.7.2 Some factors affecting rutting performance mentioned in DPG1 that could prove relevant to MMLS testing on seals

Environmental impact

Evidence suggests that wet trafficking can increase the rutting of asphalt, and moisture known to be damaging to the structure of asphalt. For this reason, the rainfall patterns (frequency, intensity, duration etc.) relative to traffic should be investigated to establish the nature of wet trafficking to be applied in a controlled environment (DPG1, 2008). As noted, moisture has an impact on seal performance as well. Wet trafficking may thus prove useful and possibly even vital for research into moisture damage of seals when placed under MMLS loading. Short and long term effects can be simulated in terms of traffic induced load cycles. The data could then be used to set up guidelines with regard to sealing with rain forecast, or identify a possible seal design that minimises the manifestation of one or more of the moisture induced failure mechanisms. These types of investigations into these failure mechanisms would require, for each, their own data set. As more testing is carried out and more data sets are obtained, seal performance could be better understood, modelled and predicted using MMLS testing.

The bituminous binder present in asphalt and seals is susceptible to aging. Seasonal temperature fluctuations along with the corresponding binder viscosity variations result in a periodic hardening and softening of the binder. Over time, the binder loses its ability to lower its viscosity. This is known as aging. Milne mentions four mechanisms of bitumen hardening (causing aging); loss of volatiles,

atmospheric oxidation, physical hardening, exudative hardening (porous aggregate). (Milne, 2004) Since in service aging of the bitumen would be time and region specific, the DPG1 highlights that aging could have a profound effect on the rutting performance of asphalt. Early trafficking would result in a much greater impact on the performance in terms of rutting, than trafficking toward the end of the service life. The DPG1 accounts for aging by reducing the expected rutting as finally estimated from the MMLS rutting performance by 30% (based on the progressive increased stiffness over time due to aging). (DPG1, 2008)

Traffic volume and related axle loads

The DPG1 emphasises the importance of the selection of the traffic volume and related axle loads based on the statistics pertaining to the critical temperature phases. Asphalt rutting, being highly dependent on temperature, and early life traffic should be considered carefully. Critical trafficking situations are generally assumed to only be prevalent during certain times of the day in the life of the pavement (DPG1, 2008).

Lateral wander of traffic affects the volume and extent of critical trafficking. In service, wheel loads do not occur along the same path consistently. This implies that the number of load cycles at a particular location along the transverse profile is reduced. Lateral wander also affects the way in which the asphalt is moulded transversely. The resulting deformation profile is normally of a Gaussian format, despite the random load distribution. The DPG1 makes mention of researchers studying the effect of lateral wander on thick asphalt layers. Supported by theoretical finite element analyses they concluded that lateral wander proved less damaging than channelized trafficking. More recent studies suggest that lateral wander on thin asphalt layers (40 mm) under high temperature could cause significantly more damage to the asphalt in terms of rutting than channelized trafficking. Supporting research to reinforce this is necessary, but to remain conservative the DPG1 suggests that designers apply lateral wander when testing thin asphalt layers. To simulate the effect of lateral wander, MMLS trafficking can be distributed transversely. This can be done by moving the wheel across the transverse profile progressively simulating a Gaussian distribution (DPG1, 2008).

Traffic speed & tyre pressure

Accurately modelling traffic speed for simulation purposes is not a simple task. Naturally, traffic speed and time of loading is variable, the effect on the pavement structure is therefore also variable. The selected trafficking speed should, as closely as possible, reflect the conditions the layer would be required to endure during its serviceable life. Distinctions should be made to account for factors

such as average speed, gradients, heavy vehicle volume, traffic flow-rate and stop-start conditions (DPG1, 2008). The DPG1 (2008) recommends the following categories for the respective conditions:

- Flat (level) free flowing conditions

- Rolling gradients and free flowing traffic with high heavy vehicle volumes

- Slow channelized traffic on steep inclines and highway intersections

- Free flowing airport runways and taxiways with high contact stresses

- Airport aprons, stop-start taxiways and runway thresholds

The MMLS has a maximum equivalent speed of 7200 load applications per hour. This trafficking speed is considered as relating to free flowing highway speeds in excess of 27km/h. Slower speeds are used progressively to simulate other more strenuous situations and are ultimately reduced to 1800 load applications per hour when complex high stress conditions are to be simulated.

The tyre pressure is said to play an important role in the performance of asphalt material, most notably when fresh. The DPG1 indicates that a tyre pressure of 800kPa would be considered appropriate when asphalt is placed under a high percentage of heavy vehicle traffic. These high pressures may however cause excessive wear on the tyres. A slightly reduced value of 750 or 700kPa should be used if the heavy vehicle percentage is not too high. Another consideration is the wheel load, since it affects the footprint. The high tyre pressure situation (800kPa) would require a wheel load of 2.9kN per axle, while the lower pressure situation needs a reduced wheel load of 2.7kN per axle. The resulting loads are then used for the life cycle performance prediction (DPG1, 2008).

Layer thickness and pavement structure

Comparative stresses between MMLS trafficking and full scale trafficking tyres are related through the layer thickness. Thinner layers yield a closer comparative stress relationship between scaled down MMLS trafficking and full scale trafficking. Generally, rutting under MMLS trafficking relative to full scale trafficking should be proportionately increased as the layer thickness is increased. Similarly, the thinner the asphalt layer, the greater the total surface rut of the structure may be influenced by the underlying layers which are usually non-asphalt and commonly unbound material. For this reason, the DPG1 emphasises the importance of measuring the rutting directly related to the asphalt. This is done by anchoring a pin under the asphalt layer and measuring the rutting in the asphalt layer separately from the settlement of the layers below it (DPG1, 2008).
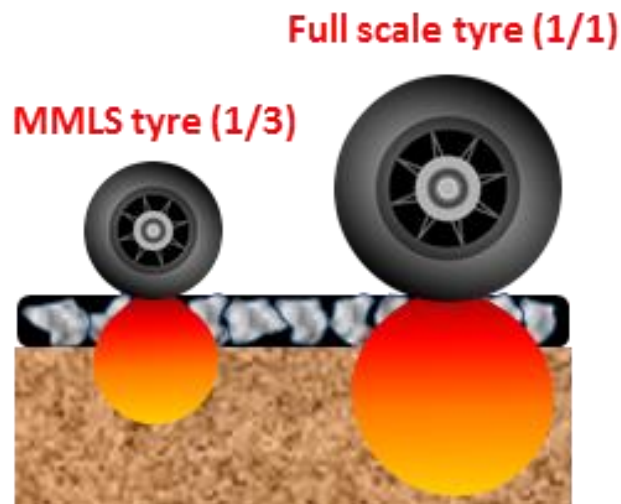
Figure 17: MMLS3 tyre vs full scale tyre stress distributions (Ebels, 2003)

The layer thickness for MMLS testing should not exceed 150 mm due to the limited depth of the stress profile related to the tyre size as shown in *Figure 17*. The nominal maximum aggregate size (NMAS) should also be less than 50% of the layer thickness of the asphalt (DPG1, 2008).

2.8 Establishing performance variables for MMLS testing on seals

Using the information from the previous sections, the performance variables for MMLS testing on seals are now provided. Naturally, these performance variables are directly or indirectly related to the factors affecting seal performance mentioned in *Section 2.2.3* and displayed in *Figure 2*. The influence factors are illustrated again in groups according to the investigation field applicable to them. *Table 5* refers to the influence factors related to the existing pavement structure and condition, *Table 6* refers to the influence factors related to traffic and the physical environment and *Table 7* refers to the influence factors related to the materials and seal design. The related numerical models, performance variables are then tabulated along with their controllability in-service as well as in the laboratory for MMLS testing. They are adapted from Dr Milne's work where he described the investigation into the identification of influence factors from theory and practice. He mentioned that the identification of these influence factors for inclusion in the numerical behaviour and experimental performance variables of seal performance was an interactive process. He examined the theory to initiate the respective models, and in the development of those models, the need arose for confirmation, determination or explanation of parameters which in turn called for further investigation into literature (Milne, 2004). The establishment of performance variables for this study will most likely follow a similar approach, now using Dr Milne's work as a point of departure.

(a) Existing Pavement structure & condition

Table 5: Influence factors relating to the existing pavement structure and condition

Investigation Field	Component variable	Performance variable	In-service	Laboratory (MMLS)
(a) Pavement, Substrate (Base or existing surfacing)	• Material type • Classification (G1 – G6) • Grading (maximum stone size)	• Density • Strength • Embedment	Controllable to some degree with sufficient preparation and pre-treatment	Controllable

(h) Traffic

(i) Physical environment

Table 6: Influence factors relating to traffic and the physical environment

Investigation Field	Component variable	Performance variable	In-service	Laboratory (MMLS)
(h) Traffic	• Equivalency Factor • Contact stress: Foot print, Pressure, Load • Time and frequency of loading	• Tyre pressure • Load • Traffic volume	Non-controllable	Controllable
(i) Physical environment	• Temperature variation • Moisture variation Their effect on stiffness & complex modulus	• Effect of temperature • Effect of moisture • Aging	Non-controllable	Controllable

34

(d) Materials & (e) Seal Design
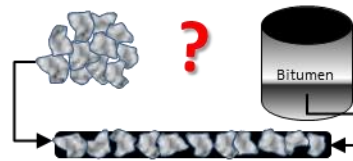
Table 7: Influence factors relating to the materials and seal design

Investigation Field	Component variable	Performance variable	In-service	Laboratory (MMLS)
(d) Materials: Bitumen type	• Penetration grade 70/100 • Emulsion: SC-E1 • Polymer Modified: S-E1 • Bitumen Rubber	• Temperature Susceptibility • Viscosity • Adhesion • Cohesion • Ductility	Controllable	Controllable
(d) Materials: Seal Aggregate	• Aggregate type • Average Least Dimension (ALD)	• Strength • Adhesive properties • Wear properties • Texture	Controllable	Controllable
(e) Seal Design	• Seal type • Seal design: application, aggregate, binder, void volume	Seal design: • Type • Applications • Aggregate • binder	Controllable	Controllable

The performance parameters highlighted above can then be used as a guideline for the experimental design of this project. The target failure mechanisms can be identified along with its related influence factors and performance variables. An idea as to the parameters which can/should be controlled and those which should vary will become clearer. This will be elaborated on further in the experimental design.

35

3. <u>MATERIALS</u>

3.1 Bitumen

3.1.1 Introduction

SABITA Manual 2: Bituminous binders for road construction and maintenance (2012) defines and describes bitumen as follows:

"Bitumen is a dark brown to black viscous liquid or solid, consisting essentially of hydrocarbons and their derivatives. It is soluble in trichloroethylene, is substantially non-volatile, and softens gradually when heated. Although solid or semi-solid at normal temperatures, bitumen may be readily liquefied by applying heat, by dissolving it in petroleum solvents or by emulsifying it in water."

Bitumen has been used by man in a wide range of applications including waterproofing and bonding applications for thousands of years. The earliest recorded uses can be traced back to between 3500 – 2000 BC by the ancient Sumerian civilisation. They used natural bitumen to bond the stones used when constructing their water tanks (Read and Whiteoak, 2003). This would serve as proof that mankind has been aware of the uses of bitumen for ages. Presently, however, the most common use of bitumen is in the road construction industry.

In seal construction, the bitumen binder is used with a stone aggregate matrix in various combinations. These two components work together synergistically to form a flexible, strong and waterproof surface. The properties and behaviour of bitumen is valuable for engineering applications due to its strength and adhesive properties in addition to being a durable and highly waterproof material. When combined with a mineral aggregate matrix, the bitumen allows for some flexibility in the seal. This is ideal under the dynamic action of traffic, since a rigid surface would be prone to cracking, nullifying the waterproofing properties of the bitumen. The highly adhesive behaviour of bitumen, when combined with mineral aggregate allows it to become a binder providing the flexibility and waterproofing while the aggregate provides the mechanical strength to transfer loads from the surface to the underling pavement layers.

3.1.2 Origin and Production

Bitumen is a naturally occurring substance and can be found in small deposits in various places around the world including the USA, West Indies, Mexico and Germany to name a few. These naturally occurring deposits vary in purity depending on its location. The largest deposit of bitumen in a fairly pure state (known as Gilsonite) can be found in Utah, United States (Milne, 2004). Other

common bitumen deposits are less pure, containing high proportions of bitumen along with a significant amount of mineral matter.

Presently, the largest source of bitumen is from the refining process of crude oil. The origin of this fossil fuel can be traced back hundreds of thousands of years. When marine organisms died, their remains sunk and came to rest on the floors of oceans and lakes. Over time these organic remains were covered with inorganic sediments. The immense pressure along with the passing of millennia caused these materials to be condensed into complex combinations of organic components. The result is the fossil fuel known today as crude oil. Known crude oil deposits have been found in some parts of the world including the Middle East, Asia, the Americas as well as the Atlantic Ocean and the North Sea (Read and Whiteoak, 2003).

Bitumen is a derivative from the process when crude oil is refined to produce petroleum. Very few refineries produce bitumen as their primary product. For most, it is but a by-product in their petroleum manufacturing processes. Since crude oil is a naturally occurring substance, it should be noted that the quality and characteristics of each crude is not consistent. The chemical composition of crude oil is dependent on the organic material from which it originates, as well as the environment in which it was formed. Maturity of the oil results in the separation of the heavier molecular components resulting in a crude that is lighter (lighter crudes contain higher proportions of petrol, gas, diesel etc.). Generally, heavier crudes would require greater degrees of refining to produce fuel. Bitumen, being a residue of the refining process, therefore also display varying compositions and characteristics which are not only dependent on the crude from which they are derived, but also on the refining process itself. All crude oils are not suitable for bitumen production. Of the 1500 different crude oils known, only about 250 are suited to bitumen production (Milne, 2004). Crude oils with higher proportions of aromatics display high contents of residue, asphaltenes and sulphur. It is these types of crudes that are most suitable for bitumen production.

3.1.3 Composition

Bitumen is a mixture of molecules comprised mainly of hydrocarbons with small amounts of functional groups containing oxygen, sulphur and nitrogen atoms along with traces of various metals (Greyling, 2012). The proportions of these atoms and molecules are dependent on the crude oil from which the bitumen is derived as well as the refining process used. Establishing the precise chemical composition of bitumen is a complex task, but despite its chemical complexity, it is possible to separate bitumen into two broad groups based on the molecular content of asphaltenes and
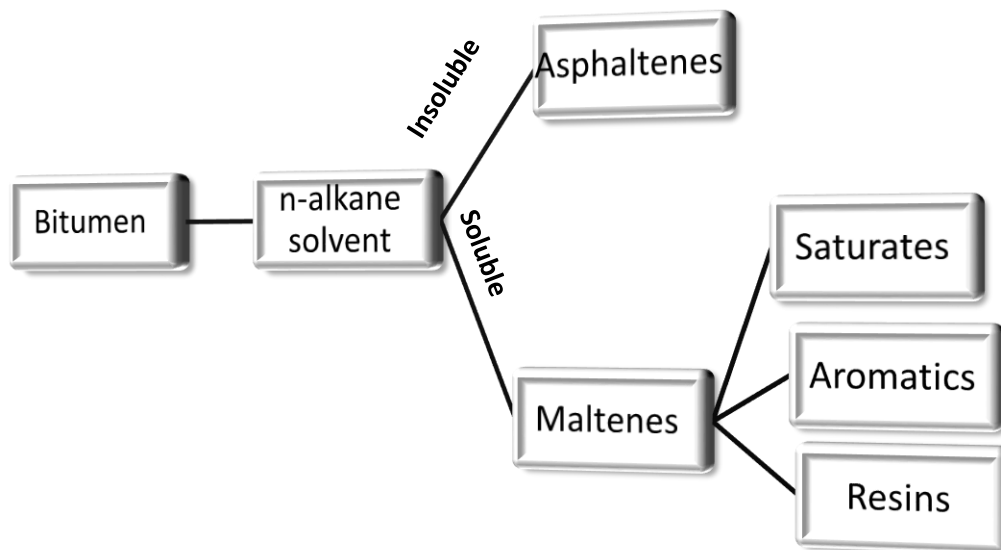
Figure 18: Bitumen groups based on asphaltenes and maltenes adapted from Read and Whiteoak (2003)

maltenes. Maltenes can then be further sub-divided into saturates, resins and aromatics. This is shown in *Figure 18* above.

Milne (2004) and *The Shell Bitumen Handbook* (Read and Whiteoak, 2003) describe these groups in great detail. A brief summary of their description follows:

Asphaltenes – The precipitate when bitumen is dissolved in pentane. They contain, in addition to carbon and hydrogen, some nitrogen, sulphur and oxygen. These materials constitute 5 – 25% of the bitumen, are very polar, black in colour, hard, with large molecules and make bitumen harder and more viscous due to their high density.

Maltenes – Saturates – consist of straight and branched chain aliphatic hydrocarbons. They are viscous oils straw or white in colour, are non-polar and constitue 5 – 20% of the bitumen.

Aromatics – consist of non-polar carbon chains. These aromatic oils are dark brown viscous liquids and constitute 40 – 60% of the bitumen.

Resins – like asphaltenes, are composed of carbon and hydrogen with small amounts of nitrogen, sulphur and oxygen. These aromatics are dark brown in colour, solid or semi-solid, highly polar, and are strongly adhesive due to their polarity.

3.1.4 Bitumen types and grades

Bitumen technology has developed significantly over the past few decades. Today, various types of bitumen exist, including various penetration grades, bitumen emulsions as well as polymer modified bitumen. With the passing of time and the development of cutting edge chemical technology, the bitumen industry now boasts a wide range of bitumen products formulated to exhibit certain behaviour under certain conditions. Although many types of bitumen are used for road construction and industrial applications, only the major grades and types of bitumen for seal applications will be briefly discussed.

3.1.4.1 Penetration Grade Bitumen

Penetration grade bitumen is the most widely used type of bitumen in road construction and, as its name suggests, is classified based on their penetration using the standard penetration test. It is manufactured in one of two ways; either by straight-run distillation or by blending two base components (the base components being different types of penetration grade bitumen) to produce the required grade. *Table 8* that follows has been adapted from the *SANS 4001 − BT1* (2014) and provides the requirements for penetration grade bitumen in South Africa.

Table 8: Requirements for Penetration Grade Bitumen adapted from SANS 4001-BT1 (2014)

1	2	3	4	5	6	7
	Penetration Grade					
Property	10/20	15/25	35/50	50/70	70/100	150/200
	Requirements					
Penetration at 25°C/100 g/5 s, 1/10 mm	10-20	15-25	35-50	50-70	70-100	150-200
Softening point (ring and ball) °C	58-78	55-71	49-59	46-56	42-51	36-43
Minimum viscosity at 60°C, Pa.s	700	550	220	120	75	30
Viscosity at 135°C, mPa.s	≥750	≥650	270-700	220-500	150-400	120-300
Flash point, °C minimum	245	235	240	230	230	220
Performance when subjected to the rolling thin film oven test: (a)mass change, % (by mass fraction, max.	-	0.5	0.3	0.3	0.3	0.3
(b) viscosity at 60°C, % of original, max.	-	-	300	300	300	300
(c) Softening point (ring and ball), °C, min.	-	57	52	48	44	37
(d) Increase in softening point, °C, max.	10	8 55	7	7	7	7
(e) retained penetration , % of original, min	-	-	60	55	50	50
Spot test, % xylene , max.	-	-	30	30	30	30

As can be seen, these specifications are based on certain test properties the aim of which is to provide different grades of bitumen to account for different climatic conditions.

3.1.4.2 Cutback Bitumen

Essentially, cutback bitumen is penetration grade bitumen that has been blended with a small amount of volatile solvents (like kerosene). The purpose of this additive is to initially reduce the viscosity to allow for easier handling and application. The viscosity of the cutback bitumen is determined by the proportion of solvent added; a higher proportion of solvent resulting in a cutback with a lower viscosity (SABITA, 2012). Once these volatiles evaporate, the bitumen reverts back to the penetration grade bitumen from which the cutback was made. Three types of cutters or flux are typically used to create cutbacks depending on the behaviour that is sought. Diesel is typically used to formulate a slow curing cutback, kerosene to formulate a medium curing cutback and white spirits to formulate a rapid curing cutback (Greyling, 2012). The advantage of using cutback bitumen is that it can be applied at lower temperatures due to its reduced initial viscosity. The downfall being that non-renewable energy sources are essentially lost through evaporation.

3.1.4.3 Polymer modified Bitumen

In situations of high stress like heavy traffic, steep inclines, intersections and sharp curves, in areas where the daily/seasonal temperatures fluctuate or experience high ambient temperatures for extended periods, on flexible or cracked pavements, or in remote areas where improved durability is required, the use of conventional bitumen can be insufficient to achieve the functional and behavioural requirements. In these extreme cases, the use of modifiers to improve the rheological properties of the bitumen becomes advantageous.

Similar to conventional binders, the physical properties of modified bitumen are primarily controlled by the fundamental properties related to viscosity, temperature and phase transition. Generally, the purpose of using a modifier would be to alter the plastic and viscoelastic phases of the bitumen. The changes in these phases would depend on the type and concentration of modifier used. Bitumen modification technology could thus provide binders that exhibit improved viscoelastic properties over a broader temperature range (Asphalt Academy, 2007). Further benefits that could be attained through polymer modification are also highlighted and include:

- Improved stiffness and cohesion

- Improved flexibility, resilience and toughness

- Improved bitumen-aggregate adhesion

- Improved consistency

- Improved resistance to aging

- Reduced temperature susceptibility
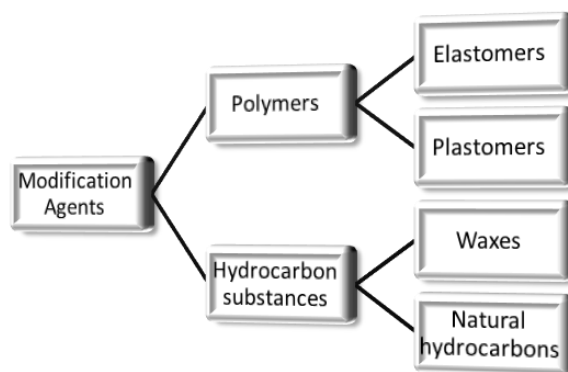
Figure 19 alongside has been extracted from TG1 (Asphalt Academy, 2007) and depicts the types of modifiers used.

Figure 19: Modifying agents (Asphalt Academy, 2007)

The TG1 (Asphalt Academy, 2007) also uses a classification system for modified binders based on the following:

Type of application – 	Seal (S), asphalt (A) and crack sealant (C).

Type of modifier used – Homogeneous elastomer (E), homogeneous plastomer (P), non-homogeneous elastomer (R), hydrocarbon (H).

Type of binder system – If the product is an emulsion, the letter "C" would follow directly after the letter indicating the type of application.

Level of modification – 	A numerical value is used to indicate increasing softening point values.

The typical modified binders in terms of the classification system as indicated above are tabulated in Table 9 below:

Table 9: Seal classification based on the modifying agents used from TG1 (Asphalt Academy, (2007))

Modifying agents		Classification
Elastomers	**Styrene-butadiene-styrene (SBS)**	*S-E2, A-E2*
	Styrene-butadiene-rubber (SBR) latex	*S-E1, A-E1, C-E1*
	Bitumen rubber	*S-R1, A-R1, C-R1*
Plastomers	**Ethylene vinyl acetate (EVA)**	*A-P1*
Hydrocarbons	**Natural hydrocarbons**	*A-H1*
	Aliphatic synthetic wax	*A-H2*

As can be seen in the classification system highlighted above, only the elastomers (SBS, SBR and bitumen rubber) are used in seal applications.

3.1.4.4 Bitumen Emulsions

By nature, bitumen is highly viscous if not solid at ambient temperatures. The usage of bitumen in road construction practices usually require the bitumen to behave as a mobile liquid for ease of transport as well as application. Principally, there are three ways to dramatically decrease the viscosity of bitumen; heating it, dissolving it in solvents, and through emulsification.

Bitumen emulsions consist of bitumen droplets dispersed in water containing an emulsifier. The result is an oil-in-water type of mixture with the bitumen particles held in suspension by an emulsifying agent. The net bitumen content in bitumen emulsions generally vary between 60 – 70% (with the exception of "inverted" emulsions where the water content is less than 20%) (SABITA-M2, 2012). *The Shell Bitumen Handbook* (2003) notes that there are four classes of emulsions:

- Cationic emulsions

- Anionic emulsions

- Non-ionic emulsions

- Clay stabilised emulsions

Of these, cationic and anionic emulsions are the most widely used.

The terms cationic and anionic stem from the electrical charges on the bitumen globules held in suspension. Cationic emulsions contain bitumen globules that are positively charged while anionic emulsions contain bitumen globules that are negatively charged. Due to these electrical charges present in cationic and anionic emulsions, the adhesive ability of an emulsion to the aggregate is greatly affected by the type and mineralogy of the aggregates used. Spray seal applications result in the direct contact of the binder and the aggregate. Thus, the selection of the aggregate and emulsion combination is of utmost importance in seal design. Acidic aggregates make up a large proportion of the aggregates used in South Africa. These negatively charged acidic aggregates, such as granite and quartzite, display a natural affinity to the positively charged cationic emulsions. As a result, cationic emulsions are more widely used since they have superior adhesive properties to a wide range of aggregates typically used in South Africa. Conversely, negatively charged anionic emulsions display good adhesion to positively charged mineral aggregates such as limestone and dolomite. Using, for example, an anionic emulsion with an acidic aggregate such as granite would

result in a delay in the effective adhesion development. Only once the water has evaporated and the emulsion reverts back to the base bitumen would effective adhesion develop (Milne, 2004).

Emulsions can be useful in certain situations, especially in seal construction. The following scenarios render the use of emulsions superior to that of hot applied binders as noted in the SABITA-M2 (2012):

- Damp or dusty aggregates in chip sealing;

- When aggregates are uncoated in chip sealing, since the adhesion of a range of aggregates to the cationic emulsion is improved.

- Requiring application at lower temperatures. This assists in lowering energy consumption, enhances worker safety, reduces emissions and extends the allowable work periods during construction.

- When lower application rates are required. Since emulsions are diluted with water, a workable volume of the emulsion can be applied.

3.1.4.5 Bitumen based precoating fluids

Precoating fluids are a fairly recent development in seal design, but over a short period has become common practice. Precoating fluids are generally a low viscosity bituminous based binder with additives such as petroleum cutters and chemical adhesion agents. The use of precoat is considered a cost effective measure to minimise the risk of poor adhesion between aggregates and the tack coat (SABITA-M26, 2006). Opening a road to traffic before adequate adhesion between the aggregate and binder has developed could result in early chip loss and stripping in seals. Poor adhesion development could be a result of dusty aggregates used during seal construction or when seals are constructed during periods of low ambient temperatures. The traffic conditions under which the seal is placed could also grant merit to the use of precoat. High design traffic volume, speeds or high stress areas have shown to be more susceptible to stripping. The use of a precoating fluid could, in these cases, be beneficial by promoting adhesion between the binder and aggregate. Aggregates are sometimes precoated to provide a dark surfacing finish. This is especially common when light coloured aggregates are used and the contrast between the finished surface and the road markings are not sufficient.

3.1.4.5 Primes

Bitumen based prime coats are used when bitumen binders ae applied to a non-bituminous granular pavement layer. Used as a preliminary treatment prior to the application of an asphalt layer of

surfacing seal, the prime coat penetrates the layer to which it is applied while also leaving a small quantity of binder on the surface. The residual binder left on the surface has a few primary functions as listed in the *South African Pavement Engineering Manual (2013):*

- Promotes adhesion between the base and the newly applied asphalt or surfacing layer.
- Allows for water evaporation from the base while inhibiting external moisture ingress into the base.
- Limits the degree of absorption of the binder into the base when the following spray operation commences.
- Binds any fine loose particles present on the surface of the base thus allowing the accommodation of light traffic for a short period of time until the new surfacing can be placed.

Primes should have a low viscosity cutback bitumen or inverted bitumen emulsion with the ability to penetrate a dense, well compacted base layer. Volatiles in prime coats should evaporate and be absorbed quickly so that it is not picked up by the tyres of construction vehicles during the next spray operation.

3.2 Aggregate

3.2.1 Introduction

The term aggregate, in the context of road construction, generally refers to crushed rock but it is not uncommon for other materials to be used. Due to the importance of the underlying base course and the influence it has on the expected embedment, for the purpose of this study, aggregates will be discussed in two categories; seal aggregates and base material aggregates.

3.2.2 Origin

Aggregates used in the road construction industry are usually obtained from quarries in a close proximity to the construction site. The rocks are generally blasted, crushed and sieved to attain the required materials as needed. The type and mineralogy of the aggregates obtained is thus dependant on the geology of the location from which the aggregates were blasted. To establish a broad idea as to the nature of road construction aggregates, the three basic rock types from which all natural aggregates originate will be briefly discussed based on literature (Tarbuck and Lutgens, 2007).

Igneous rocks – formed when molten rock cools and solidifies. They can be further subdivided into two types; extrusive (or volcanic) rock which forms when molten rock cools and solidifies at the surface, and intrusive (or plutonic) rock which forms when magma loses its mobility before reaching the surface and eventually crystallizes. Examples include granite, andesite and gabbro.

Sedimentary rocks – weathering (chemical and mechanical), transportation and deposition of clastic sediments, organic matter and chemical precipitates give rise to sedimentary rocks. The continual deposition, compaction and cementation of the particulate matter occurs at the earth's surface resulting in approximately 75% of the land surface being covered with sediments and sedimentary rock. Examples include sandstone, shale and limestone.

Metamorphic rocks – when existing rocks (igneous, sedimentary or even metamorphic) are placed under extreme conditions of temperatures and/or pressures that are significantly different from the conditions in which they were formed, metamorphism could occur. Metamorphism, which means "to change from", is a process that causes changes in the mineralogy, texture and possibly the chemical composition of rocks, giving rise to metamorphic rock. Examples include hornfels, marble and quartzite.

3.2.3 Base aggregate

In South Africa, the classification system used for unbound granular materials is based primarily on the source of the material and the way in which the material is processed rather than the layer in which the material is used, as is common in other parts of the world (such as the United States). A range of categories are defined for unbound granular materials with the highest quality being defined as a G1 to the lowest quality being a G10. G1 and G2 materials are generally used in base construction, while lower quality materials such as G9 and G10 are used as a subgrade. The material classes between those extremes are used for subbase construction and as needed according to the design requirements on the pavement.

The following descriptions of the various material classes were obtained from a research paper *Stiffness, strength and performance of unbound aggregate material* by Theyse (2002):

Graded crushed stone (G1)

Crushed stone of a G1 quality is obtained by crushing solid, unweathered rock. As a result, all the faces of the aggregate particles will be fractured. Should the gradation require any adjustment, it may only be done using fines produced from the crushing of the original parent rock.

Graded crushed stone (G2 and G3)

These classes of material are obtained from crushing rock, boulders or course gravel. It is required that at least 50% by mass of the individual fractions in excess of 4.75 mm have at least one fractured face. The grading of the crushed material may however be adjusted using natural fines from other sources other than that which is obtained from the crushing of the parent rock.

Crushed stone and natural gravel (G4, G5 and G6)

Materials of these classes can be obtained from natural gravel and boulders that may require crushing. The soaked CBR of the material is then used to determine the classification as being either a G4, G5 or a G6. All the material should pass the 63 mm sieve, and the plasticity index may be adjusted by adding small quantities of cement, lime or sand. Generally, G4 materials are used in base layers while G5 and G6 materials are used in subbase layers.

3.2.4 Seal aggregate

The aggregate is the second major component in any chip and spray seal. Its purpose is to bond with the bituminous binder to form a durable, strong and waterproof surface. The seal aggregate is required to fulfil the following six primary functions as highlighted by Milne (2004) and Greyling (2012):

1. The texture and angularity of the aggregate stone matrix should be of a particular specification in order to provide an adequate skid resistant riding surface.

2. Rock aggregate, naturally, has a degree of resistance to polishing under the dynamic abrasive forces of traffic wheel loads.

3. The aggregates' crushing resistance also allows for wheel loads to be effectively transferred to the underlying pavement structure.

4. The aggregate matrix provides a skeletal structure which accommodates the elastic behaviour of bituminous binders.

5. The aggregate skeleton structure is required to have sufficient strength and voids to prevent the bitumen from flushing to the surface when placed under traffic loading.

6. Additionally, the aggregate also protects the bitumen from the harmful ultra-violet rays of the sun.

3.2.5 Hornfels

Beneath the Earth's surface there are chambers of magma surrounded by rock. The extreme heat from the molten igneous body causes the rocks in the immediate surroundings of the magma chamber to be altered from their original state. This type of metamorphism is known as contact or thermal metamorphism. These altered rocks occur in a zone known as the metamorphic aureole. The size of the magma chamber, mineral composition of the rock surrounding it as well as the availability of water affects the size of the aureole produced. Large aureoles often have distinct zones of metamorphism with high temperature minerals such as garnet forming close to the magma body due to the extreme temperatures. When the rocks surrounding the magma chamber are
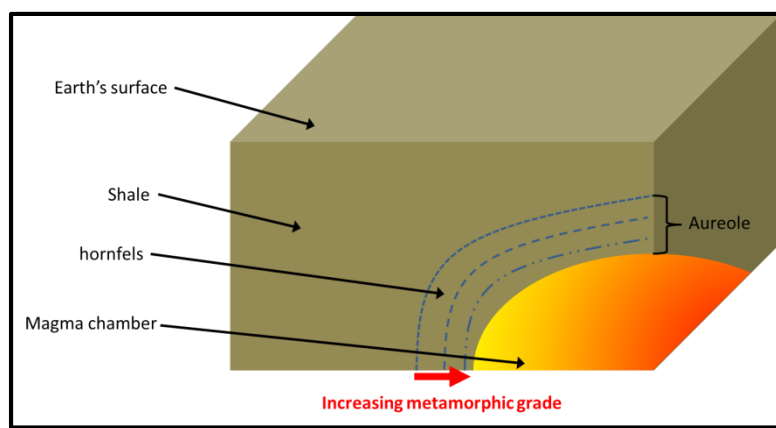
Figure 20: (a) Contact or thermal metamorphism of shale (adapted from Tarbuck and Lutgens 2007), (b) Hornfels

mudstone or shale, the clay minerals in these rocks are effectively baked under the high temperatures from the magma chamber. This results in the formation of a hard, fine-grained metamorphic rock known as *hornfels* (Tarbuck and Lutgens 2007). This process is depicted in Figure 20*(a)*. Other parent materials that could also result in the formation of hornfels include volcanic ash and basalt. Contact metamorphism typically occurs (but is not restricted to) shallow crustal depths where the temperature contrast between an intrusion and the surrounding rock is high while the confining pressure is low. Due to the lack of pressure, these types of metamorphic rocks have crystal particles which are randomly orientated. Hornfels (*Figure 20(b)*) are commonly used as a base course material in South Africa since they display good mechanical behaviour, a property desirable in road construction aggregates (Wang et al, 2011).

4. EQUIPMENT AND TEST METHODS

4.1 Introduction

In this section, the apparatus and equipment used in this study will be discussed. Equipment with standard test methods will not be discussed in great detail; however, some important key points will be mentioned about the test method and its relevance to this study.

4.2 Ball Penetration Test

The standard test method for the ball penetration test forms part of the SANS 3001-BT10 and was first included in the draft *TMH 6: Special Methods for Testing Roads (1986).* Its purpose is to quantify the penetration resistance of a road surface to a standard impact. Data from this test is used to estimate the likely embedment of the seal aggregate into the base layer under service conditions. The ball penetration test is usually conducted on a random basis, or to evaluate specific areas of a pavement where surfacing seals would be applied. Presently, this empirical test method is the only standard method used to estimate seal stone embedment.

Figure 21: Ball Penetration Apparatus

The following apparatus are required when performing a ball penetration test and they are shown in *Figure 21*:

- Standard Marshall Compaction hammer as specified in SANS 3001-AS2: Marshall Flow, stability and quotient.
- 19 mm case hardened steel ball bearing
- Circular tripod with movable cross bar and dial gauge or steel rule (0.5 mm units)
- Thermometer suitable for measuring road or pavement temperatures.

(a)   (b)   (c)   (d)
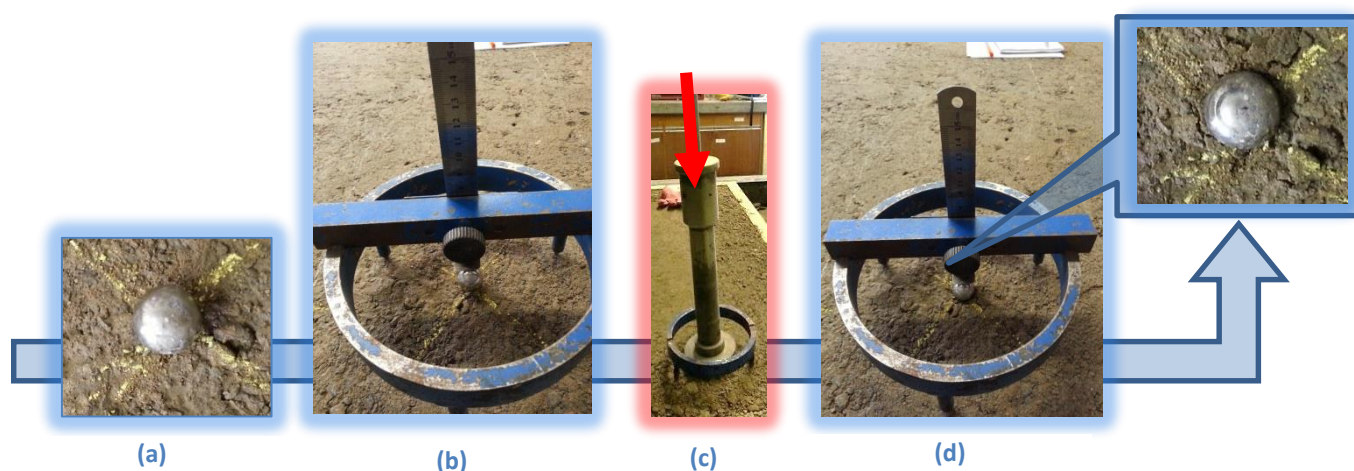
Plate 1: Ball Penetration procedure

48

The test is done by setting the ball on the spot where the penetration is to be measured *Plate 1(a),* and placing the tripod over it and measuring the initial depth (d_1) *Plate 1(b)* Without moving the tripod, the steel rule and cross bar is removed and the Marshall hammer is placed carefully on the ball *Plate 1(c).* The ball is then given a single blow by raising the sliding weight to the top and allowing it to fall. The compaction hammer is then removed and the cross bar is placed back into position The new depth (d_2) is then measured *Plate 1(d).*

The ball penetration can then be calculated as simply the difference between the initial depth and the depth after a single blow of a Marshall hammer rounded to the nearest 0.5 mm:

Ball Penetration = $d_2 - d_1$

There are further adjustments that can be made when testing surfaces which have already been sealed, due to the presence of bitumen and its temperature dependent behaviour. These adjustments are however not relevant in this study since all ball penetration tests will be conducted on the base course before the seal is applied.

Although the ball penetration test does provide a reasonable idea as to the hardness of the surface upon which a seal will be constructed, it does not accurately predict the rate of embedment that can be expected. Embedment is affected by many factors some of which include the type and intensity of traffic; aggregate shape and size; and as this test evaluates, the hardness of the existing surface. All ball penetration tests will be done without using an initial seating blow (as recommended by some practitioners). The very first blow will be taken as **d_1.** It is therefore critical that the ball be placed on a fixed position and will not move while applying the blows.

4.4 Laser Texture Meter (LTM)

Figure 22: Laser Texture Meter (LTM)

The LTM (*Figure 22*) (also known as the Texture Indication Meter) was developed after some seal testing was carried out using the MMLS3, and it became evident that some form of measuring device would be required in order to effectively monitor the surface texture and possibly even the seal stone orientation when placed under a simulated traffic loads (Milne, 2004). If this could be achieved, it would allow for comparative testing to be done using varying seal design parameters. The evolution of the LTM was concurrent to performance tests being investigated by Dr Milne, and it was noted that further work would need to be done to fully develop a prototype, and collate the laser readings to Mean Texture Depth.

Seal Design methods in South Africa (TRH3, 2007) uses the desired surface texture as a definitive design input parameter. The seal design charts available in the TRH3 provide binder application rates based directly on the required texture depth, along with other input parameters regarding the traffic (ELV), base hardness (Ball Penetration) and the aggregate shape (ALD). Additionally, texture depth provides an indication as to the void content in a seal. Milne has noted that the void content is a determining factor governing the performance of a seal, and since the texture depth relates well to the void content, it too can further be related to the performance of a seal. Milne goes on to mention that the measure of rotation and punching of the seal stones would also be of great value in describing the behaviour of the specific seal under varying traffic loading and environmental conditions (Milne, 2004). This study will, on the other hand, attempt to keep the traffic and environmental conditions controlled while varying the seal design parameters in an attempt to investigate exactly what Dr Milne suggested over a decade ago, punching of the seal aggregate into the base.

Milne envisaged the following uses for the LTM along with a few ideas for further development, some of which is now possible with the existing LTM and its data capturing software:

- Determination of Standard Mean Texture Depth (SMTD) and conversion to Mean Texture Depth (MTD).
- Enable skid resistance to be determined cheaply and with a portable, repeatable device.
- Assistance in determining road surface texture for Pavement Management Systems.
- Measuring rutting
  - ✓ Presently possible with the current LTM. Rutting does not require precise high resolution measurements and could easily be measured and observed using the LTM.
- Enable objective (measured) comparison and assessment for seal performance.
  - ➢ This aspect will be incorporated into this study

Milne's ideas for further development:

- Mechanisation of the laser movement along the datum bar.
  - ✓ This was done a few years after the prototype LTM was developed.
- Development of the road texture software to enable convenient plotting of the cross section and texture, as well as developing the algorithms needed to implement conversions of LTM measured texture to the MTD which is obtained from the sand patch test.
  - ➢ Since the development of the LTM, there have been attempts to address this issue. A study was conducted in 2010 on the performance of High Friction Coloured Surfacings (HFCS) to be used as a colouration alternative on the BRT lanes in Cape Town. The study evaluated the performance of HFCS in terms of macro texture, skid resistance, colour retention, and abrasion. Of importance is the method used to evaluate the macro texture or texture depth.

    Two methods were used to evaluate the macro texture:

    -The Austroads Sand Patch Test for performance monitoring in the field.

    -The LTM for laboratory testing using the MMLS3.

The Sand Patch test is done by spreading a known volume of sand or glass beads evenly in a circular patch. The diameter of the circular patch formed is measured at various positions (as shown in *Figure 23*) and using a relationship, the texture depth is obtained. This method is therefore a volumetric approach, using the average volume of sand required to create a certain sized patch to estimate the texture depth.
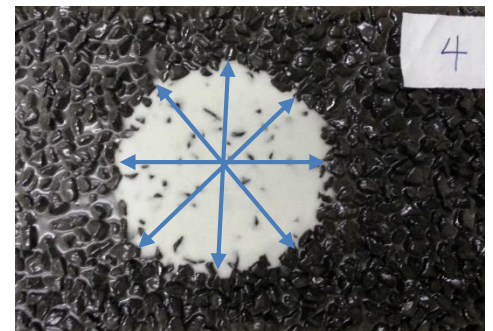
Figure 23: Sand Patch Test measurements

The study thus called for some form of mathematical algorithm using the surface profile data obtained using the LTM to calculate the texture depth. A basic overview of the mathematical formulation used in this study is outlined below.

Referring to *Figure 24*:

- The wheel path was identified from the LTM profile or by measuring the distance from the edge of the sample to the wheel path (while in the MMLS test bed) as shown in (a).
- The data required to plot the wheel path is then extracted and isolated as shown in (b).

- A polynomial regression line of the second order was then fitted where deformation took place, or a linear regression line was plotted.
- The distance between the regression line and the highest peak on the wheel path profile is then taken as the texture depth of the sample.

The texture depth calculated using this method was then compared to the texture depths obtained using the sand patch test on the field tested samples.

(a) **LTM profile of an HFCS Sample**

(b) **Developed wheel path profile from extracted data**
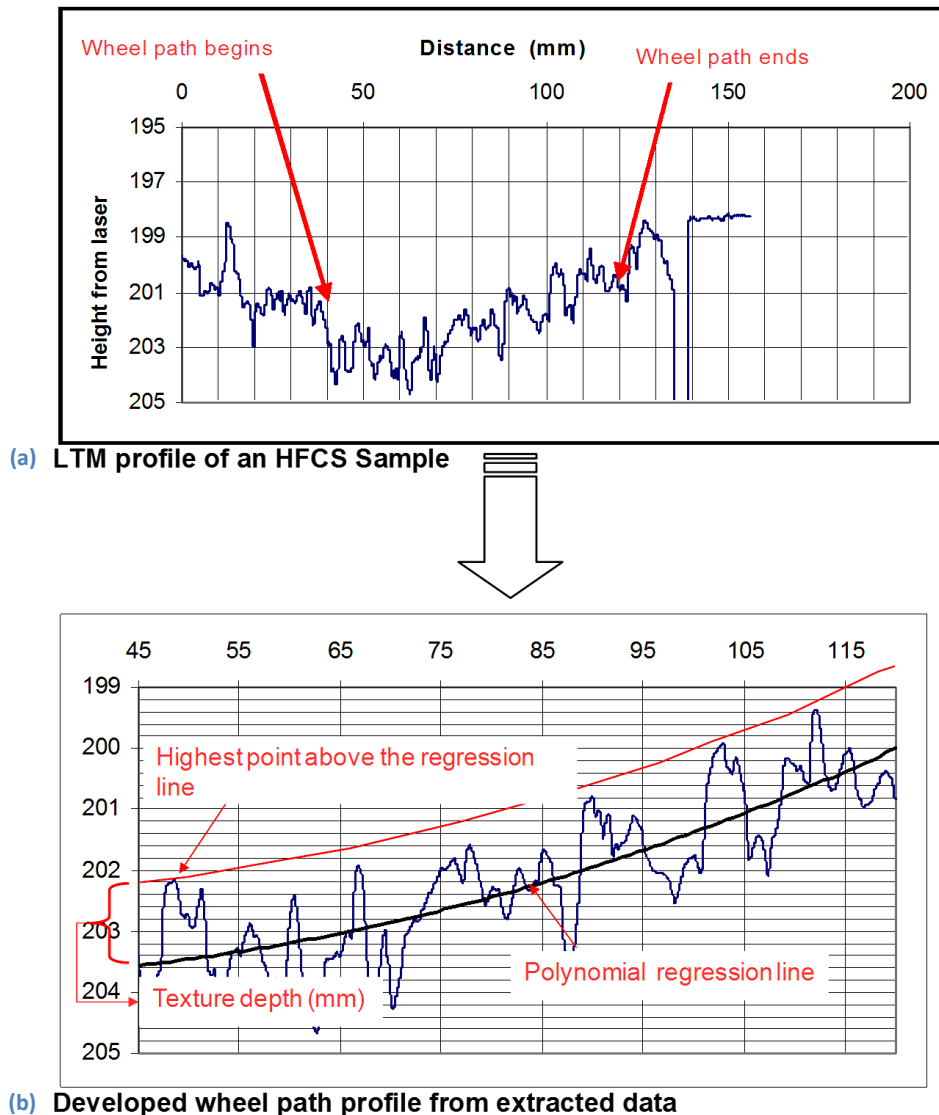
Figure 24: Calculating the texture depth from the LTM data

Essentially, the mathematical formulation used for the LTM data is based on the same principles as the sand patch test, with one major difference, the sand patch apparatus allows many peaks to govern the absolute height of the sand on the surface whereas the LTM formulation only allows a single (the highest) peak to govern the texture volume that is calculated. The LTM also captures a

52

single line with a poor average, whereas the sand patch captures an area with a more reliable average since it uses more peaks to govern the spreading of the sand. The study observed no significant correlation between the sand patch texture depths and the LTM texture depths. This observation is not surprising when the mathematical as well as physical formulation of each method is analysed. Using the LTM data to determine a texture depth accurately is thus still an issue requiring some more refinement before it can be effectively implemented.

The existing LTM system is diagrammatically illustrated in *Figure 25*.
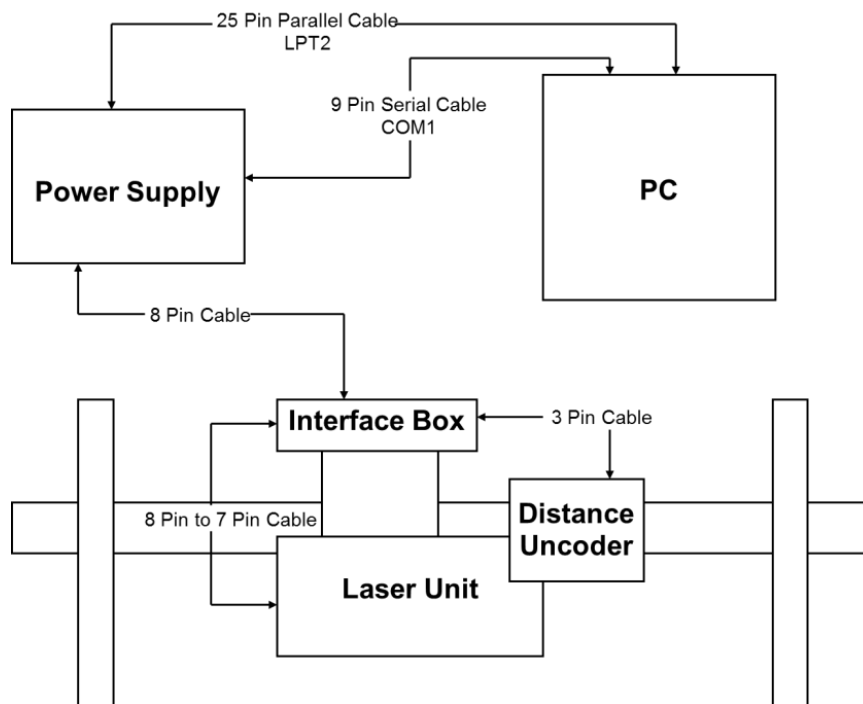
Figure 25: Diagrammatic representation of the LTM component system

The unit consists of the following components:

- Cross-beam of 1.1m
- Detachable feet
- Bracket to attach the laser unit
- Horizontal distance uncoder
- Interface box
- Power supply unit
- 3 connection cables
- Power cable

The bar has two sensors which stop the laser's movement at pre-set points on the bar. The horizontal distance encoder (which at the time of this study was not functional) served an important

53

purpose. The data obtained from this sensor could be used to keep track of the laser's translation by correlating the distance pulses to distance using a known distance. The laser records data continuously and the recording process is independent of the speed of translation. An interface unit is also available for a notebook or PC to be able to read the vertical distance (depth in mm) and the horizontal distance pulses. The software (texture.exe) at present has not been developed any further since the prototype LTM was built and is very basic providing the user with the recorded data in ASCII format (.DAT file) that can be imported to excel. The input ports are fixed to COM1 and LPT2. The power supply unit is used to power the 12V motor that drives the chain system moving the laser across the bar. The scan length of the laser can be adjusted by moving the stop sensors on the rail as required. The software is however only capable of storing 15 000 data points at a time. This translates to approximately 30 seconds of recording time. The sensor unit also has an indicator LED. A red light indicates that the laser is out of range and would not record the depth position, while a green light indicates that the laser is in the centre position which is the ideal position with the most accuracy. No light on the indicator LED means the laser would record data but with a slight risk of an inaccurate reading.

4.5 MMLS3 APT (Accelerated Pavement Tester)

4.5.1 Introduction

Figure 26: Model Mobile Load Simulator 3 (MMLS3)

The MMLS3 (*Figure 26*) is a scaled down heavy vehicle simulator used for accelerated trafficking of model or full scale pavements. The *MMLS3 Operator's Manual (2012)* describes the technical specifications of the machine in great detail, some of which are highlighted below:

54

- The four 300 mm diameter single wheels can typically apply 7200 real wheel loads per hour, at maximum speed of 2.5 m/s which translates to 9km/h.

- The trafficking speed is set using the control box which also serves as the power control and has a meter measuring mileage (in terms of load cycles) of the machine.

- The pneumatic tyres are normally inflated to 700 kPa, but have the capacity to be inflated to 800kPa.

- The maximum wheel load that can be set on the MMLS3 is 2700 Newton (2.7kN).

- With a tyre width of 80 mm, the corresponding footprint area is 34 cm².

- Capable of applying lateral wander (± 75 mm).

Milne (2004) notes that in the hierarchy of performance tests, full scale APT tests simulate reality the closest, but scaled down tests are an economically viable alternative to prioritise the test variables. Literature (van de Ven, Jenkins, 1998) indicates that the MMLS3 is an economically and technically viable testing apparatus for assessing pavements and surfacing performance through the theories of similitude. In the case of seals, where the contact area of the tyre on the seal aggregate is to be examined, the contact stress has similitude and thus reflects a model of reality.

As mentioned previously, the MMLS3 has been used successfully for testing rutting and moisture susceptibility in asphalt. This provides a degree of confidence that MMLS3 testing on seals could indeed hold promise for the future. *The MMLS3 Operator's Mannual (2012)* provides a detailed guideline regarding the use, calibration and maintenance of the machine; key points worth discussing are provided below.

4.5.2 Wheel load application

The 1/3 scale factor in terms of size of the wheel contact area provides a 1/3 × 1/3 area of an E80 tyre. This factor translates approximately to a 1:9 scale factor of area and load, while the contact stress is a 1:1 scale of reality (between 600 and 700 kPa) (Milne,2004). A wheel load of 2.1 kN is thus used as a representation of one wheel of the dual axle wheels on an E80. This wheel load is consistent with previous research using the MMLS3 on seals (Milne, 2004 and Cilliers, 2006).

The wheel load on the MMLS3 is set by adjusting the suspension springs on the bogies (MMLS 3 tyres). The key feature of the MMLS3 which makes its application successful is the design of the suspension system. The design is such that the wheel load is practically independent of the vertical displacement of the wheel. This allows for the wheel load to be set beforehand and as long as it stays within the specified displacement range during operation, vertical displacement of the

pavement surface or the machine frame will not affect the wheel load (MMLS Operators Manual, 2012).

4.5.3 Measuring and setting the wheel load

A calibration unit is provided to aid in setting the wheel load. It is mounted on the channel beam on top of the machine and fixed using two bolts. Each wheel is then moved manually and positioned directly beneath the flange of the calibration unit. With the bogie held firmly in place, the crank on the calibration unit is turned so that the flange moves down, exerting pressure on the bogie. The important step in the calibration process is observing one of the two rubber stoppers on the wheel trailing arms. As the wheel is pushed down, the rubber stopper will move away from the frame of the bogie. The crank is turned until this gap is approximately 10 mm (as shown in *Figure 27*).
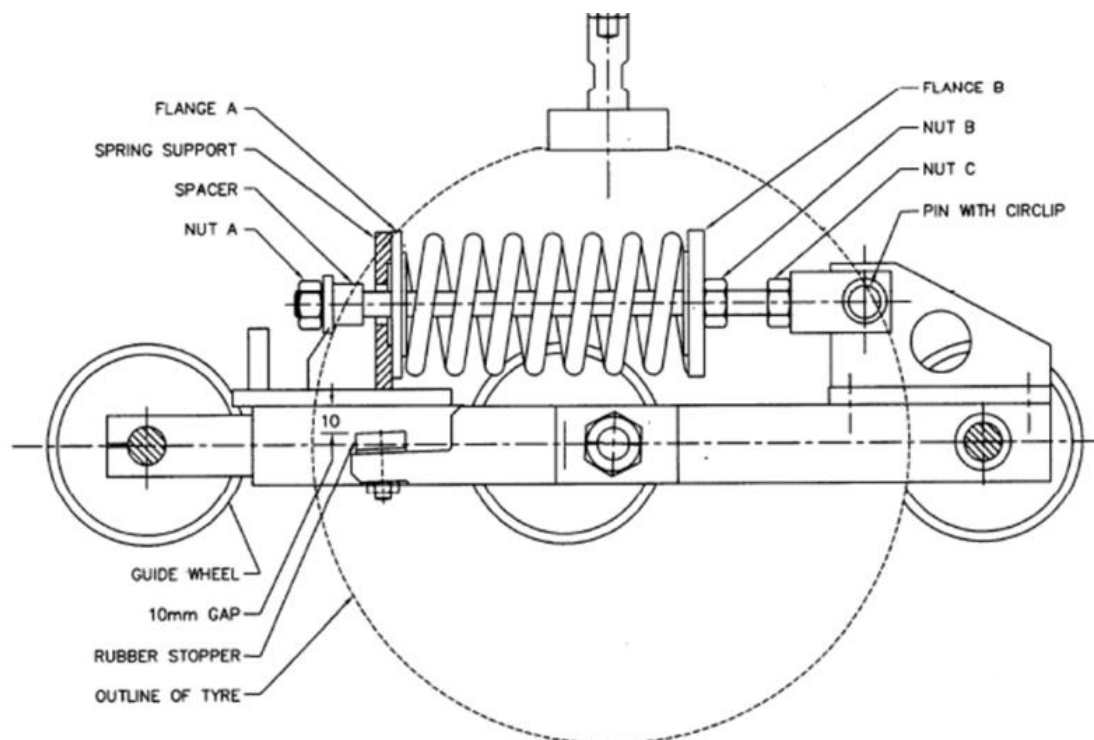
Figure 27: Measuring and setting the wheel load (MMLS3 Operators manual, 2012)

The load is shown on the digital display of the calibration unit. If the load shown is above or below the desired value when the gap between the rubber stopper and the bogie frame is at 10 mm, the load needs to be adjusted. If the load is too low and needs to be increased, the springs would need to be compressed by tightening the lock nuts and rotating the spring clockwise. If the load is too high, and needs to be decreased, the spring should be relaxed by loosening the lock nuts and rotating the spring counter-clockwise. The number of turns of the spring should be carefully monitored and the compression (or relaxation) of the spring should be done in increments of at

56

most 5 mm in length. The second spring is then tightened or relaxed using the same number of turns. The spring lengths should not differ by more than 2 mm. Once this is done, the load is increased until a 10 mm gap is achieved. If the load is still not at the desired value, the number of turns and the wheel load increment can be used to calculate the number of turns required to obtain the desired load.

Once the desired wheel load is obtained (in the case of this study, 2.1 kN as shown in *Figure 28*) this process can be repeated for the other bogies.

Figure 28: Measuring the wheel load using the MMLS3 load cell
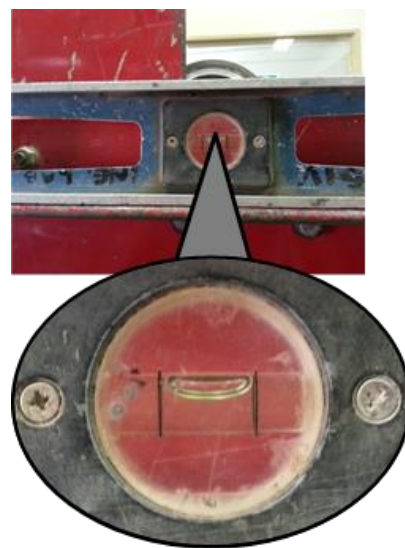
Plate 2: Checking that the MMLS3 is level

The importance of the 10 mm gap between the rubber stopper and the bogie frame comes into play when setting the machine in place for testing. The MMLS3 has four legs that can be adjusted independently of each other, this allows for the machine to stand levelled on an uneven surface or pavement. Once the machine is in place, the first step would be to ensure that the machine is level. This can be done using the bubble level on the machine or using a straight edge bubble level. The legs are adjusted accordingly until the correct level is achieved (horizontally as well as laterally) as shown in *Plate 2*. Once the correct levelling of the machine has been established, all the legs are cranked upwards or downwards until the 10 mm gap between the rubber stopper and the bogie frame is observed when the wheel is on the surface to be tested. The wheel system can then be rotated so that each bogie is checked for the 10 mm gap. A spacer is provided for convenience and

should fit snugly between the rubber and the frame. Once this is done, the machine is calibrated and is ready for testing.

4.5.4 Lateral wander

As previously noted, the MMLS3 wheel system is capable of moving laterally. This allows for the wheel loads to be spread laterally from the centre line of the wheel track on the pavement as shown in *Figure 29*. The maximum lateral displacement is 75 mm on either side of the centre line and with the wheel width of 80 mm provides a total maximum track width of 230 mm. The lateral wander system is applied to achieve a normal distribution, and thus spends more time near the centre line of the track than at the edges. Displacement takes place at constant intervals of 25 seconds while the increments are varied to achieve a normal distribution (MMLS Operators Manual, 2012).

Lateral wander will not be used in this study. Channelised traffic, as noted by Milne (2004), will facilitate the concentration of the applied load which would equate to anywhere between 1.5 to 3 times normally distributed traffic.
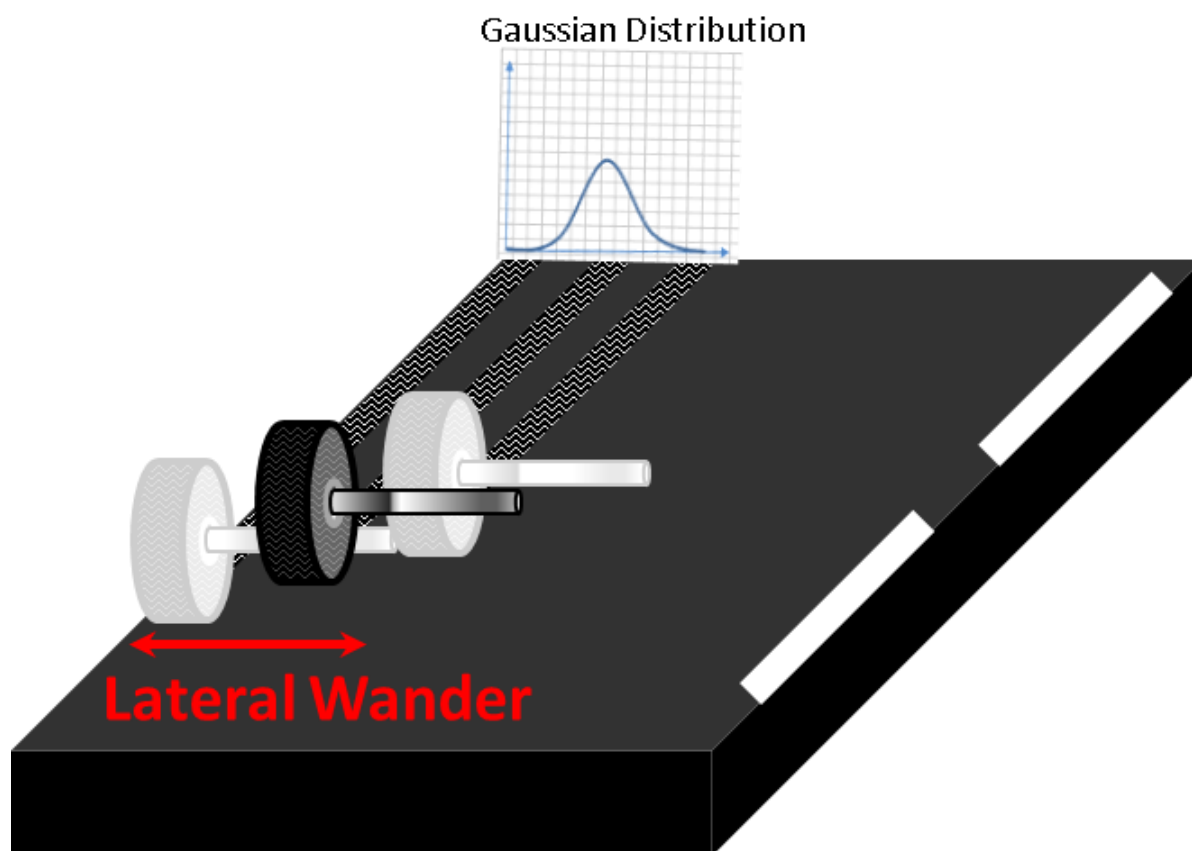
Figure 29: Concept of lateral wander

5. RESEARCH METHODOLOGY

An outline of this chapter is provided in *Figure 30* below:
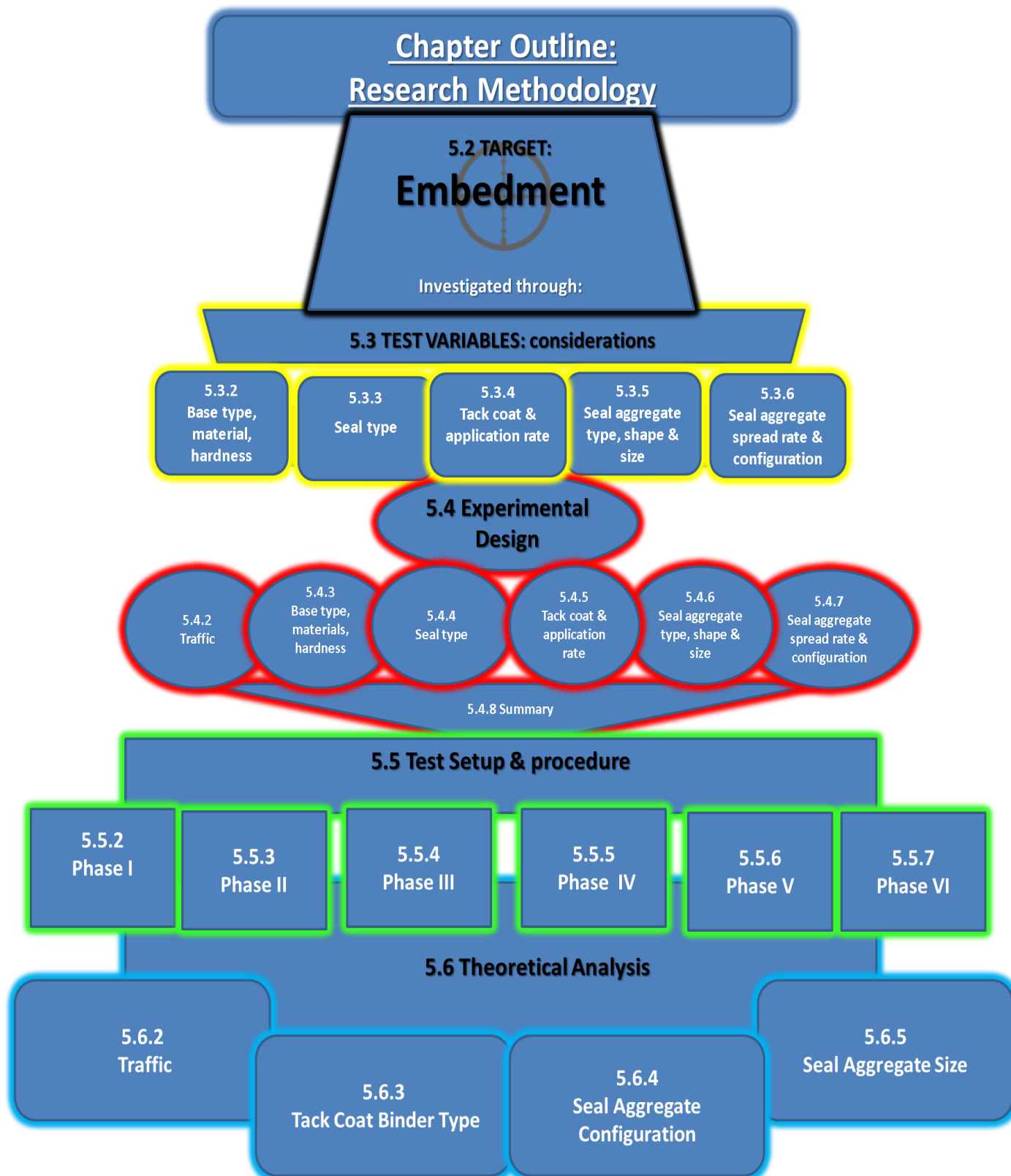
5.1 Introduction

In order to obtain a successful protocol for MMLS testing on seals, for any given failure mechanism there would be a necessity for the collection of a wide range of test data. The data would need to describe the component as well as performance variables affecting the failure mechanism, and provide benchmark values for the number of loading cycles required for the failure to manifest under certain conditions. Since this study aims to be the groundwork for the protocol, the data that will be gathered will be steered by what is required in the seal construction industry, while attempting to condense the testing requirements to fulfil a Masters Research project.

This section will build on *Section 2.3.2* as well as *Section 2.7* and will describe in detail the test variables that will be manipulated in order to obtain useful data regarding parameters that influence seal stone embedment. Due to the practical nature of this experiment and the possible influence it could potentially have on seal design practice, advice was sought from Gerrie van Zyl (2014), an experienced practitioner of seal design and construction. Van Zyl, having decades of experience working with seals, has provided valuable insight into the component variables that would most likely provide the greatest wealth of data for the failure mechanism that will be investigated and his input made a large contribution to the processing and direction of this section.

5.2 Target Failure Mechanism: Embedment

As discussed in *Section 2.3.2*, excessive embedment of the seal aggregate into the base will have undesirable effects on skid resistance. This can be attributed to the loss of texture due to the loss of voids accompanied by the bleeding of the binder. The mechanism refers to the gradual immersion of the aggregate into the underlying road surface through the action of traffic. The degree of embedment that would manifest would be largely dependent on two key factors; the type and intensity of traffic, as well as the hardness of the underlying surface (Cilliers, 2006).

As mentioned in *Section 2.3.2,* a certain degree of embedment is required during the construction of a seal. This initial embedment would allow the stone to be held in place during the spraying of the binder and would also facilitate the prevention of early whip-off once the road is opened to traffic. Excessive embedment would however be detrimental to the serviceability of the seal by decreasing the voids causing bleeding of the binder. This would in turn result in fattiness and texture loss on the riding surface.

The gradual process of embedment is said to approach equilibrium after a certain time or load cycle period, affected largely by the traffic conditions. Hanson's approach dictating the mat thickness that

equals the ALD of the stone would see embedment as the ALD minus the depth of the stone layer above the average road substratum Cilliers (2006).

The concept is illustrated graphically in *Figure 31* below.
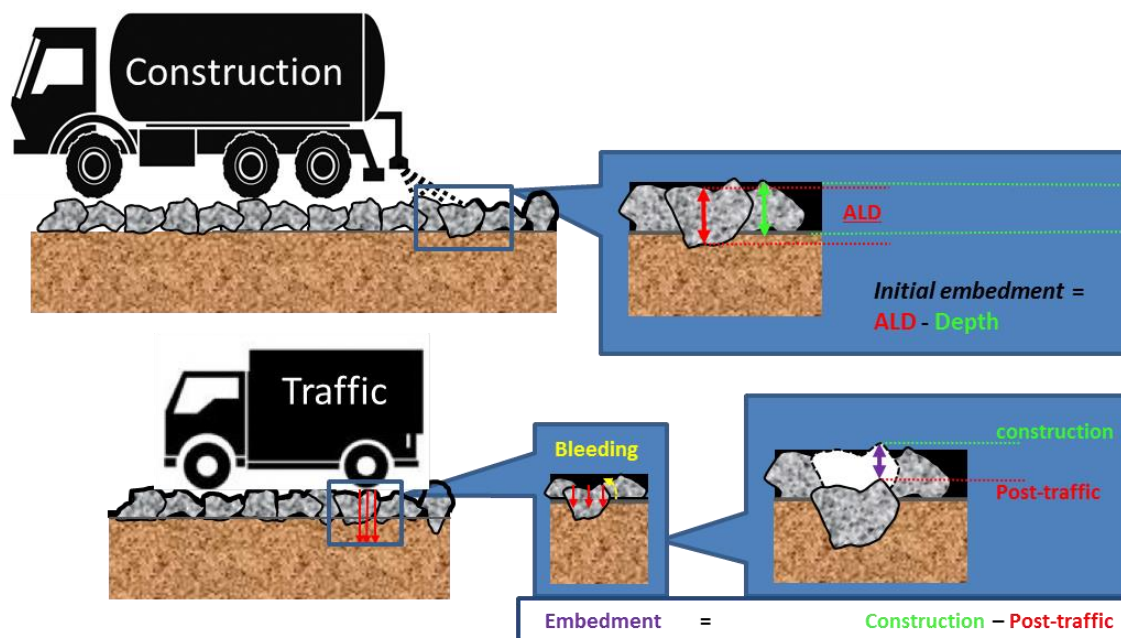
Figure 31: Concept of seal stone embedment

5.3 Test variables: Considerations

5.3.1 Introduction

Due to the wide variety of variables that require consideration when designing and constructing seals, giving attention to all of them would not be possible, let alone feasible. This is beyond the scope of this study. Bearing in mind that the aim of this research project is to be the groundwork upon which further studies can be done, the seal design process is examined and the variables scrutinised. Emphasis will be placed on the testing procedure using the equipment available (discussed in the previous section) to establish if the test method could provide quality data about seal stone embedment. Since the testing procedure would require much thought along with some trial and error, the focus will not be to have a very large experimental matrix. This would allow for detailed testing to be done on a few samples as opposed to less data on a larger number of test samples. If the testing procedure proves to be of value, further research can be done by broadening the experimental matrix. This will be discussed further later in this section.

The variables directly affecting embedment were carefully considered, along with the fact that the construction process would need to be modified so that it could be done on a much smaller scale i.e.

in a laboratory environment, while still being representative of seal construction practice. With van Zyl providing insight as to the needs of the seal construction industry, the following factors were carefully considered.

5.3.2 Base type, material, and hardness

The base serves as the primary structural layer of sealed pavement structures. As mentioned, the seal does not act as a structural layer, and is therefore expected to effectively transfer the forces of traffic to the layer beneath it while serving as a waterproof skid resistant riding surface. In practice, the base material selection is largely based on the aggregates available within the location of the construction site. Due to the large volumes of aggregate required for road base construction, materials are usually sourced from quarries that in close proximity to the site reducing transport costs. For the purpose of this study, a similar approach will be followed. Aggregate will be sourced from the nearest quarry that provides high quality G2 type material.

Research by Gerber (no date) makes mention of the upper regions of the base holding the most influence on the embedment behaviour of a seal. Of particular importance in this study will therefore be the resulting hardness of the upper portion of the base. It is this region of the base that affects embedment the most and obtaining consistency will be an important challenge to overcome. Quantifying the hardness of this upper region of the base will be done using the ball penetration test. This empirical test method will provide valuable insight as to the surface hardness, and is used widely in practice.

In practice, the construction of a high quality base is regulated stringently. And the materials used must be according to strict specifications. The subbase upon which the base layer is compacted should be well levelled and stabilised to provide the anvil required to attain the degree of compaction required. The spacing of the truck loads to be stockpiled in the middle of the road should be carefully calculated and planned so that the required compacted layer thickness can be obtained. The completion of a G1 quality base is attained through a process known as slush-compaction (Kleyn, 2012). The basic concept of slush-compaction involves using water with a sufficient amount of compaction energy to effectively expel fines from the base course. As the fines are expelled the density increases leaving behind an aggregate matrix with a maximum degree of particle interlock. Research done by Roelofse (2014), concurrently with this study, investigated the importance of slush compaction.

As noted by Roelofse (2014), achieving a particular base hardness within the confines of a laboratory presents a challenge in itself. Reliable compaction methods would need to be established in order to

construct a base that is within the specifications of a G2 base. Industry construction methods would need to be carefully analysed and a reliable method would need to be proposed and tested using the ball penetration test to establish if the method is effective or not.

5.3.3 Seal type

The selection of the appropriate seal type is based largely on the experience of road authorities and practitioners of seal design and construction. For surfacings on newly constructed roads, the most important influencing factors, which will perform well under specific situations, are provided in the TRH3. A process is then provided whereby inappropriate surfacing seal types are eliminated. It is important to note that this is but a guideline, and in no way ensures the success of a particular type of surfacing for a given scenario. This is most likely due to the inability to fully capture and predict the conditions under which the seal will be placed during its serviceable life. The TRH3 (2007) discusses the selection of appropriate surfacing seals under the following headings:

- Traffic volume
- Traffic actions
- Gradient
- Maintenance capability
- Surface texture required
- Construction techniques
- Environmental conditions
- Quality of the base
- Special conditions
- Initial cost basis for comparison

As can be seen, many of the influencing factors as mentioned in *section 2.2.3* are taken into account during the selection of the appropriate seal type. Of particular importance to this study is the guideline provided in the TRH 3 (2007) for construction techniques. The following extract is taken directly from the TRH 3 (2007) *section 4.3.7 Construction techniques*:

"Although seal construction techniques are basically the same, irrespective of the type of seal, the experience of the construction team should be taken into consideration in the selection of the seal to be used. Also, some types of seal are also more 'forgiving' than others, lending themselves more readily to the construction of an acceptable quality wearing surface."

63

Since the construction techniques referred to in this section of the TRH3 will not be applied in this study, it will be important to select seal types which will be constructible, given the small scale to which the seals will need to be constructed in a laboratory environment.

The three basic steps of seal construction i.e. spraying of the bitumen, spreading of the aggregate and roller compaction of the aggregate should be replicated as closely as possible, so that the resulting seal can be considered a good representation of seals constructed in practice.

5.3.4 Tack coat and application rate

The tack coat is a thin bituminous layer used to bind the seal stone matrix together so that the seal exhibits a mat like behaviour. The tack coat also provides a waterproof layer protecting the base from moisture ingress. Various types of bitumen and bitumen emulsions are used as tack coats for seals, and the choice of tack coat is made based on the various elements like climatic conditions, traffic speeds, road geometry etc. The application rate of the tack coat is based on the aggregate shape, spread rate, as well as the required texture depth. Flaky aggregates would require less stones (by mass) to cover the same area as less flaky angular stones. Flaky aggregates also have larger surface areas that require coating to prevent whip-off as opposed to less flaky particles. The void content would also decrease with an increase in flakiness. These are important considerations since voids are required to prevent fattiness and bleeding of the tack coat.

Figure 32: Tack coat application in seal construction (van Zyl, 2015)

The application method for the tack coat would need to be well thought out. In practice, construction vehicles designed for this purpose systematically drive and spray the tack coat as shown in *Figure 32*, followed closely by the truck pouring the seal stones (*Figure 33*) before it is finally compacted providing the required initial stone embedment and reorientation. This process will prove challenging to replicate on a small scale. The binder cools

Figure 33: Aggregate application in seal construction practice (van Zyl, 2015)

rapidly after spraying, allowing only a small window to effectively spread the aggregate and compact it. Should the binder temperature decrease too much before the stone is applied and compacted,

the adhesion between the binder and the stone surface would be negatively impacted. Although the binder aggregate adhesion does not affect embedment as much, it is important to achieve representative test samples. Spraying the tack coat alone could prove to be challenging. An alternative method would possibly need to be applied. This alternative application method would, however, still need to capture the essence of seal construction in practice.

5.3.5 Seal aggregate type, shape and size

The stone type generally used in practice would depend on the types of aggregate in the vicinity of the construction site to minimise transportation costs. The stone type would need to have sufficient resistance to crushing and polishing while also have the appropriate mineralogy and more specifically the appropriate charge when the seal is constructed using emulsions.

As mentioned previously, the aggregate shape and size would affect the degree of embedment. Aggregate properties such as the particle angularity may affect embedment directly through the force distributions in the particle and stress concentrations at the seal-substrate interface. There is not much information to provide insight into the particle size and how it relates to embedment. Read & Whiteoak briefly mention that smaller aggregate sizes could lead to early embedment. This phenomenon would still largely depend on the type and intensity of traffic and the resulting failure occurs when the binder fills all the available voids in a seal causing bleeding (Read and Whiteoak, 2003). Larger aggregate types are generally used for heavier traffic loads due to the fact that they have a higher void content and thus allows for more space for the binder to flow when the void content decreases as a result of embedment.

As can be seen, the existing literature does not provide much clear evidence of the influence of aggregate shape or size on the degree of embedment, the selection of the stone size based rather on the traffic scenario which is said to be the largest factor influencing embedment.

5.3.6 Seal aggregate spread rate and configuration

The TRH 3 discusses the aggregate spread rate rather briefly. It is indicated that the aggregate should be applied at a rate that would achieve a complete and uniform mosaic, with all the design assumptions based on the aggregate particles lying shoulder-to-shoulder, in a single layer and in a tightly knit pattern. (TRH3, 2007) It is further highlighted that a spread rate which is too high or too low could exhibit undesirable characteristics during its serviceable life. Some of these include ravelling of the seal if the spread rate is too low and whipoff of the bonded aggregate due to excess aggregate being forced into the seal mat.

Specifications governing the aggregate spread rate are not provided in the TRH3 (2007) since the ideal spread rate may vary based on various factors such as the aggregate properties, seal purpose and even the designer's personal preference. The images alongside are however provided (*figure 30*). They display the approximate aggregate spread rate for the two typical configurations: dense shoulder-to-shoulder and open shoulder-to-shoulder matrices and are based on a flakiness index of 15 percent (TRH3, 2007). The configuration is thus determined visually, and would be either one of these basic configurations.

Embedment of the stone could possibly be affected by the two different configurations since the open shoulder-to-shoulder configuration *Figure 34*(a) sees the bitumen as the continuous phase with the seal aggregates dispersed in it. Movement of the stones would thus be governed by the adhesion of the stone particle to the bituminous tack coat as well as the stiffness of theselected binder. Dense shoulder-to-shoulder mosaic *Figure 34*(b) would allow the stones to transfer forces to each other since they are closely knit. The tight packing of the stones would also decrease the space available for the stones to move, and the movement of the stones would essentially be governed not only by the binder, but by the aggregate strength and resistance to abrasion and crushing. The interaction of the seal aggregates with each other as well as the behaviour of the seal as a whole would thus be governed by the spread rate and configuration of the aggregate and could therefore also affect the degree of embedment that would manifest.

(a)

(b)

Figure 34: (a) open shoulder-to-shoulder and (b) dense shoulder-to-shoulder configurations (TRH3, 2007)

5.4 Experimental Design

5.4.1 Introduction

Based on the considerations discussed in the previous section, the experimental matrix has been identified. Since this is the first study which would attempt to quantify embedment through comparative APT testing, the focus will be placed on ensuring the testing procedure is reliable and repeatable. Furthermore, emphasis will be placed on doing a number of repeat tests as this would provide insight as to the level of repeatability of the experiment and could ensure better confidence in the data acquired. Once a test method is established, the experimental matrix can be extended to

gather more data in the future. For the purpose of this study, uncontrollable factors such as climatic conditions and traffic scenarios will not be considered as test variables. Instead, these will be kept consistent allowing seal design variables to be the focus.

The number of possible test variables worth considering is countless. With the help of van Zyl (2014), who provided insight as to what could presently be beneficial for the seal construction industry, the following test variables are identified and deemed appropriate for the purpose of this study:

5.4.2 Traffic

In this study, a load of 2.1 kN was chosen as a representation of one of the dual axle wheels of an E80. The tyre inflation pressure was also fixed at 700 kPa since the typical inflation pressure of an E80 is usually between 600 and 700 kPa. Previous researchers using the MMLS3 on seals used a similar configuration as mentioned in *Section 4.5.2*. Since the contact stresses at the tyre seal interface would directly influence the degree of embedment, a conservative choice is made to use the higher end of the typical range i.e. 700 kPa. A total of 100 000 load cycles will be applied to each seal sample.

The TRH3 specifies that single seals can accommodate 750 to 2000 elv/lane/day, increasing up to 2000 to 5000 elv/lane/day with the use of modified binders. The TRH3 also specifies the following expression to calculate traffic volume:

ELV = L + 40 × H

> Where:
>
> L = number of light vehicles / lane / day
>
> H = number of heavy vehicles / lane / day

The equivalency factor of 40 is deemed an acceptable one for use as a conversion from heavy vehicles to their equivalent light vehicles.

Based on this information, and using the upper limit of the traffic volume allowance for single seals, the life expectancy of a single seal can be estimated as follows:

2000 elv/lane/day (in the case of conventional binders)

= 730 000 elv/lane/year

= 18 250 HV/lane/year

Five years of traffic would thus be equal to 91 250 HV/lane.

Table 10: Measurement intervals and time equivalents using 2000 elv/lane/day as the traffic forecast

Thus, 100 000 load cycles would translate to over 5 years of traffic on a single seal. Furthermore, this can be increased based on the fact that the traffic would be channelised and the effect of lateral wander (as in practice) is not simulated. Milne (2004) indicates that this effect of channelised traffic could lead to an even further conservative factor of up to 3.

Reading number	Load cycles	Time equivalent (2000 elv/lane/day)
1	0	Construction
2	100	2 days
3	500	10 days
4	1000	20 days
5	5000	100 days
6	10 000	200 days (± 6 months)
7	25 000	500 days (± 1 year 4 months)
8	50 000	1000 days (± 2 years 9 months)
9	75 000	1500 days (> 4 years)
10	100 000	2000 days (> 5 years)

The seal profile will be measured at various intervals during the 100 000 load cycles. *Table 10* details the intervals that were selected along with an estimate as to the approximate time equivalent.

Due to the lack of effective roller compaction equipment, the seal stones are expected to reach their initial construction embedment during the early stages of MMLS trafficking. The TRH3 (2007) assumes an initial embedment of half the embedment potential that is established using the Ball Penetration test for design purposes. In order to effectively approximate the point at which the initial embedment has been reached, the readings taken during the beginning of the trafficking phase are done more frequently. The initial movement of the stone can thus be monitored in greater detail allowing for a more accurate estimation of the initial embedment. This will be discussed in more detail in the analysis phase of this study.

5.4.3 Base type, material and hardness

Due to the precise construction requirements and methods (slush-compaction etc.) required to successfully obtain a high quality G1 base layer, it is highly unlikely that G1 base layer will be constructible (feasibly) within the confines of a laboratory using the equipment available. For this reason, the aim is to attain a G2 quality base layer using the vibratory roller system available in *Stellenbosch University's Fred Hugo MMLS Lab*. The material used to construct this layer will therefore be of a G2 type material adhering to the Fuller curve requirements for a G2 material. The hardness of the base layer will be assessed using the Ball Penetration test. Once the layer is effectively compacted and the moisture content reduces to at least 50% of OMC, the surface will be primed using MC10 at an application rate of 0.8 ℓ/m^2.

5.4.4 Seal type

Since this study would be one of the first that aims to quantify a failure mechanism and comparatively analyse the influence of selected seal design parameters using an APT, it would be logical to begin with the most basic seal type i.e. a single seal. This would allow other design parameters to be investigated in more detail.
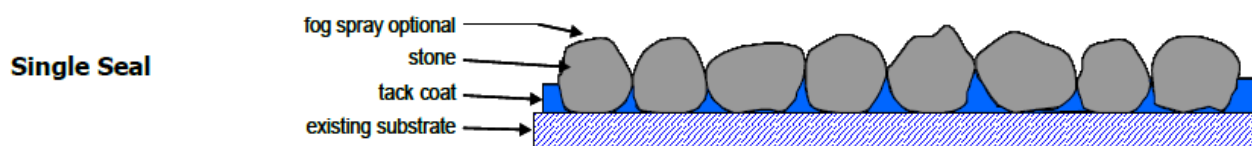
Figure 35: Single Seal (TRH3, 2007)

Figure 35 shown above depicts the basic structure of a single seal. Being the most basic seal type, it consist of a single layer of seal aggregate laid on top of a tack coat and sprayed with a bituminious cover or fog spray layer. In this study, a common cover spray with the same application rate will be used on all the seals constructed. This will help prevent aggregate loss and its application is common practice with newly constructed seals. Stone loss usually occurs at high traffic speeds and the since the maximum trafficking speed of the MMLS3 is a mere 9 km/h, the cover spray will be a diluted (50/50) spray-grade cationic emulsion applied at the lowest rate specified in the TRH3 0.8 l/m^2.

5.4.5 Tack coat and application rate

There are various types of bitumen used as tack coats in practice. Four different types will be tested:

- Conventional 70/100 Penetration Grade (pen 70/100)

- 70/100 Penetration Grade modified with SBS polymer applied to precoated aggregate (pr.SE-1)
- Cationic spray grade bitumen emulsion (CAT65)
- Elastomer (SBR latex) modified bitumen emulsion (SC-E1)

The inclusion of polymer modified binders as part of the experimental matrix formed part of the recommendations by van Zyl (2014). This recommendation is reinforced based on literature found on the use of bitumen rubber in spray seals as mentioned in *Section 2.3.2.*

The application rates used will vary according to the aggregate spread rate and stone size. A standard application rate of 0.8 ℓ/m^2 will be used for the dense shoulder-to-shoulder configuration and will be maintained for each bitumen type. This means that for the same test variables, the tack application rate will be the same for each bitumen type. It should however be noted that in the case of emulsions, the application rate would need to be adjusted (increased) based on the net cold binder. The volume of emulsion applied would be higher compared to hot binders since the emulsion has a certain amount of water present. Once the emulsion breaks and the water evaporates, the binder left behind would be the net cold binder. Essentially, the volume of net cold binder applied, in the case of emulsions, should be the same as the volume of hot applied binder.

Additionally, the application rate applied should be adjusted according to the stone size as well as stone spread rate. Larger stones would typically require a higher binder application rate to ensure effective adhesion. The void content is higher when using larger stones allowing more space for the binder to fill before bleeding would occur. The increase in application rate will be governed by the ALD and the adjustment calculations are detailed in *Appendix A1*.The application rate adjustment for the aggregate spread rate can also be found in *Appendix A2*, and is determined using an experimental method governed by the aggregate wetted height. These adjustments will be based on the standard application rate of 0.8 ℓ/m^2 for the 13.2 mm dense shoulder-to-shoulder configuration.

All tack coats will be applied at the application temperatures recommended by the manufacturer. The product data sheets can be found in *Appendix C* for information purposes.

In the case of polymer modified SE-1, the aggregate will be precoated. This is common practice when using polymer modified hot binders and will ensure better adhesion of the aggregate to the binder. Additionally, all the seal tiles will be sprayed with a cover coat. This will ensure the aggregate particles are effectively bound together and will minimize the risk of stone loss. Cationic spray grade emulsion diluted (50:50) with water will be used as the cover spray. This was recommended by van Zyl (2014), the very same recommendation can be found in the TRH3 (2007).

5.4.6 Seal aggregate type, shape and size

As in the case of seal construction practice, the aggregate type was selected based on what could be sourced locally i.e. Hornfels. Hornfels is found in abundance in the Western Cape and surrounding areas and are thus commonly used as a road construction material.

The ALD and flakiness index of the material obtained will be assessed (*Appendix B2* and *B3*). These will not be variables, but are important material properties which could influence embedment. The information found would then be documented and used as part of the determination of the required binder application rates.

Two aggregate sizes will be used:

- 13.2 mm
- 19 mm

13.2 mm aggregate is typical in the case of single seals. Despite 19 mm stone being uncommon in single seal construction due to the noise generated, the increased void content could provide important information regarding embedment and its relation to an increased void content and is thus included as a test variable.

5.4.7 Seal aggregate spread rate and configuration

Seal design in South Africa is based on the guidelines, recommendations and specifications provided by the *TRH3: Design and Construction of Surfacing Seals (2007).* In this best practice guideline it is noted that the binder application rate is highly dependent on the aggregate spread rate. This can be rationalised by the fact that in the case of cubical aggregate particles, theoretically, the more closely packed the particles are, the lower the void content will be. Consequently, the amount of binder that can be accommodated in the seal will decrease and the possibility of bleeding would effectively increase. It is then further noted that the general belief is that the first layer of single sized aggregate should lie "shoulder-to-shoulder". This term, however seems to differ for the various road authorities within SA. The ideal spread rate, according to the TRH3, will depend on the specific aggregate and should finally be determined on site by spreading the aggregate to obtain the desired matrix and then measuring the bulk volume used to cover a specific area.

Using the concepts highlighted in the TRH3 (2007) regarding the aggregate spread rate and configuration, the following configurations were decided upon:

- **Dense shoulder-to-shoulder packing.**

This configuration would see a larger volume of aggregate spread across the seal tile area that would be constructed. The aggregate particles should be closely knit and have many contact points.

- **Open shoulder-to-shoulder packing**

This configuration would see a lesser volume of aggregate spread across the seal tile area compared to the dense shoulder-to-shoulder configuration. The aggregate particles should still be touching each other, but the packing would not be as tight as with the dense shoulder-to-shoulder configuration. The use of this configuration will be limited to the typical 13.2 mm aggregate size. This would provide at least some degree of insight as to the effects of the differing aggregate spread rate configuration on embedment.

As recommended in the TRH3, the volume of aggregate to be applied will be determined visually. However instead of using the bulk volume, the mass will be used. This seems appropriate since the amount of aggregate that will be used on each tile will be considerably less, and a greater degree of accuracy will be achieved using the mass of the aggregate as opposed to the bulk volume.

The photographs below show the three configurations that were deemed reasonable to represent the spectrum of variables related to the aggregate configuration: 13.2 mm dense sh-sh *Plate 3(a)*, 13.2 mm open sh -sh *Plate 3*(b) and 19 mm dense sh-sh *Plate 3*(c), sh-sh being "shoulder-to-shoulder" as it will now be referred.

| (a) | (b) | (C) |

Plate 3: (a) 13.2 mm dense sh-sh, (b) 13.3 mm open sh-sh, (c) 19 mm dense sh-sh

Aggregate particles were packed and arranged in such a way that they were laying on the plane with the ALD perpendicular to the surface. This provided the best packing and corresponding mosaic and ensured a degree of consistency between the three different configurations as shown above. The

mass of aggregate used to achieve these configurations were then measured and used for all the seal tiles constructed.

5.4.8 Experimental design summary

Base Hardness[b]	Binder type (tack)	Binder Application rate[b]	Stone size	Spread configuration
Low (out of spec)	Pen 70/100	Low	13.2mm	Dense sh/sh[a]
				Open sh/sh[a]
			19mm	Dense sh/sh[a]
	S-E1	Low	13.2mm	Dense sh/sh[a]
				Open sh/sh[a]
			19mm	Dense sh/sh[a]
	SC-E1	Low	13.2mm	Dense sh/sh[a]
				Open sh/sh[a]
			19mm	Dense sh/sh[a]
	CAT65	Low	13.2mm	Dense sh/sh[a]
				Open sh/sh[a]
			19mm	Dense sh/sh[a]
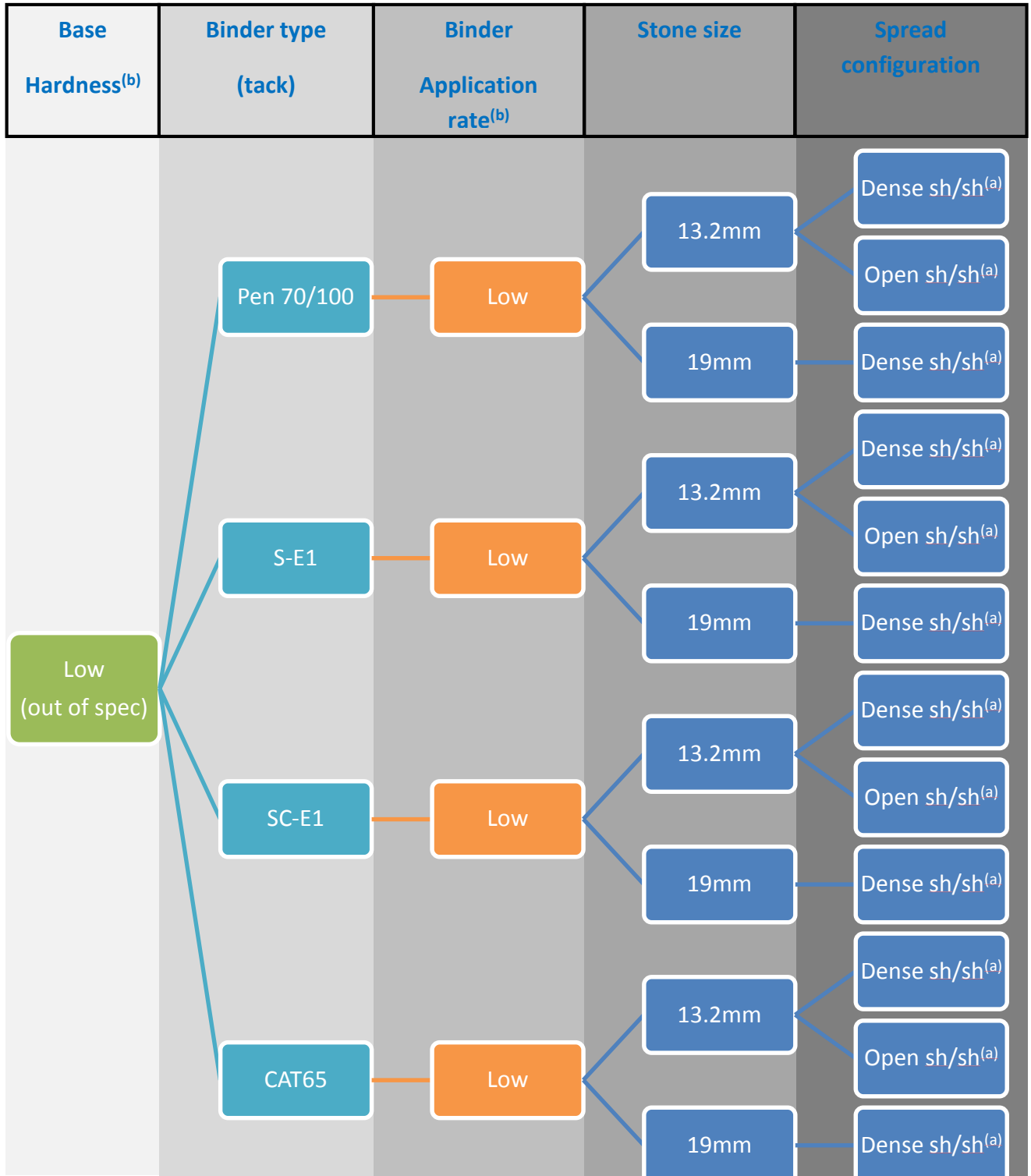
Figure 36: Experimental design summary

[a]refers to 'shoulder-to-shoulder'

[b]These mark variables which were initially included as part of the experimental matrix but were subsequently excluded due to time constraints. These would be good places to start if the expansion of this matrix is considered in the future.

5.5 Test setup and procedure

5.5.1 Introduction

As previously noted, constructing seals within the confines of a laboratory presents various challenges due to the scale of the construction. Methods used in practice will not be applicable, and alternative methods for the construction of seals needed to be employed. This section will detail the procedure followed in this study using the equipment and following the test methods discussed in *Section 4*.

The experimental setup and procedure detailed in this section is divided into various phases, which highlight chronologically how the procedure was developed and implemented. In order to develop a standard test protocol, the testing procedure should be repeatable. With this in mind, and since this would be the first attempt at investigating embedment using the MMLS3, the procedure followed is detailed fully with the relevant results summarised with additional detail provided in the appendices.

5.5.2 Phase I: Pre-construction investigations, preparation and testing

The following investigations and tests are conducted prior to construction. The information obtained is then used in the subsequent phases of the testing procedure.

5.5.2 (a) Base Material: G2 Hornfels
Sieving the base material

All the material used in the base was passed through a 19 mm sieve. This would ensure that all stones in the base are at least of a smaller fraction than the largest seal aggregate size. The material obtained from the sieving is then crushed and blended with the virgin material. This blend is then used to construct the base course.

Optimum Moisture Content (OMC) and Maximum Dry Density (MDD)

The OMC and MDD is determined using the standard test method A7 provided in the TMH1 (1986):

This method would yield the moisture-density relationship of the material from which the moisture content required to obtain the maximum dry density can be determined. This information is of vital importance during the base construction and would provide an indication as to the required moisture content during compaction. The resulting degree of compaction would inevitably affect the hardness of the base. The OMC can be requested from the supplier but due to storage methods and the ease with which moisture could find its way into the material while it is stockpiled, it is

74

recommended that the hydroscopic moisture content (if not the OMC) be determined close to the time of construction which would provide more reliable results. The details of the OMC tests done can be found in *Appendix B1.*

Grading Analysis

A grading analysis is done on the virgin material using the standard Test Method A1 in the TMH1 (1986). The material used to construct the base will not be blended to a desired grading; however the grading curve of the material would need to adhere to the requirements for a G2 base course material. For this purpose, a grading analysis can be done or requested from the supplier shown in *Figure 37*.
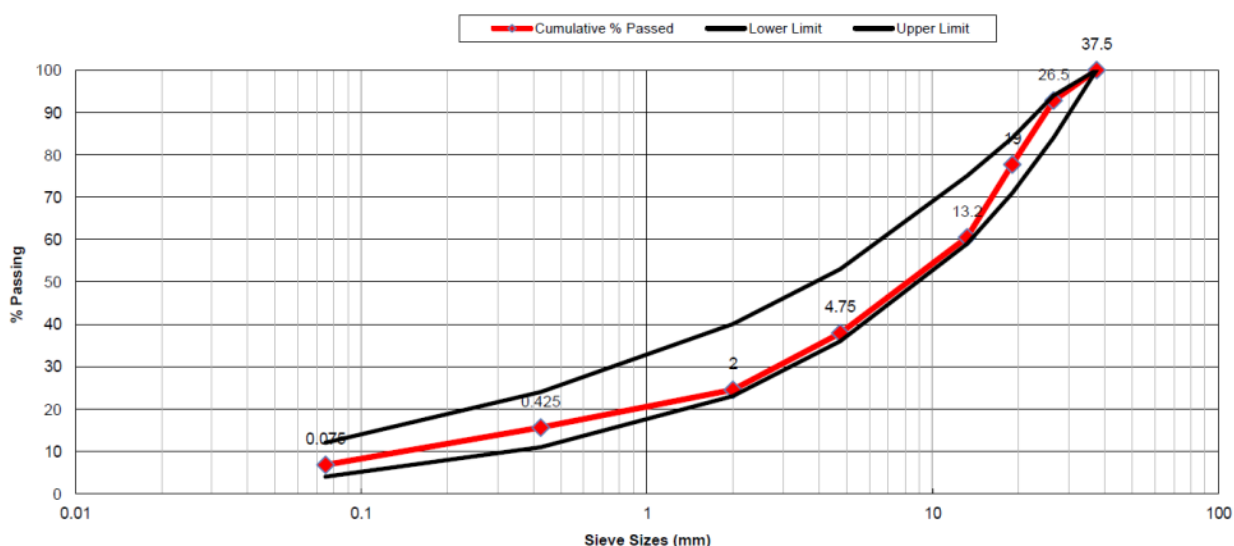
Figure 37: Grading curve for the G2 material used in this study

5.5.2 (b) Seal aggregate and tiles

Average least dimension (ALD)

The ALD is determined using the standard test method B18 (a) in the TMH1 (1986). This test method also provides a definition for the ALD:

> *"The least dimension of an aggregate particle is the smallest perpendicular distance between two parallel plates through which the particle will just pass. The average least dimension is the overall average of the least dimension for a number of particles." (TMH1, 1986)*

The details of this test are fully outlined in *Appendix B2.* The following results were obtained:

13.2 mm: ALD = 8.4mm

19 mm: ALD = 11.8 mm

Flakiness index

The flakiness Index is determined using the Standard Test Method B3 in theTMH1 (1983). This test method also provides a definition for the Flakiness Index:

"The Flakiness Index of a course aggregate is the mass of particles in that aggregate, expressed as a percentage of the total mass of that aggregate, which will pass the slot or slots of specified width for the appropriate size fraction. The width of the slots is half that of the sieve openings through which each of the fractions passes." (TMH1, 1986)

The following results were obtained:

13.2 mm: Flakiness Index = 13.2 %

19 mm: Flakiness Index = 21.9 %

The details of these results are provided in *Appendix B3*.

Seal tile moulds

The moulds used to construct the seal tiles are sized so that the tile is wide enough to provide an area adequate to capture the entire zone of influence, while also being small enough to allow for multiple seals to be constructed on the base.

Since the tyre width of the MMLS3 bogie is 80 mm, the mould with the dimensions indicated in *Figure 39* is deemed appropriate to capture the entire zone of influence. All quantities and application rates will thus be based on an area of 0.1008 m².

Binder application rates and method

The application rates will be adjusted based on the ALD of the two different stone sizes as well as the wetted height obtained using the standard application rate of 0.8 ℓ/m² for the dense sh-sh packing. The application rate for the open sh-sh configuration will be such that it provides a similar wetted height that is seen in the dense sh-sh configuration. These adjustments are detailed in *Appendix A2*.
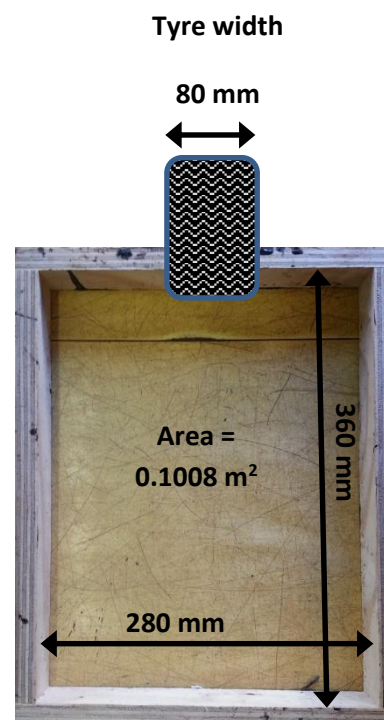
Figure 38: Seal tile mould and tyre width

Due to the difficulty and challenges experienced by researchers attempting to use a bitumen spray-bar within the confines of a laboratory, it was decided that for the purpose of this study, a spray-bar was not used. Instead, the tack coat will be applied using a squeegee. This presents a challenge in the case where the tack coat used is a hot applied binder (Pen 70/100 and SE1). Due to the rapid cooling nature of hot binders, the spreading of the tack coat would need to be done swiftly, and the seal aggregate would need to be applied within seconds of spreading the tack coat. To accommodate this, a custom made squeegee was made as shown in *Figure 39*. The

Figure 39: Custom made squeegee

rubber squeegee blade is simply attached to a plate with two arms that fit comfortably on the seal tile mould. Round arms are used to facilitate a sliding action along the frame, so the tack coat can be effectively spread.

The cover coat will be sprayed using a pneumatic paint spray-gun. The application temperature is what prevents the use of this device for the application of the tack coat. Since the cover coat will be a dilute emulsion for all the tiles, which does not require a high application temperature, the cover coat can be applied using the spray-gun shown in *Figure 40*. The nozzle can be adjusted to change the flare angle. The flare angle should be calibrated appropriately prior to seal construction by testing the gun using water. The flare angle should be wide enough to just about cover the width of the tile while the spray-gun is held at least 300 mm from the surface. The spray-rate for the emulsion used is determined beforehand by spraying the gun for 5 seconds and measuring the mass of emulsion that leaves the spray-gun. This is repeated a few times and the average is determined. The spray-rate for dilute cationic

Figure 40: Pneumatic Spray-gun

emulsion with the spray-gun used is determined as approximately 4.2g per second. This proved to be a more accurate way of applying the binder uniformly over the area.

Aggregate application method and compaction

As previously discussed, the application and compaction of the seal aggregate during the construction of seals plays a huge role in the long term performance of the seal. The primary functions of the roller compaction of the seal stones is to (a) provide the initial embedment required to prevent whip-off; and (b) to orientate the seal stones such that their ALD is perpendicular to the surface. A roller will not be used to compact the stones in this study. A compaction plate will be used

to provide at least some degree of initial embedment and orientation and since the compaction plate would not provide the same compaction effort as a roller would in practice, it will be assumed that the initial embedment would take place during the first 100 to 1000 load cycles of MMLS3 trafficking. This would address the issue of the initial embedment; the orientation of the particles would however need to be addressed in another way. The stones need to be applied in such a way that they are orientated on their ALD. Individual packing of the stones would not be possible due to the rapid cooling of the hot applied binders. Instead, the method that provided promising results during the trail investigation is the use of a plate with rods on either side similar to the one used to make the customised

Figure 41: 19 mm, dense sh-sh, aggregate packed with their ALD perpendicular to the plate.

squeegee (*Figure 39*). The stones are then packed individually laying them on their ALD and packing them to the desired configuration as shown in *Figure 41*. Once the tack is applied, the plate can then be placed on the mould and by simultaneously lifting the plate upwards on the free end and moving the plate backwards, the stones would slide down (some would roll) and land mostly in the same orientation as they were packed. This method does not provide the perfect simulation of in practice seal construction, but was found to yield the best results in terms of stone orientation.

5.5.2 (c) LTM measurements

As indicated in Section 4, the sensor unit on the LTM has an LED which provides an indication as to the sensor range status. Trial runs using the LTM on seal samples indicate that the "centre" (Green light) is a narrow 10-12 mm, with a total depth reading band of 65 mm. Outside this 65 mm band, the laser is out of range and will not capture data. This concept is illustrated in *Figure 42* alongside. It is therefore imperative to ensure that when LTM readings are taken, the sensor remains in range during the entire scan.
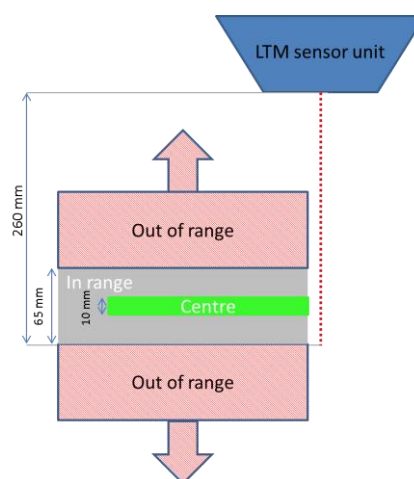
Figure 42: LTM depth sensor range

Further preliminary testing with the LTM shed light on another issue during the scanning process. Freshly sprayed seals are usually shiny (especially when a cover coat is applied) and have an almost wet appearance as shown in *Plate 3(a)*. Using the LTM on a seal with a glossy surface causes the LED indicator to flash red throughout most

of the scan causing a large amount of data loss. This is most likely due to the reflection and refraction of the light emitted during the reading process. After various attempts at addressing this issue, it was found that brushing the seal with fine material (passing the 0.075 mm sieve) yielded the best results. Since the seal is dust free upon construction, the fines readily adhere to the aggregate surface (which is very similar to what happens to newly constructed seals in practice). This effectively dulls the seal as shown in *Plate 3(b).* Excess fines are then blown off using compressed air. Although the fines do not cover the entire surface of the seal stones, especially in between the stones and the laser still misfires from time to time, the average data loss decreased by more than 70%. Since the particle size of the fine material is smaller than one tenth of a millimetre, the application of fines should not impact the depth readings obtained using the LTM.

(a)   (b)
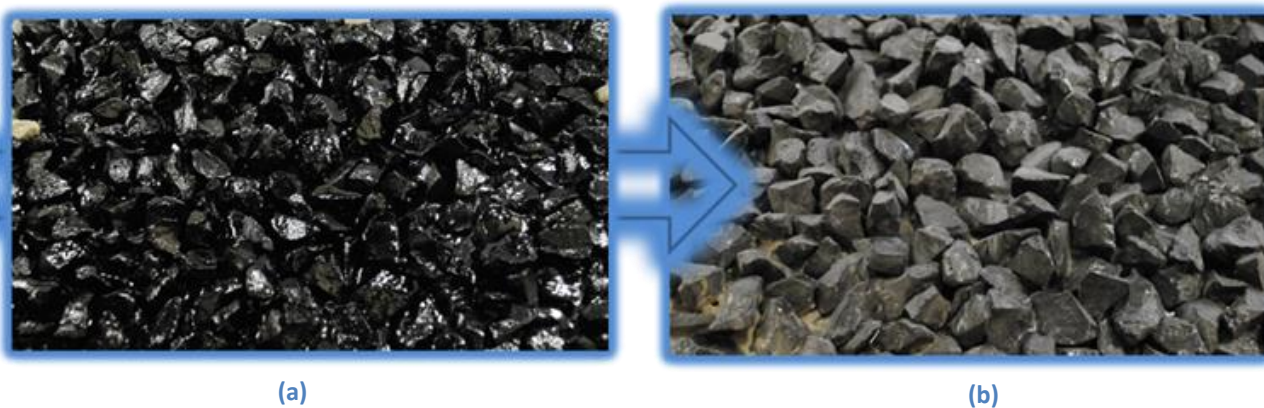
Plate 3: (a) Newly constructed seal (b) dulled seal surface using fines

What has also become clear during these preliminary trials is that the LTM's rate of data loss due to misfiring of the laser is not consistent. Scanning the same sample yields a different degree of data loss and level of accuracy (data is at times captured, but is very obviously inaccurate). Possible consideration will be given to scanning the samples multiple times and using the combination of scans to improve the degree of accuracy in the data sets. This will be discussed further in a later section of this chapter.

5.5.3 Phase II: Base construction

Using the information obtained in *Phase I*, the base can now be constructed. With the hygroscopic moisture content known (*Appendix B1*), the amount of water to be added during the mixing process can be determined by simply subtracting the hygroscopic moisture content from the OMC since the base will be compacted at OMC to achieve the maximum dry density or 'MDD' (refer to *Appendix B1*). The resulting percentage would then be the fraction of water (by mass) to be added to the mix. The amount of material required would be governed by the volume of the base required and the MDD obtained in Test Method A7 (TMH1, 1986).

(a)

(b)
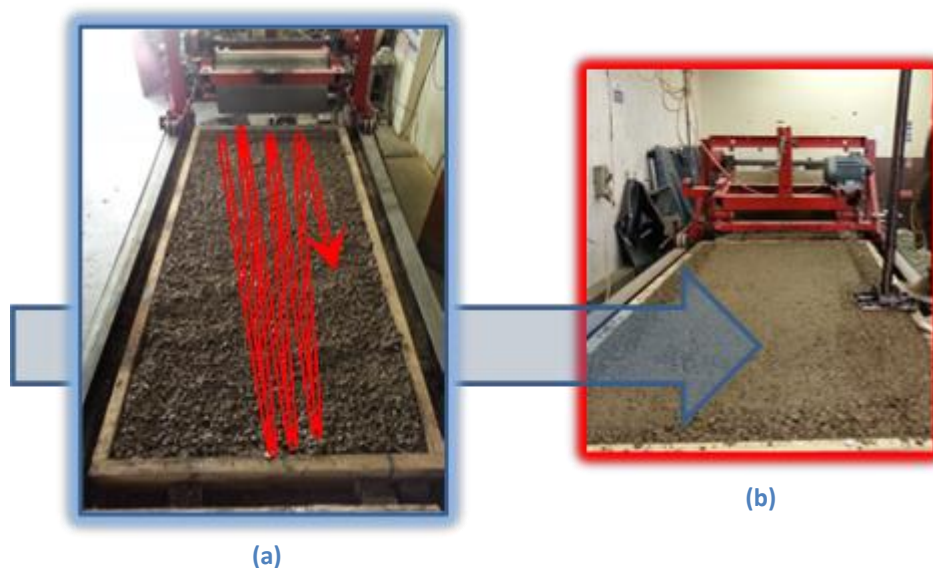
Plate 4: (a) Base before compaction (b) base after roller compaction and during manual compaction of the edge

Due to the large amount of material requiring mixing, the base is split into three sections along the length, and the mixed G2 material is added by wheelbarrow evenly between the three sections. This process is similar to the stockpiling of the base aggregate prior to compaction, but on a much smaller scale. The material is evened out using a shovel and rake, the result shown in *Plate 4(a).* With the required amount of material in place and sufficiently levelled, the compaction process should begin immediately. A vibratory roller compaction device should be used with sufficient compaction effort to attain the MDD. The University of Stellenbosch's Asphalt and Geotechnical section have, in the Fred Hugo MMLS laboratory, a vibratory roller on guide rails that is used specifically for this purpose. The roller is allowed to pass over the material as many times as required until the material appears to be fully compacted. The roller is lowered gradually after every one or two passes using a crank mechanism. When the roller is unable to lower any further, this signals that the maximum degree of

compaction has been reached. Since the roller is unable to traverse laterally, the sides of the base is compacted using a hand tamper *Plate 4(b).* This is done for each layer that is compacted after every 3 to 4 passes.

The compacted base is then allowed to dry using infra-red lights simulating the effect of the sun (*plate 5(a)*). The lights are left on the base for 10 - 12 hours a day and its position is switched from the left side of the base to the right after 5 to 6 hours to distribute the heat evenly. The surface

(b)

(a)
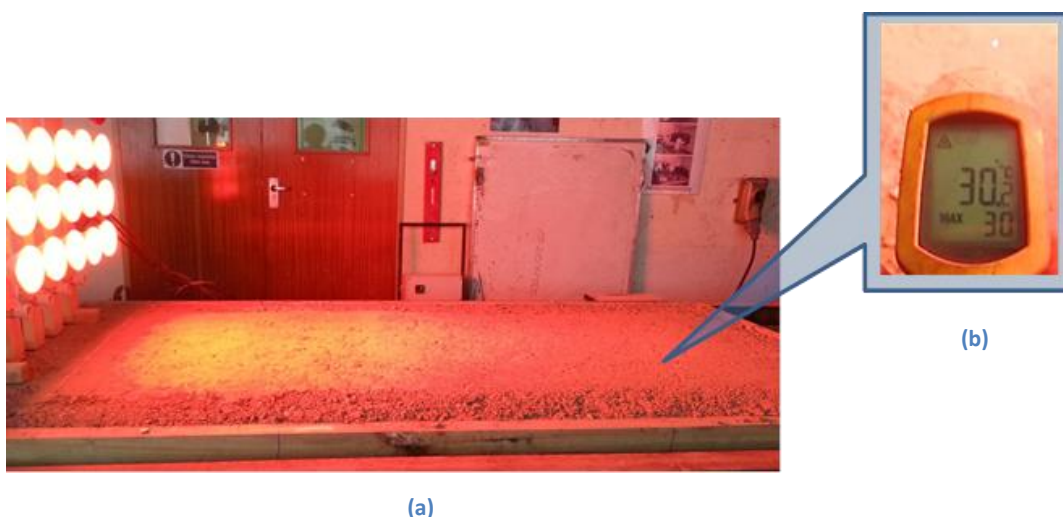
Plate 5: (a) Drying of the base layer using infra-red heat globes, (b) base maintained at about 30°C

exposed directly beneath the lights is heated to about 30°C as shown in *plate 5(b)*. The TRH3 (2007) specifies that the moisture content in a base needs to reduce to 50% of the OMC before seal work can commence. After a few days, the base should then be dry enough to proceed.

The Ball Penetration Test as described in *Section 4.2* is then conducted at various points on the base to establish the hardness of the surface and embedment potential. The positions of the tests are planned and conducted outside of the proposed position of the wheel tracks as shown in *Figure 43* alongside. This ensures that the surface below the wheel track is undamaged and intact. This test is also used to provide an indication as to the moisture content of the base. A few tests are conducted a few days after the base is constructed, and then every few days from then until the apparent ball penetration remains consistent. As the moisture content

Figure 43: Planned approximate locations for the ball penetration tests and the wheel track

81

decreases, the base attains strength and stiffness and once the penetration value remains practically unchanged it can be considered to have reached the maximum stiffness and would thus have a moisture content below 50% of OMC. The ball penetration test is used sparingly, and will be used again once the trafficking phase of the testing process is complete. These final ball penetration test results will be assumed to be the governing embedment potential of the base.

To complete the base construction, the surface is broomed to remove all loose particles. A prime coat (MC10) is then applied to the surface using a squeegee. The low viscosity prime coat penetrates the top 10 mm of the base with the the aid of a cutter, whilst depositing a thin film of bitumen on the surface to provide adhesion between the base and the seals that will be constructed. The application rate and temperature used is in line with the manufacturer's recommendations. The primed surface (*Figure 44*) is then allowed to dry. The use of additional heating is optional and would speed up the evaporation of the cutters in the prime. Once the prime is dry to the touch, the surface is ready for the next phase.

Figure 44: Primed surface

82

5.5.4 Phase III: Seal construction

Using the custom built apparatus discussed in *Section 5.2.2(b),* the seals can now be constructed.

Table 11: Test Variable key

Tile number	Tack coat	Aggregate size (mm)	Aggregate spread configuration
1	pr.SE-1	13.2	Dense sh-sh
2	Pen70/100	13.2	Dense sh-sh
3	Pr.SE-1	13.2	Open sh-sh
4	Pen70/100	13.2	Open sh-sh
5	pr.SE-1	19	Dense sh-sh
6	Pen70/100	19	Dense sh-sh
7	SC-E1	13.2	Dense sh-sh
8	SC-E1	13.2	Open sh-sh
9	Cat65	13.2	Dense sh-sh
10	Cat65	13.2	Open sh-sh
11	Cat65	19	Dense sh-sh
12	SC-E1	19	Dense sh-sh
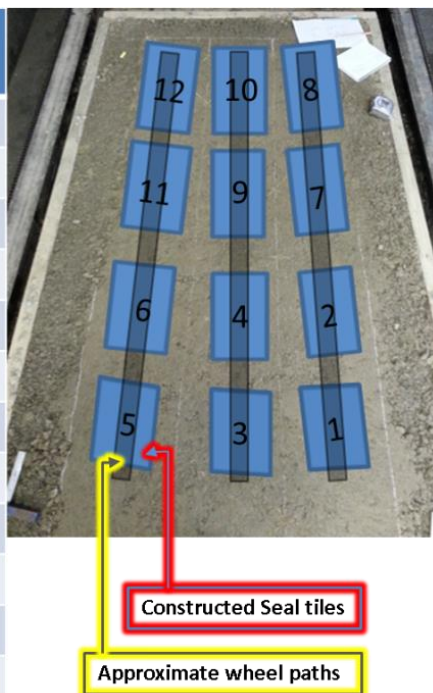
Figure 45: Mapped seal tiles and approximate wheel paths

Figure 45 maps the variables on the base and *Table 11* provides the corresponding variable key.

The first step would be to apply the tack coat. The binders used are all applied at the temperatures recommended by the manufacturer. The data sheets for all the binders used can be found in *Appendix C.* The application rates are also calculated for the various seals and are detailed in *Appendix A.* Due to the small quantity of bitumen that needs to be applied, the required amount is determined by mass, and placed into a measuring beaker. The binder is then poured out of the beaker, and the weight of the beaker is then set to zero on the scale before the required mass of bitumen is re-added. This would take into account the residual binder that would effectively be left in the beaker once the binder is poured out. The binder is poured in a zig-zag pattern inside the mould, and is immediately spread using the squeegee. The aim is to spread the binder as evenly as possible covering the entire area. This process is illustrated in *Plate 6.*
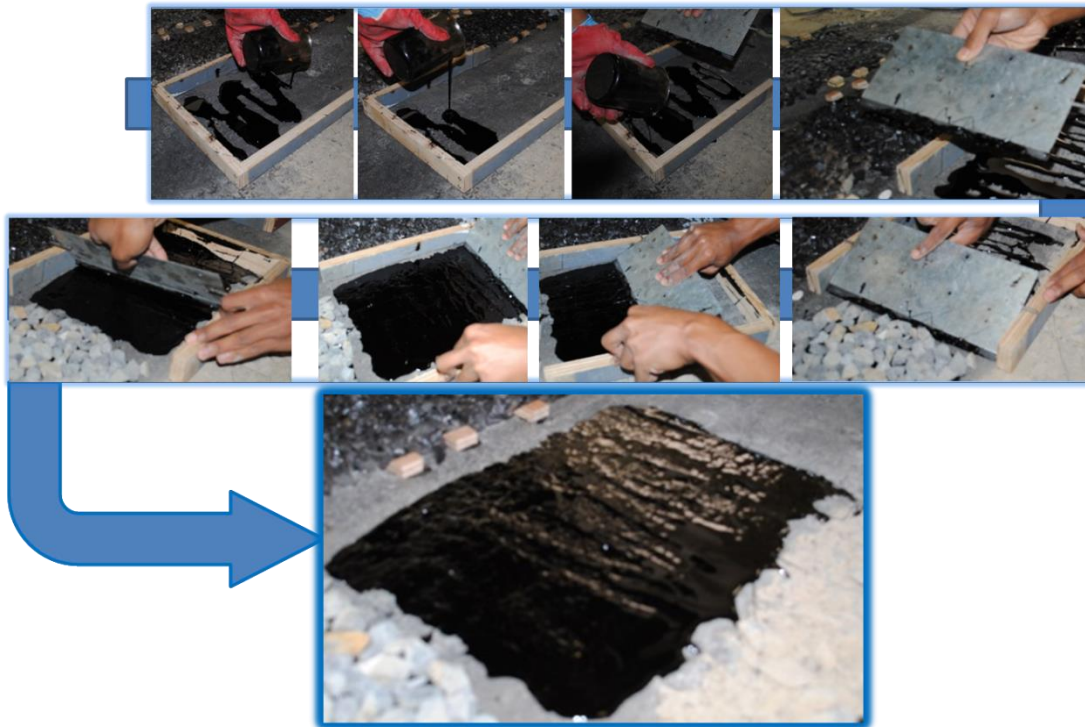
Plate 6: Tack application process

Once the tack coat has been applied, the aggregate should be applied immediately. The pre-packed aggregate plate is placed carefully on the mould. By lifting and moving the plate backwards, the seal stones are allowed to slide and fall into position. Any stones that fall off the plate or that are laying on top of another stone can be carefully placed into any gaps that can be seen. After removing the mould, a mat is placed on the stones the plate compactor is then used to press the stones into place

Plate 7: Aggregate application and plate compaction process

and provide some force to orientate the stones that rolled over on to their ALD. The force applied and number of oscillations used is kept consistent for all the seal tiles. This process is illustrated in *Plate 7*.

The cover spray can now be applied. The spray-gun is connected to a compressed air supply with the pressure used during the calibration of the spray-gun. With a measured spray rate of approximately 4.2 g per second, and a required mass of approximately 75 g per tile, the emulsion is sprayed evenly across both tiles. Spending 17 to 18 seconds on each tile would yield the required application. *Plate 8* shown below illustrates this cover spray process.

Plate 8: Cover spray process

The seals are then allowed to cure for at least a full day. In the case of an emulsion used as a tack coat, the curing time should be increased significantly to ensure that the emulsion breaks and all volatiles evaporate. After at least a day or two the adhesion can be checked by attempting to remove a stone outside of the planned wheel track. If the stone dislodges easily, sufficient adhesion has not developed and the seal would need more time to cure. The curing time is an important aspect during seal construction, but its effects are restricted to chip loss which is a short term failure mode. Embedment, being a long term failure mechanism would thus be much less affected by the curing time. When the seal stones are held firmly by the binder and cannot easily be dislodged by hand, the next phase can begin.

5.5.5 Phase IV: LTM data capturing

As noted in Section *5.5.2(c)* the seal is first dulled by lightly brushing fines over the surface followed by blowing the excess fines off the surface using compressed air.

In order to effectively monitor the seal profile, the laser should scan the same position each time. To achieve this, wooden markers are fixed into position on the base alongside each tile. Fixing the markers to the base away from the wheel path and not on the seal would ensure that they remain in a fixed position and do not move as the stones displace under traffic as shown in *Figure 46*.
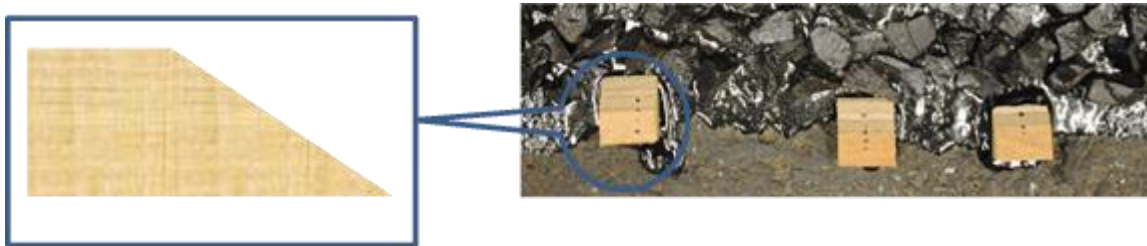
Figure 46: Wooden marker design and positioning

The design of the wooden markers serves additional purposes.

Based on the findings during Phase I as noted in *Section 5.5.2(c),* and after a significant number of trials using the LTM and observing the data sets obtained, it was decided that to improve the level of accuracy of the scans taken, each scan will be repeated five times. The data obtained would then be plotted on the same set of axes and although there may be a few outliers, the governing seal profile would be clear based on the path followed by most of the repeat readings taken. This process is discussed in detail in *Section 5.5.7* later in this chapter.

The movement of the laser along the rail and the point at which the data starts being captured does not occur simultaneously. These two functions are controlled independently. It is found that the best way to conduct the readings is to begin the data capturing first, which would mean the LTM would be capturing a constant depth value (on the flat portion of the wooden marker as shown in *Figure 47(a)*). Since the laser would be stationary. Once the motor switch is triggered, the laser would scan the wooden marker before the seal as shown graphically in *Figure 47(a).*

(a)　　　　　　　　　　　　　(b)
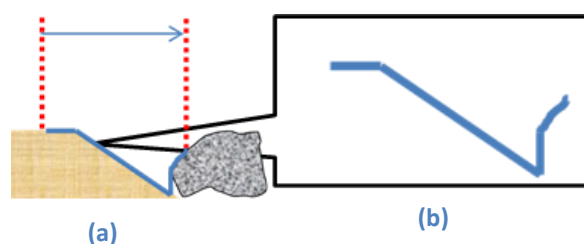
Figure 47: (a) Concept of LTM scanning process (b) resulting profile shape

86

Since the horizontal distance sensor is not functional, the shape of the marker would provide a reference from which these repeat readings can be overlaid given that the resulting profile shape from each scan would be easily identifiable as shown conceptually in *Figure 47(b)*.

Another function of the wooden marker is to provide a reference height from which to calculate the displacement of the stones. The marker remains fixed so the relative height difference between the stones and the marker would yield the displacement from which the embedment can be calculated. This will also be discussed further in *Section 5.5.7*.

Figure 48: Position marking

Using the LTM as a guide, markers are then fixed at the start and end points of the desired scan length. Before the first scan is done, the precise point of the laser is marked using an ink permanent marker. Two or three additional points are made using the laser as a guide to further improve the accuracy of the setting. This is illustrated in *Figure 48* alongside. This is done on both ends of the scan length so that once the laser is moved out of position, the precise point of the start and end of each scan can be used for the scans thereafter.

Figure 49: LTM bubble level

The LTM is also equipped with a bubble level (*Figure 49*). Each leg of the LTM can be adjusted independently of each other using bolts. This allows for the LTM frame to be levelled when scanning on an uneven surface. The LTM is levelled before each scan.

When the LTM needs to be put back into position after MMLS trafficking, it is placed back on the surface and its position is carefully calibrated before the scan is done. This process is tedious due to the size and position of the LTM. It is an iterative process whereby one end of the LTM is positioned so that the laser is precisely on the marked start spot as shown in *Figure 50(a)*. Switching the motor

(a)   (b)
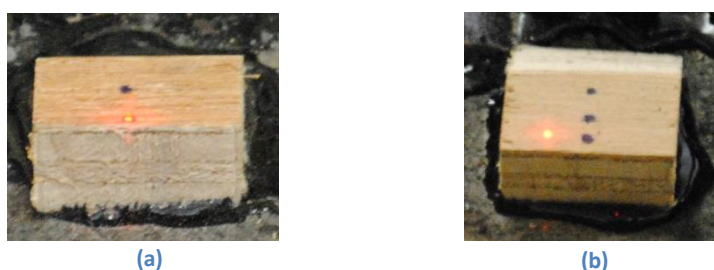
Figure 50: (a) Laser point on required position (b) laser point off required position

on allowing the LTM to move to the end point of the scan would then see the laser point being out of position on that marker as shown in *Figure 50(b).*

This side is then shifted so that the laser point is on position as shown in *(a)* which would effectively shift the opposite side (which was in position) slightly out of position. The motor is then switched on moving the laser across and this side would now need to be shifted, although not as much as the previous time. This iterative process is done until the laser is precisely on the marker as shown in *(a)*. At this stage, the position would be calibrated, and the scan can be done.

This is an important process and will determine the quality of the data obtained. A slight shift to the left or to the right could result in an unusable scan. It is therefore vital to calibrate the position of the laser as accurately as possible before commencing with the scan.

Once the laser is calibrated, the software program can be initiated (TEXTURE.EXE). This simple program reads the depth information transmitted by the sensor. The interface is shown in *Figure 51* below.

Figure 51: Interface of the LTM software (TEXTURE.EXE)

The commands can be seen on the bottom right of the window. The column labelled "V-Dist" displays the depth value for the last 20 data points read by the sensor. The value displayed in the top right corner of the window labelled "data in buffer" indicates the amount of data points currently stored in the buffer and is ready to be written to a file. The column labelled "H-Dist" is the horizontal

distance counter and as mentioned, was not functional at the time of this study. The scanning process is carried out step-by-step as follows:

1. Check that the bar next to the "Receiving" label is rotating. This indicates that the software program is receiving the data transmitted by the LTM sensor. Also ensure that the depth value is constant for all 20 points displayed in the V-Dist column which means that the laser is stationary and the depth is thus constant.

2. Press F1 (start capturing data) followed closely by flipping the switch controlling the motor. This would ensure that the software starts collecting data before the laser starts moving. Doing this allows for the constant depth value to be captured for a few hundred points (which would become the datum) before any change is seen in the depth value.

3. Allow the laser to traverse the length of the sample until it reaches the opposite marker ensuring that the software registers the data throughout the run. The software program is not without its "bugs" and loses transmission from time to time.

4. Once the motor stops running, allow a second or so before pressing F1 again stopping the data capturing function.

5. The number of data points stored as indicated on top of the window should now be fixed showing the amount of data points stored. This value should be roughly the same for each run (plus or minus a thousand or so). In the case of this study, the scan length is approximately 255 mm which translates to about 10 000 data points per scan.

6. Press F2 to store the captured data as a .DAT file. The file will be labelled TEX-001.DAT and will be stored in the same directory from which the program (TEXTURE.EXE) is run. Each file written thereafter will be labelled TEX-002.DAT etc.

7. The files should then be moved after every group of tests to another directory. Once the program is restarted, the files will be written starting from TEXT-001.DAT again and will override any existing data file previously stored under that name.

5.5.6 Phase V: MMLS3 Traffic simulation

After the MMLS3 is set up and calibrated (as discussed in *Section 4.5*) the traffic simulation can begin. MMLS3 trafficking is carried out at the maximum operating speed of 7200 cycles per hour. The total MMLS run time on each sample is therefore 13 hours 53 minutes and 20 seconds which translates to the required total of 100 000 load cycles. *Table 12* provides the breakdown of the total run time into the run times required to accommodate the LTM reading points. The running of the MMLS is timed using a stopwatch and the load cycle counter is used to confirm the number of cycles completed after each run.

Table 12: Load cycles translated to MMLS run times

LTM Reading number /Trafficking Phase	Load cycles (Cumulative)	Required MMLS run time (h:m:s)
1	0	0:00:00
2	100	0:00:50
3	500	0:03:20
4	1000	0:04:10
5	5000	0:33:20
6	10 000	0:41:40
7	25 000	2:05:00
8	50 000	3:28:20
9	75 000	3:28:20
10	100 000	3:28:20
		Total Run time = 13:53:20

5.5.7 Phase VI: LTM data processing

5.5.7 (a) Introduction

The data files collected for each sample scan should be collected and stored in such a way that it makes this phase simpler to execute. Since each scan is repeated a few times, the aim is to take each of the five repeats and plot it on the same set of axes. Once this is done, reliable measuring points can be identified by viewing all the profiles obtained after each traffic simulation interval as highlighted in the previous phase (*Section 5.5.6*).

The LTM device and the data capturing process yields a large amount of data. This data is however only usable once it has been effectively processed due to various equipment related issues. This section addresses these issues and provides the data processing methodology followed in this study.

5.5.7 (b) Importing data to Excel and trimming the data sets

The .DAT files obtained from the texture program for each repeat scan is collected into a single excel spreadsheet. This is done using Excel's import function. The data file is selected and imported as delimited, using the 'space' delimiter. This effectively splits the two data sets (one being the depth, the other being the horizontal distance which, in the case of this study, is always zero) stored in the .DAT files into two separate columns in excel. The repeats are then imported one at a time starting in the same row.

Since the collection procedure is operator controlled, the number of data points captured per scan repeat is variable but should be roughly the same if the procedure is followed correctly. Each data set should show a fixed value for at least a few hundred points before changing indicates that the motor switch was turned on and that the laser has begun moving on the rail. The lower end of the data sets should show a similar trend with the end depth value being repeated for a few hundred data points indicating that the laser has stopped moving. In order to ensure that the data sets are consistent during the next processing step, the data sets are trimmed so that each of the repeats has the same number of data points. The start and end values (which are constant due to the laser being stationary) are removed to accommodate this allowing the data sets to be resized accordingly.

5.5.7 (c) Removing the misfire (zero) points

As the laser traverses the scan length, there are points where the light is reflected and the sensor is unable to capture the depth reading. This is discussed in *Section 5.5.2 (c)*. Dulling the surface caused a significant improvement with regard to this issue, but did not resolve it completely. Since the horizontal distance sensor on the LTM is not functional, the distance of each depth data point is

calculated based on the total scan length and the number of data points obtained through the scan. The scan length remains fixed throughout the testing phase of this study at approximately 255 mm.

If the number of data points obtained is on average about 10 000, the distance between each data point would therefore be as follows:

255/10000 = 0.0255 mm

Plotting the raw data set obtained without removing the zero points provides a profile that is difficult to analyse as shown in *Figure 52*.
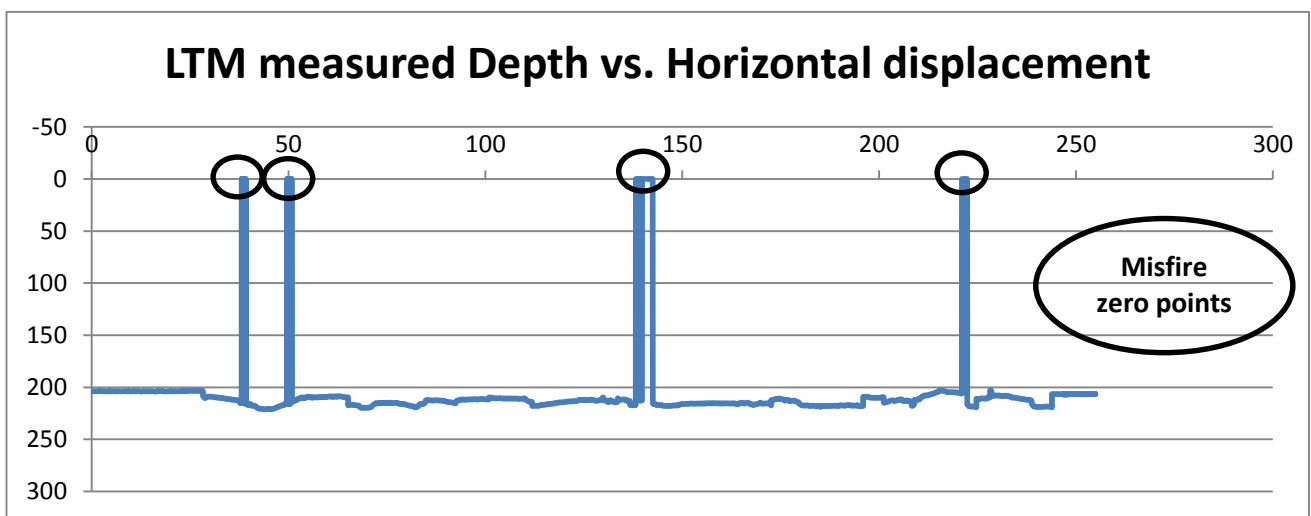
Figure 52: LTM measured depth vs. Horizontal displacement (zeros included in data set)

To provide a more usable plot, the misfire points are removed from the data set, along with their corresponding distance value. This would result in the plot skipping this point entirely and moving to the next available non-zero data point essentially averaging the depth value in between. This yielded
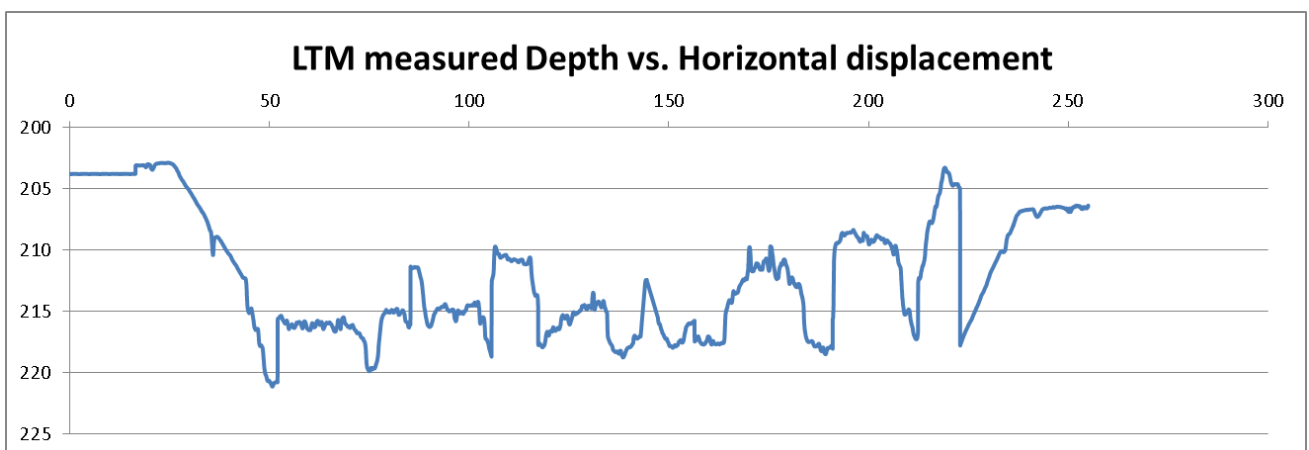
Figure 53: LTM measured depth vs. Horizontal displacement (zeros removed)

a much better plot (as shown in *Figure 53*)

On average, the scan misfires for about 10 to 15% of the scan length. These misfires are not continuous but split over the length of the scan. The highest noted misfire length is around 200-300 data points consecutively.

Using the distance between data points calculated above, this translates approximately to 5.1 - 7.65 mm. and this would be clearly visible by a straight line. This result is acceptable given that the stones are identified using manual identification and using a broad base of plots. This would ensure that these slight misfire points do not affect the embedment values determined from the plots, even when the misfires occur consecutively for hundreds of points at a time, though these occurrences are seldom.

5.5.7 (d) Plotting the repeats on a set of axes and aligning them

Plotting the repeat scans on the same set of axes yielded a plot shown in *Figure 54*.

(The process described up to this point has been automated using a MACRO in Excel. The template containing the MACRO can be found as part of the data CD provided with this report. File name: *final LTM data template MACROv3.xlsm)*

The plot obtained is not usable for analysis as yet. The resulting data sets would first need to be aligned. Since the data sets were trimmed, the point which the laser starts moving is variable for each scan repeat. What has also become apparent is that the LTM seems to slow down at certain points. This is most likely due to friction within the mechanical system that moves the laser along the rail. This slight decrease in speed is not visible with the eye, but can clearly be seen in the data captured. A slight decrease in speed (even by a second) at any point along the scan could mean hundreds of additional depth points are registered at different points in each repeat scan. Since the number of depth points determines the frequency and the position where the depth points are plotted, additional data points captured would result in the graphs being phased out of each other even when they are lined up at certain points. In an attempt to remedy this, the data from each scan is individually looked at, and the horizontal position of the data points is shifted manually and incrementally until the plots line up with each other. This time consuming process eventually yields a plot which is much better and shows a much greater promise for effective analysis as can be seen in *Figure 55*.

Given the degree of manipulation of the horizontal distance required to yield the profile shown in *Figure 55* it should be noted that the horizontal distance effectively loses reliability (this reliability would probably be regained with upgrades to the horizontal displacement sensor on the LTM). Since

this study is focused on embedment, which is essentially the movement of the stones in the vertical direction, this lack of reliability in the horizontal direction is of little consequence. The stones measured would still need to be identified manually based on the visual representation of the data and will not be determined using the horizontal position.

Considering *Figure 55*, one is clearly able to identify a profile of seal stones across the length of the scan, and despite the outlier data sets (being the data set displayed in green) and points, most of the repeat scans follow a similar profile indicating a degree of reliability in the plot based on the concentration of corresponding data points. The outlier data set could, however, also provide valuable information in certain cases. The plots shown are 5 repeat scans done without any interference with the laser position. This indicates that despite the laser being fixed, there is still a degree of lateral movement as the sensor moves along the guide rail. This outlier data set is thus just an outlier in terms of the position relative to the four other scans. Looking at *Figure 55,* the profile displayed by the green line also exists, but is found slightly to the left or to the right of the four other scans at certain points. This slight movement appears to occur during the scan since some of the data points agree with the other scans, but some are distinctively different. This movement could bring into question the reliability of the data captured from the scan but could also provide a second profile and relative position from which to observe the movement of the stones. The visual analysis of the seal profiles would dictate which of these two scenarios are more prominent.

Combined plot of repeat scans
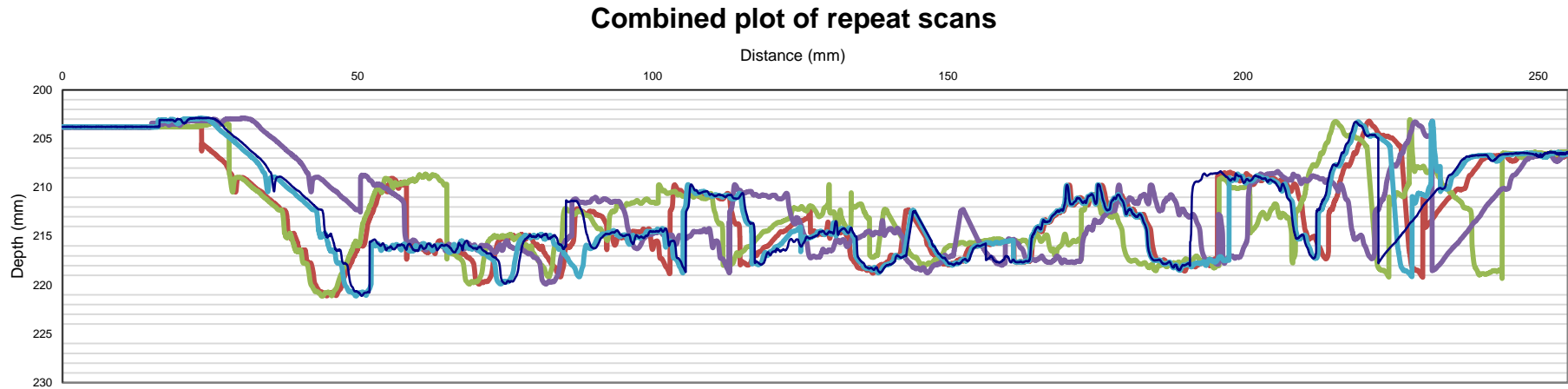
Figure 54: Combined plot of repeat scans

Shifted combined plot of repeat scans
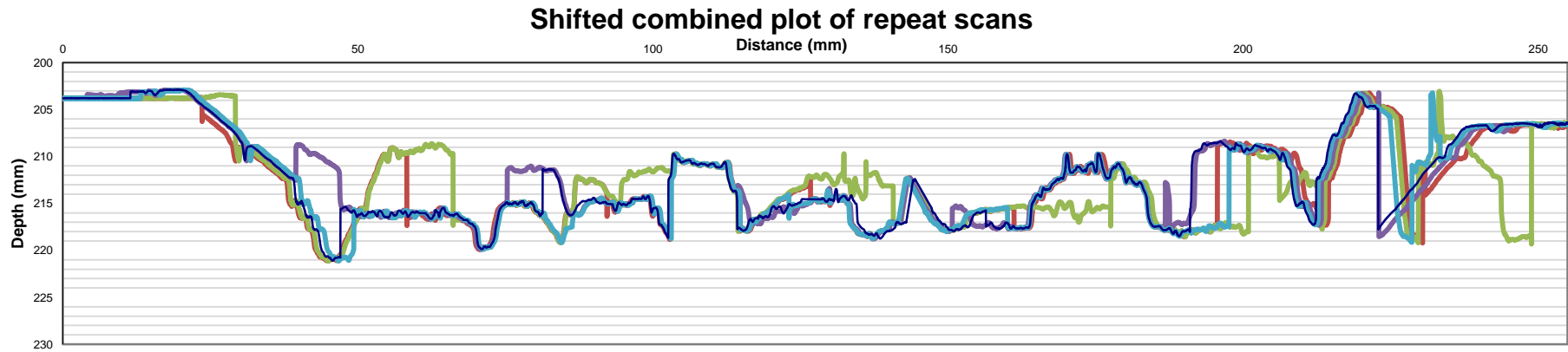
Figure 55: Shifted combined plot of repeat scans

95

5.5.7 (e) Identifying measurable stones in the profile

To establish the embedment taking place during the various trafficking phases, consistent measuring points would need to be identified within the wheel path. This is done manually by visually assessing each set of scans at each different load cycle phase. *Plate 9* displays how this is done. The orange pointers indicate the place where the laser passes the wooden marker as discussed previously. In order to gain a better idea about the profile, an image of the tile is used. Photographs taken after each trafficking phase provides a reference and further increases the confidence in the scan data obtained. Stones that are visibly very similar are then identified using the coloured boxes. They should also be in the same relative horizontal position provided the scales are the same. The profile should also look fairly similar before and after the identified stone, providing further confidence in the stones chosen. The photograph also provides an idea of the wheel path position. Stones in the wheel path are visibly abraded and dulled after being trafficked. Stones within the wheel path are therefore the most important. Stones outside the wheel path can also provide valuable information about the laser position relative to the previous load cycle phase. Essentially, the effects of trafficking should be much less prominent on stones well outside the wheel path, provided the laser is in the precise position it had been when the scans were done after the previous trafficking phase. These effects should also be more pronounced the nearer the stones are to the zone of traffic.

Stones are thus identified across all the load cycles. If a stone is unidentified in one of the phases, it is skipped, and the relative position of that stone at that phase would be unknown. As many stones as possible are identified within the wheel path allowing for as much information to be extracted from each scan. In *Plate 9*, three stones are identified within the wheel path, and one well outside the wheel path. At least one stone outside the wheel path will be identified in addition to the ones within the wheel path.

Once all the measurable stones are identified, the embedment can be measured. This process is described in the subsection that follows.
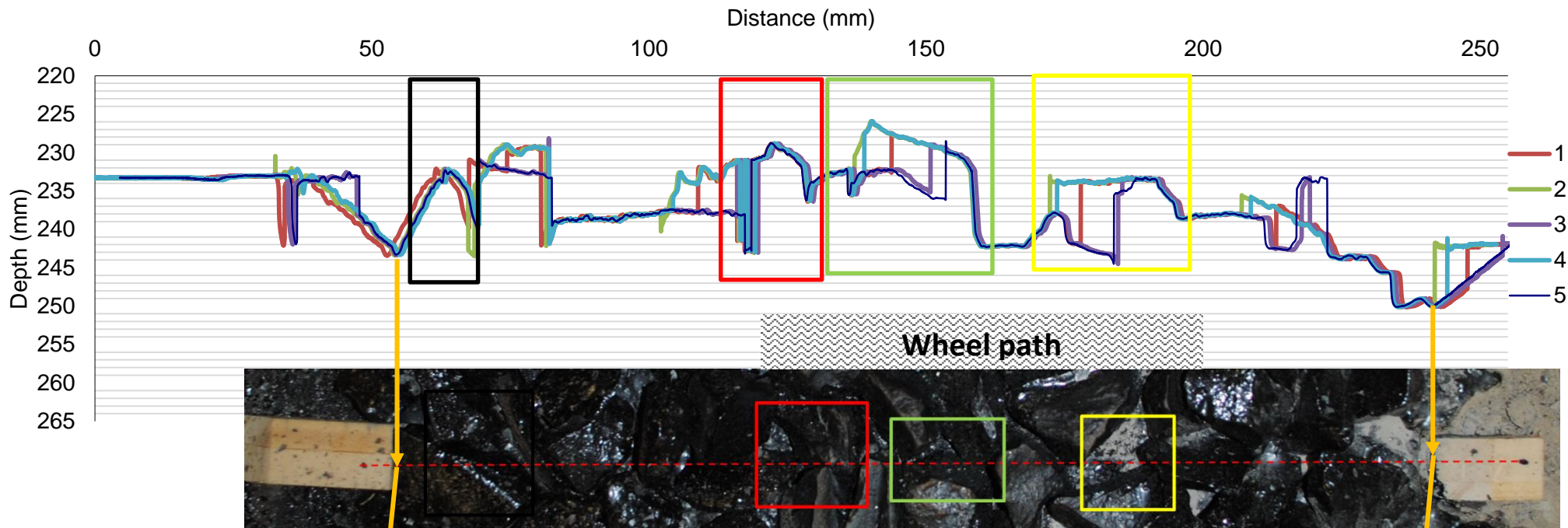
Plate 9: Identifying measurable stones
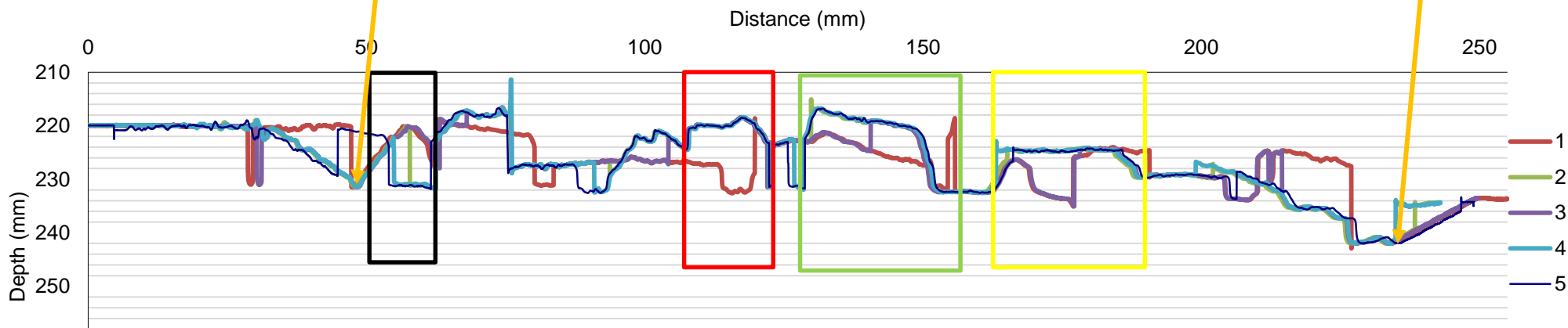
5.5.7 (f) Measuring and quantifying embedment

In order to quantify the embedment of each identified stone, the stones need to be measured against a reference point. The wooden markers provide this datum level and since the scan always begins at precisely the same point, this depth value can be used as the reference depth. The vertical displacement of each identified stone relative to this position therefore indicates the movement of the stone. The relative position is established by subtracting the level of the stone from the level of the datum. This relative position is then determined again after a trafficking phase. The difference between these two levels would indicate a movement. Due to the amount of data points captured during the scan, the depth of the stone is determined by taking the average of the 10 highest points on the identified stone. This approximates to the average of the highest 0.26 mm on the stone surface. This is done for each of the repeat scans. If all the scans describe the identified stone, the average of the relative depth is calculated using all 5 scans. If however some of the scans do not describe the identified stone, these scans are omitted when this average is calculated.

With the amount of data available, doing the embedment measurement manually is not feasible. In order to minimize the degree of error possible when calculating the embedment, an automated method needed to be established. This was done in two separate phases.

Automation Phase 1: The extraction formula

The first phase uses a formula to extract the average of the 10 highest points from the data sets at each load cycle phase using an upper and lower limit as shown in *Figure 56* below. Once this average
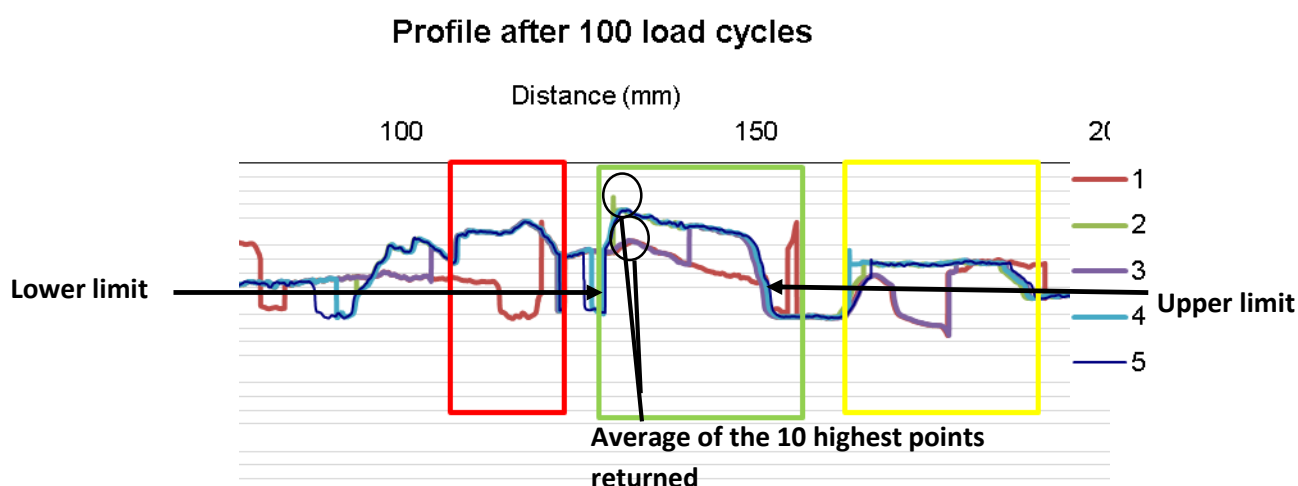
Figure 56: Establishing the depth of the stone

of the 10 highest points is extracted, the depth obtained is subtracted from the level of the very first point in the data set (the point captured by the laser before the scan begins as shown in *Section*

5.5.5 Figure 46). The value obtained is then the height of the stone relative to the reference point for that particular scan.

The stone that has been identified is however not descibed by scan 1 and 3 (red and purple lines), and is described by scan 2, 4 and 5 (turquoise and blue lines). The average of the relative height is therefore determined from scan 4 and 5 only. This value now describes the relative height of the stone using all the scans that describe the identified stone.

fx =(SMALL(INDEX('100'!$B$1:$B$11198,MATCH(BK123,'100'!$C$1:$C$11198,1),1):INDEX('100'!$B$1:$B$11198,MATCH(BK124,'100'!$C$1:$C$11198,1),1),BA125))

				100							
										omit? (1)	1
Lower Limit	129.8152174										
Upper Limit	144.7261473										144.7261
	1	2	3	4	5	6	7	8	9	10	**MEAN**
	#N/A	#N/A	#N/A	#N/A	#N/A	#N/A	#N/A	#N/A	#N/A	#N/A	**#N/A**
ref (START	219.97							Current depth			#N/A
										omit? (1)	
Lower Limit											129.8152
Upper Limit											144.7261
	1	2	3	4	5	6	7	8	9	10	**MEAN**
100	216.77	216.77	216.77	216.78	216.78	216.78	216.78	216.78	216.78	216.78	**216.78**
ref	219.97							Current depth			-3.19
										omit? (1)	1
Lower Limit											
Upper Limit											144.7261
	1	2	3	4	5	6	7	8	9	10	**MEAN**
100	#N/A	#N/A	#N/A	#N/A	#N/A	#N/A	#N/A	#N/A	#N/A	#N/A	**#N/A**
ref	219.94							Current depth			#N/A
										omit? (1)	
Lower Limit											129.8152
Upper Limit											144.7261
	1	2	3	4	5	6	7	8	9	10	**MEAN**
100	216.76	216.76	216.76	216.76	216.76	216.76	216.77	216.77	216.78	216.78	**216.77**
ref	219.93							Current depth			-3.16
										omit? (1)	
Lower Limit											129.8152
Upper Limit											144.7261
	1	2	3	4	5	6	7	8	9	10	**MEAN**
100	216.81	216.81	216.81	216.81	216.81	216.81	216.81	216.82	216.82	216.82	**216.81**
ref	219.95							Current depth			-3.14

Figure 57: Extract from Excel spread sheet which establishes the relative height of the identified stone for each scan

Figure 57 is an extract of the table used to collect the data (for the stone described in *Figure 56*). The formula tab above the table also provides the formula used to extract each data point. Essentially, what the formula does is very similar to a "V-Lookup", known as an "Index-Match" formula. Its purpose is to match the values of the upper and lower limits in the sheet containing the data for load cycle phase 100, and return the smallest (first smallest since its linked to the cell above it) value (since the lowest depth value is the highest point) between the limits provided. The cell in the column immediately next to this one would then return the second lowest value and so on. The value alongside the cell indicating "ref" is the reference point used (ie. The first value in the data set). The blue cells are used to omit a scan from the subsequent calculation. Since scans 1 and 3 are

not describing the identified stone, the blue cells have the value 1. This triggers the omit function which causes an error described by "#N/A". The scans to be ommited would generally have a relative depth varying significantly (more than 0.3 mm) from the ones describing the identified stone. The collection table used contains a table like the one described above for each trafficking phase alongside one another.

Figure 58 is an extract from the Excel spreadsheet and describes the table used to collate the data from each trafficking phase and calculate the embedment. The table shows the relative height established from each scan for each trafficking phase. It then also provides statistical information for each set of scans showing the average, standard deviation and coefficient of variation. The column labelled "strength" provides the percentage measure of the amount of scans which describe the identified stone. The embedment is quantified in the last 3 columns. The first column in this group labelled "per measurment" indicates the movement of the stone relative to the previous measurement (a positive value indicates that the stone has moved downward relative to the previous measurement). The second column labelled "last from first" indicates the embedment value of the stone after the final measurement relative to the first measurement. The last column labelled "cumulative" indicates the cumulative embedment up to that point.

Embedment Calculation										embedment		
	run 1	run 2	run 3	run 4	run 5	average	strength	std dev	COV	per measurement	last from first	cumulative
0		-7.41		-7.34		-7.38	0.4	0.044548	-0.00604			
100		-3.36		-3.16	-3.14	-3.22	0.6	0.122854	-0.03814	4.2		4.2
500	-2.24	-2.23		-2.22	-2.26	-2.24	0.8	0.01734	-0.00775	1.0		5.1
1000						#DIV/0!	0	0		0.0		5.1
5000	-1.95	-1.95	-2.02	-1.97	-1.97	-1.97	1	0.029126	-0.01477	0.3		5.4
10000	-0.50	-0.50	-0.50	-0.47	-0.50	-0.49	1	0.01176	-0.02383	1.5		6.9
25000		-0.83	-0.82			-0.82	0.4	0.008485	-0.01031	-0.3		6.6
50000			-0.65	-0.70	-0.75	-0.70	0.6	0.049031	-0.06994	0.1		6.7
75000	-1.28	-1.26		-1.28		-1.27	0.6	0.013429	-0.01055	-0.6		6.1
100000	-0.60	-0.66				-0.63	0.4	0.03677	-0.05836	0.6	6.7	6.7
								0.122854	0.006039	6.7		

Figure 58: Extract from Excel spread sheet which collates the relative height data and calculates the embedment

Figure 58 also indicates that this stone could not be identified in the scans taken after 1000 load cycles. This value is therefore omitted and the embedment is not known for this phase. The last

value in the "per measurement" column is the sum of the embedment values obtained after each trafficking phase. The fact that this value is equal to the last value in the "cumulative" column provides confidence that the stone being observed is the same throughout the trafficking phases.

In order to successfully use this formula, the templates provided must be used in precisely the same format. The formula references the sheets and cells based on the structure used in this study. (The template for this table is found as part of the data CD.

Automation Phase 2: The Identifier MACRO

The second phase of the automation process makes use of Excel's Visual Basic programming environment (VBA). This automation phase was completed during the data processing phase of this study and was successfully used to process about half of the data. What the MACRO allows is to simply click on the lower and upper limits for each set of scans, and the values are automatically entered into the upper and lower limit cells shown in *Figure 63*. Once the two limits are entered, it then also requests the user to input the run to be followed (this would be one of the runs/scans visibly describing the identified stone) and would highlight the upper and lower limit cells blue (instead of their original grey). It also has a function that clears the upper and lower limits of all the trafficking phases and colours all the upper and lower limits to their original grey.

The commands of the MACRO are described below along with a brief description of their functions.

FIX ME

This MACRO can be accessed using the MACROs tab in Excel's "developer" ribbon. This clears the cache allowing the other MACROs to initiate successfully. This MACRO must be executed once the sheet has been set up accordingly.

CLEAR (Ctrl+H)

This command brings up the input box shown in *Figure 59,* and clears the upper and lower limit values and also sets the upper and lower limit cells back to their original grey colour. Inputs include 0, 100, 1000 etc to clear a specific trafficking phase's limits, and 'all' which would clear all the limits and set them all back to grey.
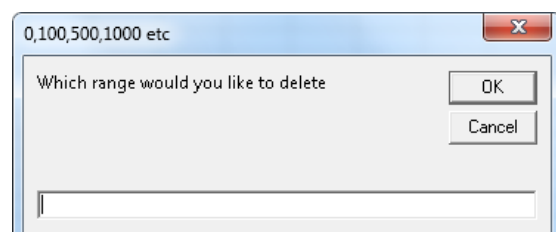
Figure 59: Clear (Ctrl+H) command input box

START (Ctrl+Q)

Once this command is initiated, the MACRO would be active.

A first click on any of the charts (click must be on a data series) would enter the clicked position into the lower limit of that specific scan data set and bring up the textbox shown in *Figure 61.* The textbox provides details about the clicked point. Of importance here is the "X" which is the value that is entered as the lower limit. One should also ensure the "Index" corresponds with the chart being clicked. (it should be in order: the first chart being 0 load cycles should be
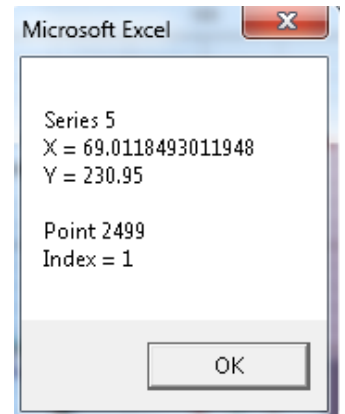
Figure 61: Information textbox

index 1, the second chart being 100 load cycles should be index 2 etc.). The second click would then enter the clicked position into the upper limit of that specific scan data set and pop up the same textbox shown in *Figure 61*. If there are already values in the upper and lower limit cells of the data set, the textbox shown in *Figure 62* will appear (values can be cleared using CLEAR function described previously). Once the upper limit is added, the input box shown in *Figure 60* will appear. A numerical input is required (between 1 and 5) to indicate which repeat scan describes the stone that is identified. This would then highlight the upper and lower limit cells of that specific run blue as shown in *Figure 63*.
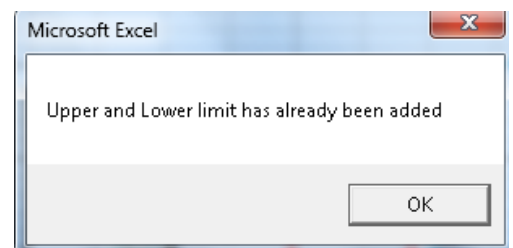
Figure 62: Values present textbox
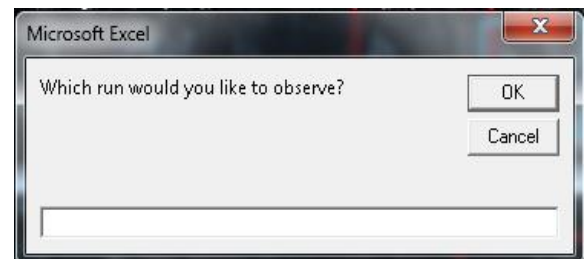
Figure 60: Observation input box
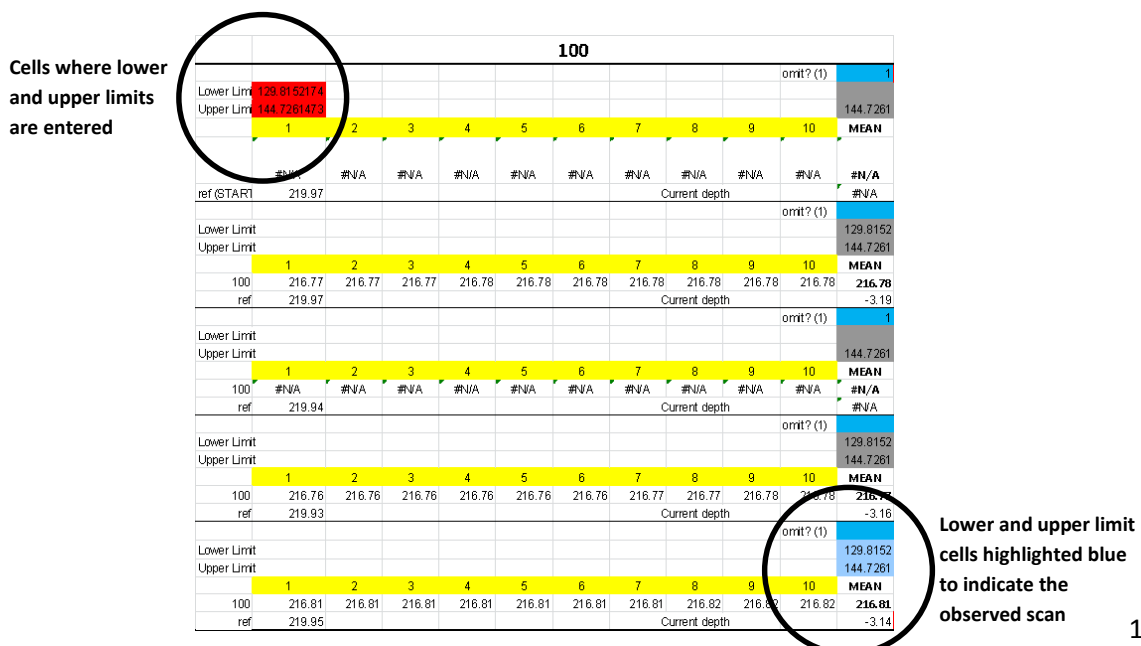
Figure 63: Where clicked limits are added and observer scan is highlighted

102

Once a table has been completed, it should be copied and pasted somewhere before the next measurement is started. The MACRO is linked to specific cells so the position of the table should be kept consistent for the MACRO to function correctly.

STOP (Ctrl+W)

Stops the MACRO functionality.

The successful implementation of this seemingly simple MACRO signifcantly decreased the processing time during this study and could possibly aid future studies with similar data processing requirements. The MACRO can easily be modified and improved by a capable VBA programmer.

The MACRO files can be found on the data CD provided with this report and can be added to the spreadsheet once all the charts are present (charts should be copied to the sheet in order to maintain the correct index values).

5.5.7 (g) Summary

The following points summarise the process described above:

1. Import data to Excel and trim the data sets as described in *5.5.7(a)*
2. Copy these values into the corresponding sheets in the spreadsheet *final LTM data template MACROv3.xlsm* into the "laser height column
3. Input the length of the laser track
4. Repeat this for runs 2, 3, 4 and 5
5. Click "COMBINE" on the sheet labelled "RUN 5"
6. Align the repeat scans as described in *5.5.7(d)* and rename this sheet to load cycle phase
7. Copy this sheet into the template *embedment template v2.xlsm*
8. Repeat for all load cycle phases
9. Copy aligned charts from each load cycle phase sheet into the embedment sheet
10. Identify measurable stones as described in *5.5.7(e)*
11. Copy MACROS into spreadsheet
12. Run "FIX ME"
13. Clear cells (Crtl+H)
14. Initiate MACRO (Ctrl+Q) and measure embedment as indicated in *5.5.7(f)*

5.6 Theoretical Analysis

5.6.1 Introduction

The behaviour of a seal under the dynamic effects of traffic is not very well documented in literature. Details as to the effects of traffic on a seal are not easily found and seal designs are based largely on empirical methods as well as experience. Literature on embedment specifically, as a failure mechanism in seals, is even scarcer. There are a few studies that have been conducted, very few specifically investigating embedment in seals, yet still provide some insight and information regarding this phenomenon. This section will aim to analyse such existing literature and based on this and the knowledge gained from research done on the subject matter, predict the behaviour of the seal from an embedment standpoint.

If the seal stones are embedded to a proper depth, the adhesive ability of the binder is greatly improved, and the potential for aggregate loss is reduced (Shuler, 2010). It is clear from literature, that a degree of embedment is desirable during the construction process of the seal. Seal designs in SA use this principle as part of the design method for single seals. It is indicated that although the degree of embedment may vary, for design purposes it is taken as 50% of the embedment expected with time, and this embedment potential is established using the ball penetration test (TRH3, 2007). This implies that the construction process i.e. rolling and compacting of the aggregate, should orientate and embed the aggregate 50% of the total embedment that is expected. The rest of the embedment would then take place under the influences and forces of traffic. This study will aim to establish the rate at which this post-construction embedment occurs and also the total degree of embedment that can be expected using the comparative seal design parameters that follow.

5.6.2 Traffic (0 to 100 000 load cycles)

As noted previously, a degree of embedment is desired for the long term effectiveness of a seal. This initial embedment induced through the construction process of a seal in practice will not be effectively mimicked in this study due to the lack of a suitable compactor for this purpose. It is thus noted that the seals in this experiment, after its construction, would achieve that initial embedment through the trafficking forces applied using the MMLS3. It is expected that the seal stones would reach its "post-construction" orientation and initial embedment after a maximum of 1000 load cycles. And the embedment that occurs thereafter would be considered as long-term embedment. This rationale will be confirmed and possibly adjusted based on the data collected in this study. The expectation then is that the seals experience a very high rate of embedment initially, followed by a

slower rate of embedment approaching the maximum degree of embedment equal to the embedment potential (ball penetration).

5.6.3 Tack coat binder type (Pen 70/100 vs. SE-1 vs. CAT65 vs. SC-E1)

It is expected that the rate of embedment for the hot applied binders should be very close to their emulsion counterparts since the application rate of net cold binder used will be the same. It should be interesting to see the difference between the modified hot binder (SE-1) used and the modified emulsion (SC-E1) since they have been modified using different polymers (SBS and SBR latex repectively). The study done on *Bitumen Rubber Chip and Spray Seals in South Africa* by Hoffmann and Potgieter (2007) allures at the idea that the use of the SE-1 (since this study was conducted on bitumen rubber specifically) could possibly see a lesser degree of embedment compared to the conventional binders due to the increase in stiffness and softening point compared to conventional binders although perhaps not as pronounced in the case of the use of bitumen rubber which has shown to have a much higher softening point and elastic recovery compared to straight binders.

The TRH3 discusses the use of modified binders in seal design. It is indicated that much research work is still required to perfect the theory of application rate design, taking into account all the factors influencing the initial and long term performance of a seal. It is then noted that the application rate used with modified binders is increased using a single function applied to the application rate when using conventional binders. The functions used to make these adjustments are based on the experience and opinions of a panel of current practitioners. For the purpose of this study, the application rates will not be adjusted when using the modified hot binder SE-1 or the modified emulsion SC-E1. This would ensure that the application rate itself is not a variable and will allow the binder type to be isolated as an influence factor.

5.6.4 Seal aggregate configuration (dense sh-sh vs. open sh-sh)

The two configurations are distinguished by the number of contact points between each aggregate particle with the dense sh-sh having significantly more points of contact than the open sh-sh configuration. It is expected that the open sh-sh configuration would allow for much more initial stone reorientation, but once this has occurred, the degree of embedment should not be dramatically different from the dense sh-sh configuration. Embedment in seals with an open sh-sh configuration would however be governed by the bitumen type more so than the seals that are densely packed. This would be due to the bitumen being in a more continuous phase compared to the densely packed seal where the aggregate would be the continuous phase. It should however be

noted that the behaviour of the seals in these varying configurations would also depend on how effectively these configurations can be imitated and constructed in a laboratory environment.

5.6.5 Seal aggregate size (13.2 mm vs. 19 mm)

Being only a limited study in this project, the use of 19 mm stone will only be applied in a dense sh-sh packing. Literature vaguely describes that the use of stones which are too small could lead to early embedment leading to loss of texture and, in extreme cases, excessive bleeding; while the use of stones which are too large may result in the immediate failure of the surface seal due to stripping of the binder from the aggregate under traffic loading (Read & Whiteoak, 2004). Since stripping and corresponding chip loss is largely affected and induced at high traffic speeds, and the trafficking speed that will be applied to seals in this study is considerably lower than the traffic speeds on seals in practice, stone loss should not occur. If Read & Whiteoak's (2004) statement holds true for the entire spectrum of seal aggregate sizes, then a higher degree of (initial) embedment should be seen in the smaller sized aggregates compared to the larger 19 mm aggregates.

6. RESULTS AND INTERPRETATION

6.1 Introduction

The testing phase of this study presented many challenges and unforeseen obstacles, all of which are discussed in detail in *Section 5.5.* Many of them only presented once the testing began and were only then addressed. Due to this, the first MMLS trafficking run on Tiles 1 and 2 became the trial samples. Due to the restrictions during the testing phase (time, sample preparation time and space etc.) it was not feasible to reconstruct and test these tiles. They did however serve a valuable function as the calibration tiles for the rest of the testing phase. The data obtained from these tiles should be seen as preliminary tests, rather than identifying governing behaviour. Their use as the trial samples proved to be vital for the tests that followed.

This section will present the results of some of the pre-investigations followed by the LTM data after the accelerated testing. The data, after passing through an intensive processing phase, is presented as plots indicating the stone levels against the number of load cycles, essentially representing the movement of different stones on each tile at various positions relative to the wheel path over time. The various parameters are then compared and observations and trends are noted. Interpretations of the results are made as the comparisons are discussed and an overall summary is presented thereafter. The last section of this chapter details regarding important recommendations based on the challenges during the research and experimental testing phase of this study.

6.2 Results

6.2.1 Ball Penetration Tests

6.2.1 (a) General

Throughout the testing phase of this study, consideration was given to the ball penetration tests. This test, being the only test that attempts to quantify seal stone embedment was deemed an important control to be used in conjunction with the physical embedment measurements. Since the ball penetration test essentially penetrates the surface effectively damaging the base, the decision was made to do the ball penetration tests once the traffic simulations had been completed. This would allow the base to be largely intact during the trafficking phase of the tests and would also provide an idea about the hardness and embedment potential after the moisture content of the base had stabilised. It is assumed that these ball penetration measurements describe the embedment potential of the constructed base as it had been during the trafficking phase. The spaces in between the seal tiles provided sufficient room to do ball penetration tests close to the measured

stones. The results of the ball penetration tests once the trafficking phase had been completed are tabulated (*Table 13*) and *Figure 64* provides the positions where the tests were done. A colour key is provided to visually indicate the embedment potential with yellow being the lowest potential for embedment and red being the highest potential for embedment.

Table 13: Ball Penetration Test results

			Ball Penetration Tests				
Test number	d_1 (mm)	d_2 (mm)	Ball penetration (mm)	Test number	d_1 (mm)	d_2 (mm)	Ball penetration (mm)
1	50	53	3	25	51.5	53.5	2
2	52	54.5	2.5	26	54.5	57	2.5
3	52	54	2	27	52.5	54.5	2
4	52	54	2	28	54	56.5	2.5
5	51	54.5	3.5	29	53	55.5	2.5
6	55	57	2	30	52	54.5	2.5
7	51.5	54	2.5	31	53	55.5	2.5
8	50.5	53.5	3	32	52.5	56	3.5
9	52	54.5	2.5	33	51	53.5	2.5
10	51.5	54	2.5	34	53	55	2
11	52	54	2	35	53	55	2
12	51	53.5	2.5	36	53.5	56	2.5
13	51	53.5	2.5	37	53.5	56	2.5
14	51	53	2	38	51	53.5	2.5
15	52	54	2	39	53.5	56	2.5
16	54	55	1	40	51.5	54	2.5
17	54	56.5	2.5	41	53.5	56.5	3
18	52	55	3	42	52	54	2
19	52.5	55	2.5	43	56	58	2
20	53	55	2	44	53.5	56	2.5
21	51.5	54	2.5	45	59.5	61.5	2
22	53	55	2	46	54	56	2
23	54	56	2	47	53.5	56	2.5
24	53	55.5	2.5	48	53.5	55.5	2
					Mean		2.36
					Standard Deviation		0.43
					COV		0.18

Statistically, the results appear to be satisfactory. The high standard deviation is due to the seemingly wide range across which the values present. The simplicity of the test would warrant a relatively high standard deviation due to the magnitude of the values obtained. In terms of the practicality of the test itself, this result is acceptable. The coefficient of variation also indicates that the degree of variability is much lower than the level of deviation from the mean. This provides additional confidence in the ball penetration test results obtained.
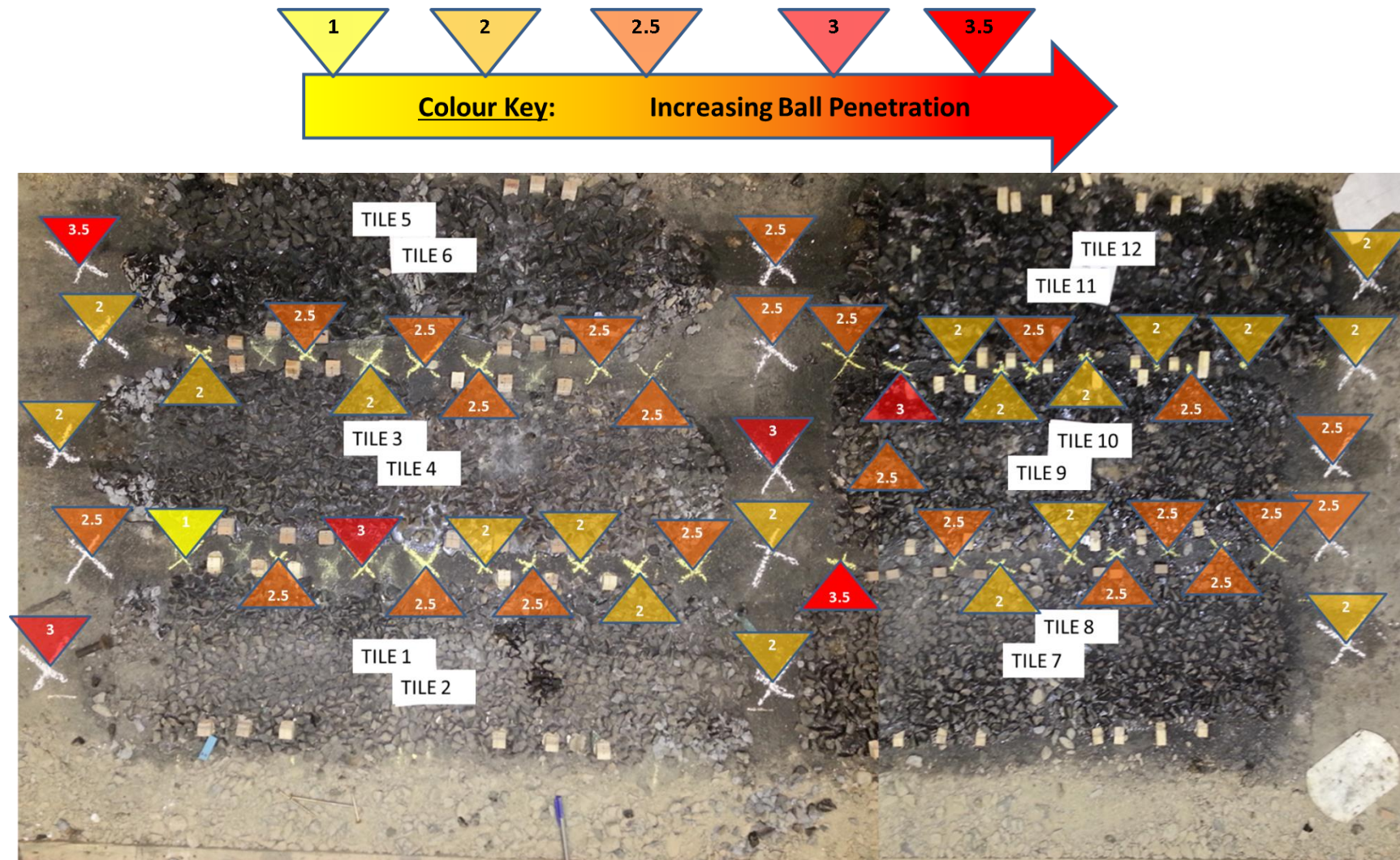
Figure 64: Ball Penetration Test positions

The ball penetration values vary between 1 mm and 3.5 mm with very few results measuring these extreme values. The average ball penetration across the entire base is about 2.5 mm and the measurements appear to vary randomly with no indication of a distinct pattern.

As previously noted, the TRH4 (2007) seal design method assumes that 50% of the total embedment that seal stones will undergo, measured using the ball penetration, is achieved during construction. It is unclear whether this assumption takes stone reorientation into account but for the purpose of this study it will be assumed that it excludes the change in the maximum height of the stones due to stone reorientation. This can be rationalised by the fact that the absolute height of the stone could change dramatically if an accurate line of measurement is maintained. Roller passes during seal construction ensures that the stones are effectively reoriented. This reorientation most likely takes place during the first or second pass. The passes that follow would then embed the stone to the initial embedment depth. If the assumption in the TRH's seal design process is accurate, the initial embedment (equivalent to the 'construction embedment') once the stones have been reoriented would be approximately 1.25mm and the maximum embedment would be around 2.5 mm on average. The ball penetration results do however indicate that this maximum embedment could be up to 3.5 mm.

This concept will be kept in mind during the analysis of the embedment data obtained in the subsections that follow. The LTM analysis will provide further insight as to the movement of the stones and perhaps verify merit of this critical design assumption.

6.2.1 (b) Embedment potential for each tile

The ball penetration values obtained in the vicinity of each tile are averaged and used as an indication of the relative embedment potential of that area. This provides additional information for the analysis of the seal design parameters that follow. The properties of each tile are provided along with the established embedment potential based on the ball penetration results in the vicinity of that tile.

Figure 65 below graphically indicates the zones of each tile. The embedment potential is taken as the average of the embedment values that fall within the zone of the tile (zones are separated using different colours in each row). Measurement points occurring in overlapping areas will contribute to the embedment potential of all relevant tiles. The results are then summarised in *Error! Reference source not found.*
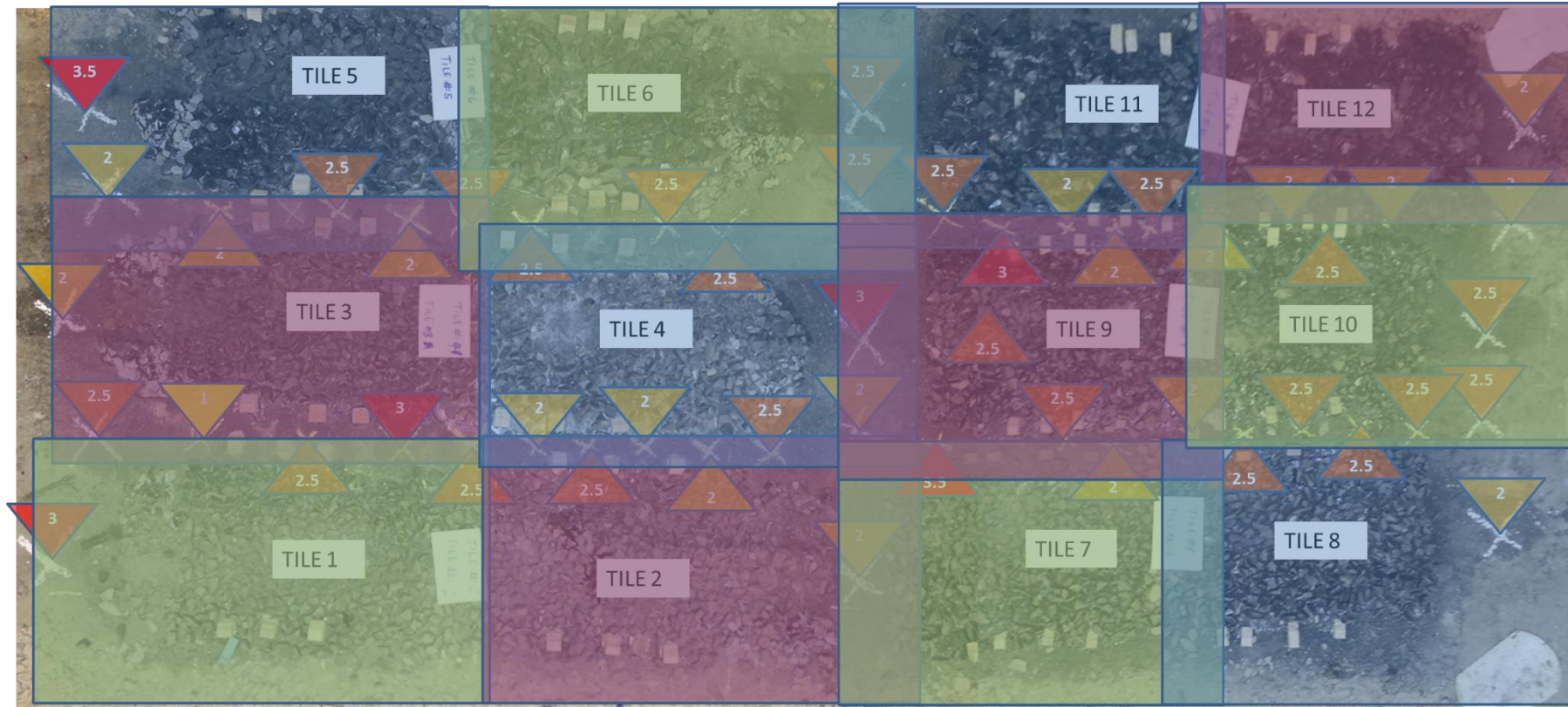
Figure 65: Embedment potential zones

Table 14: Embedment Estimations based on allocated zones

Tile Number	Design Parameters			Statistics				
	Binder	Aggregate Configuration	Aggregate Size (mm)	Number of measurements in vicinity	Mean (mm)	90th Percentile (mm)	Standard Deviation	COV
1	pr.SE-1	dense sh-sh	13.2	6	**2.4**	**3.0**	0.74	0.30
2	Pen 70/100	dense sh-sh	13.2	8	**2.2**	**2.5**	0.26	0.12
3	pr.SE-1	open sh-sh	13.2	10	**2.3**	**3.0**	0.59	0.26
4	Pen 70/100	open sh-sh	13.2	11	**2.4**	**2.5**	0.32	0.14
5	pr.SE-1	dense sh-sh	19	6	**2.4**	**3.0**	0.58	0.24
6	Pen 70/100	dense sh-sh	19	6	**2.5**	**2.5**	0.00	0.00
7	SC-E1	dense sh-sh	13.2	5	**2.4**	**3.1**	0.65	0.27
8	SC-E1	open sh-sh	13.2	7	**2.4**	**2.5**	0.24	0.10
9	Cat65	dense sh-sh	13.2	11	**2.4**	**3.0**	0.38	0.16
10	Cat65	open sh-sh	13.2	12	**2.3**	**2.5**	0.26	0.12
11	Cat65	dense sh-sh	19	8	**2.4**	**2.7**	0.35	0.15
12	SC-E1	dense sh-sh	19	6	**2.1**	**2.3**	0.20	0.10

As expected, the standard deviation is generally high. As mentioned previously, this is due to the sensitivity of the values to the varying ball penetration measurements. It is very difficult to assign a particular ball penetration value to each stone, LTM position or tile measured. Averages range between 2.1 mm and 2.5 mm indicate that the embedment potential is very similar for all the tiles with the statistics indicating a significant degree of variation is to be expected.

6.2.2 LTM measurements: Overview

As discussed previously, as many stones as possible were identified within the wheel path and measured. There were also stones (at least one) identified outside of the wheel path and measured at each position. It became apparent that even stones well outside the path of traffic experienced some degree of displacement. This displacement also followed a distinctive pattern based on the distance from the centre of the wheel path. The graphs that follow are the cumulative embedment measurements on tile 7. Each plot indicates a different zone of measurement described in *Figure 66.*

Figure 66: LTM measurement zones as

Figure 67: Embedment plots for TILE 7 in different measurement zones

113

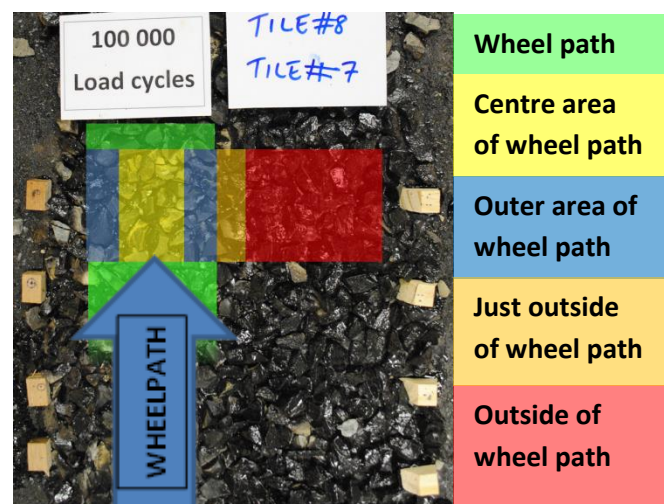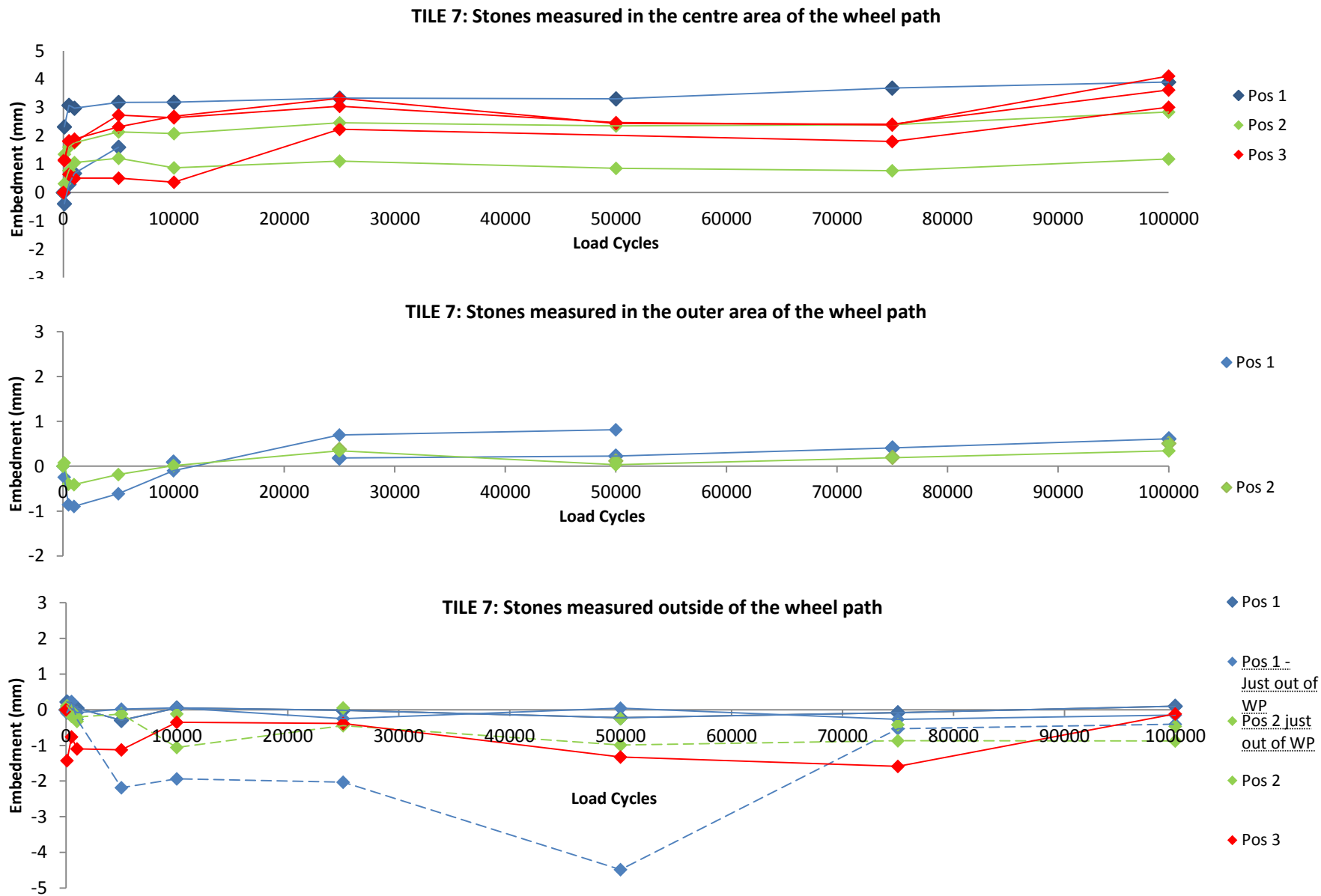The collection of graphs shown in *Figure 67* displays the embedment measurements in the different measurement zones described in *Figure 66*. The legend in each of the graphs indicates which position on each tile the measurements were taken. In the case of the last graph, the legend also indicates the "just outside of wheel path" measurements. The embedment axis, in the case of all the plots that will be shown and discussed, represent the cumulative displacement of the stones through the various load cycle phases.

Although the stones were measured at different positions (as indicated by the wooden markers in *Figure 66*) the different measurement zone plots are the collected measurements from these different positions and a distinct correlation can be seen between the various positions. The plots follow a very similar pattern when looking at the measurements taken in the centre of the wheel path zone. This correlation is also visible in the second graph which describes the measurements taken in the outer area of the wheel path. Together, these two zones describe the wheel path area and show very clearly that the degree of movement in the centre zone is much higher than in the outer zone. This distinct difference is what motivated the division of the wheel path area into two zones. The stones in the centre of the wheel path appear to be affected more directly by trafficking forces when compared with the stones in the outer area of the wheel path. Most of the stones in the centre area reached embedment values in the range of 3 to 4, whereas the stones in the outer area experienced much less vertical displacement.

The last plot provides an indication as to the movement of the stones outside of the wheel path. This zone is also divided into two distinct areas, the zone just outside the wheel path and the zone further from the wheel path. It has been noted that the stones just outside the wheel path tend to move upward relative to their initial position and these effects decrease in measurements taken further from the wheel path. This is illustrated by the dotted lines in the last plot in *Figure 67.* This upward movement (2) of the stones just outside the wheel path occurs due to the downward movement (1) of the stones inside the wheel path. As they are displaced, they force the stones next to them to move away (3) from the zone of trafficking. The stones closest to the wheel path are affected directly and could possibly tilt depending on the orientation of the stones. One side of the stone could shift upward while the other is forced downward. This concept is illustrated in *Figure 68* and would explain the negative embedment values (indicating an upward displacement) of the stones just outside the wheel path.

The overview of the LTM measurements are generalised here using TILE 7, but these concepts indicate the general behaviour and movement of the stones relative to the zone of measurement in all the seal tiles that were tested.

For the comparative purposes in the subsections that follow, only the stones measured in the centre of the wheel path are used when comparing the effects of the various seal design parameters. The measurements taken without an initial "zero" load cycle identifier is also omitted from the comparative plots. These results were thought to provide information about the trend, and not so much regarding the actual embedment reading since it lacked a critical initial benchmark measurement. Since the measurements on each different position correlate fairly well, there are a considerable number of measured stones with a benchmark initial measurement for each parameter and the inclusion of these trend supporting stones were deemed unnecessary. They would effectively overpopulate the plots allowing the trends to be less discernible.

Sections 6.2.4, 6.2.5 and *6.2.6* comparatively analyse the key seal variables that were investigated. In these sections, the results are summarised in the form of a table. Average, maximum and minimum plots are also used to indicate the embedment of the different stones measured at selected load cycle phases during the 'seal life period' (this concept is explained in Se... which provides a comparative view of the different variables when seen side...

Figure 68: Concept of negative embedment of the stones just outside the wheel path along with the images taken before and after trafficking

6.2.3 Traffic

Figure 70 displays all the measurements taken in the centre of the wheel plot seems overpopulated, the aim of this is to establish the general tre... vertical displacement from a traffic perspective. The plot is then divided int... (A, B and C as shown in *Figure 70*), classified based on the degree of movement measured... the measurement before it. Each of these periods displays a visible trend, perhaps not adh... all the samples, but by enough to describe a generalised behaviour pattern.

A – Initial Embedment Period

Commonly seen at the start of trafficking is the initial erratic movement of the stones where they are orientated and reoriented. After the first 100 – 500 cycles a large degree of embedment is
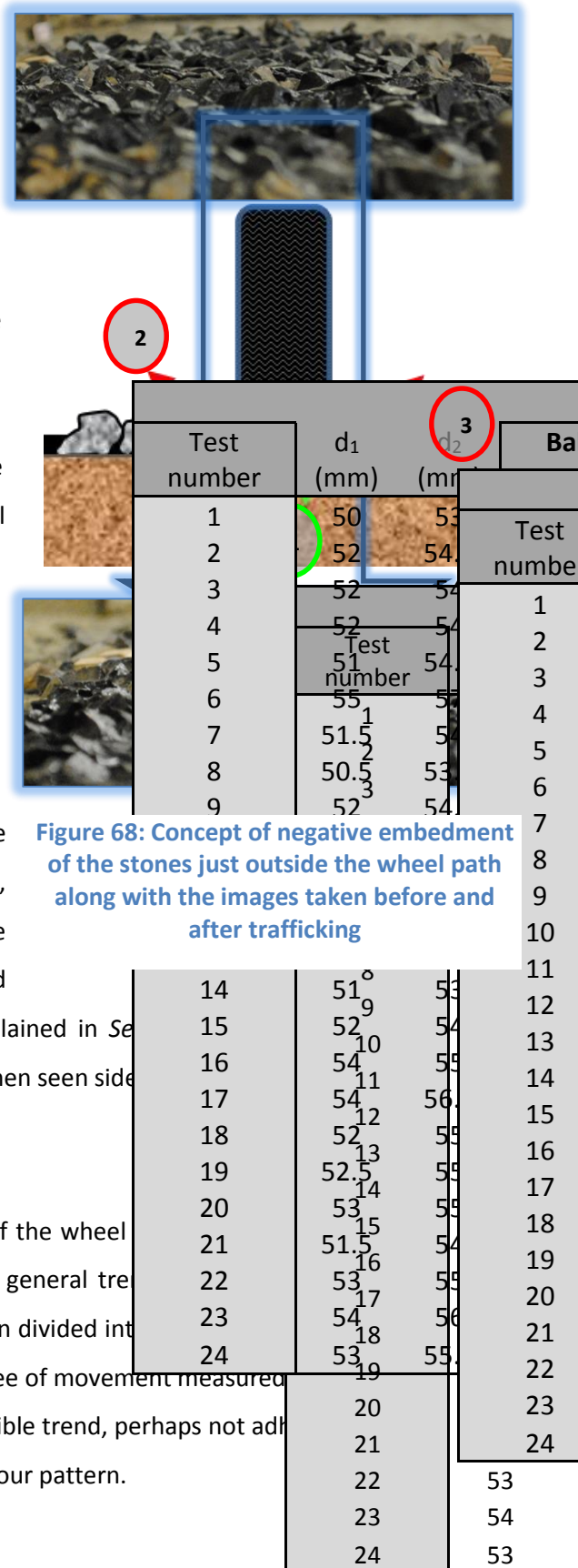
115

generally observed thereafter the stones orientate themselves until they eventually stabilise around 10 000 cycles. This stabilisation was initially predicted to be much sooner, but the forces of drum rollers in construction was dramatically underestimated. It is thus estimated that it takes approximately 10 000 MMLS load cycles to effectively produce the embedment induced during construction. During this period, the behaviour of the stones in terms of vertical displacement is unpredictable. Some stones would show an increase in apparent embedment as the stones orientate themselves onto their ALD, whereas others would show a decrease in embedment most likely due to the same mechanism of movement, but because the line of measurement remains constant, and the stones are irregular, it could easily be that the stone would indicate an increase in absolute height relative to the line of measurement. This would explain the typical decrease in embedment after 5000 load cycles. Thereafter, the stones typically would have orientated themselves effectively, and the next 5000 load cycles cause the typical increase in embedment until stabilisation at 10 000 cycles. In practice, the construction of the seal would facilitate this initial movement and embedment of the stones and the seal life would essentially only begin thereafter.

B and C – Seal Life Period

When looking at a cluster of data, the behaviour of the stones during this period varies dramatically. Both of these periods do however indicate that the movement of the stones is slight, and this behaviour is what is generally expected during the seal life. Many stones show the typical gradual increase in embedment over time (time of course relating directly to the number of load cycles). Some stones in period **B** do display a slight decrease in embedment, which could be attributed to one of two things. 1) The initial orientation had not stabilised yet (which would explain the decrease in embedment between 10 000 and 25 000 cycles). 2) The stones were beginning to dislodge and were again reorientating themselves due to the loss of adhesion between the tack coat and the stone surface (which could explain the decrease in embedment at some point after 25 000 cycles). Despite the mechanism governing the movement, the rate of change in the embedment measurements remain relatively small. This behaviour stretches on into period **C**, but what is also observed here in a number of cases is the relatively large increase in embedment after the 75 000 cycle mark.

This could be explained by some of the same mechanisms that were just discussed, but could also be due to the shearing forces of the irregular particles on the uppermost portion of the base. Conceptually shown in *Figure 69*, the top 5 to 10 mm of the base experiences load concentrations (2) due to the irregularities in the stone surface that is in contact with the base and with constant orientation (1) could cause abrasion and softening of this uppermost part of the base due to the

resulting shear forces (3). This behaviour has been verified through research done by Gerber (no date). His work involved the analysis of this region of the base using a 2-dimensional finite element model. He notes that the uppermost parts of the base (top 5 to 10 mm) have much higher shear forces compared to the lower regions. This loss of stiffness typically presents a large number of load cycles and would cause the rate of embedment to increase significantly as the base allows the stones to penetrate more rapidly due to the loss of shear strength.

Looking at the measurements in a much less populated plot and with fewer variables could provide a better understanding as to which of these different mechanisms of movement are manifesting throughout the seal life cycle for the various seal design parameters.
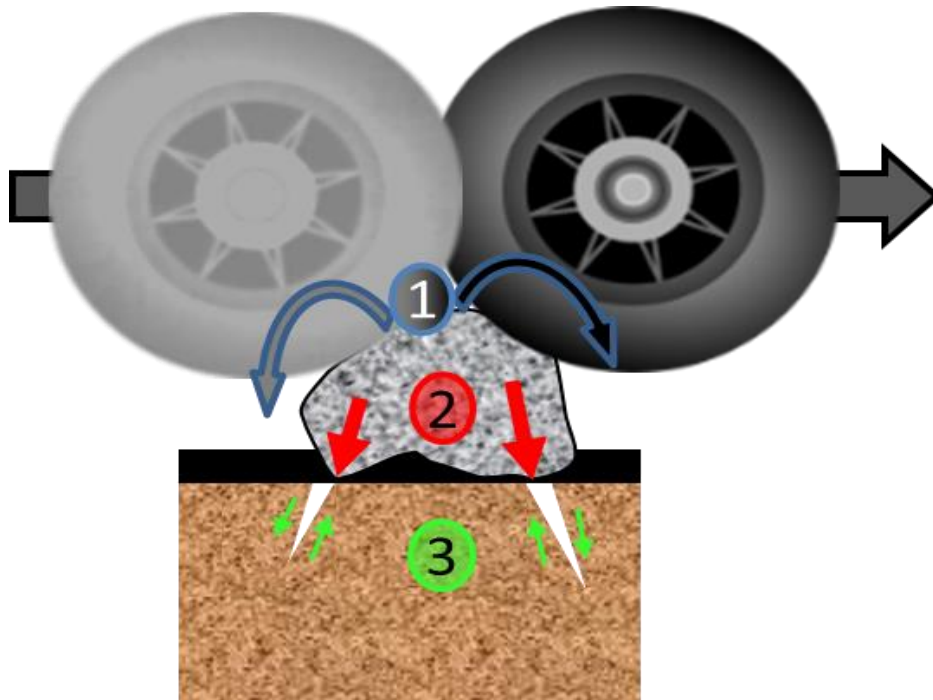

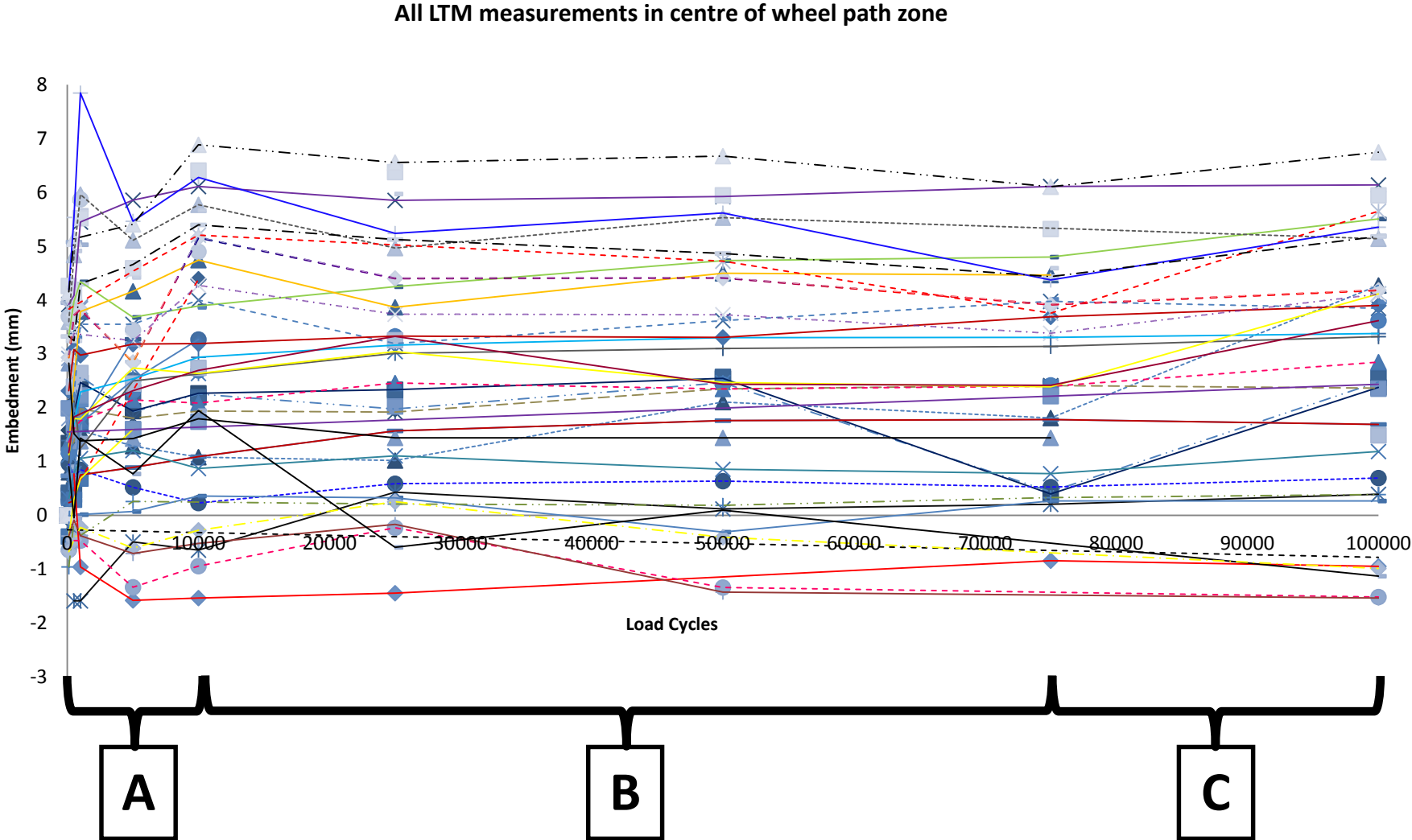**Figure 69: Stone orientation causing shear forces at the stone-base interface**

Figure 70: Plot of all LTM measurements in the centre of wheel path zone

6.2.4 Tack coat binder type

Figure 66 shows the plot of the various binder types for two different seal design parameter sets; dense sh-sh, 13.2 mm aggregate and open sh-sh, 19 mm aggregate. In both sets, the hot applied binders appear to outperform the emulsions with the penetration grade 70/100 binder clearly displaying superiority. *Table 12* that follows provides the final embedment ranges for the different binder types based on the various stones measured.

Table 15: Embedment ranges for binder type comparison

	Binder type	Range (mm)	Number of stones
Configuration:	PEN 70/100	0.3 – 3.4	5
Dense sh-sh	Pr.SE-1	2.5 – 4.5	5
Aggregate size:	CAT 65	2.0 – 6.9	5
19 mm	SC-E1	4.1 – 6.7	6
Configuration:	PEN 70/100	0.7 – 5.5	4
Open sh-sh	Pr.SE-1	2.4 – 6.1	4
Aggregate size:	CAT 65	-1.5 – 1.5	6
13.2 mm	SC-E1	0.4 – 6.1	3

Figure 73 provides the better representation of the ranges shown in the table above and provides additional details that support the deduction that the hot applied binders perform better than the emulsions. Three trafficking phases are also graphically displayed. The hot binders generally reach stability earlier (at around 5000 load cycles) and the penetration grade binder shows a very gradual increase in embedment in both variable sets. The precoated SE-1 shows a similar gradual increase in the case of the dense 19 mm tile, but also indicates a loss of adhesion leading to a dip and subsequent jump in embedment during the seal life period. In the case of the dense 19 mm aggregate, the emulsions tend to display a large total embedment relative to the hot applied binders along with the loss of adhesion during the seal life. In open 13.2 mm tiles, the emulsions perform very poorly indicating a loss of adhesion from early on in the seal life period. The CAT 65, open sh-sh 13.2 mm aggregate tile behaved particularly poorly in adhesion and was the only tile to exhibit a large degree of aggregate loss as shown in *Figure 71.* This resulted in a complete loss of adhesion in many of the stones measured on this tile due to the lack of aggregate interlock causing them to reorientate themselves and result in a negative final embedment measurement.

Figure 72 below provides a graphic representation of the average embedment measurements at three different load cycle phases during the seal life period for the two variable sets; (a) dense sh-sh, 19 mm aggregate (b) open sh-sh 13.2 mm. The graphs also indicate the maximum and minimum values providing an indication as to the range of the value. The plots reiterate how slight the movements of the stones are during the seal life period (with the exception of the CAT65 tile showing stone loss). These plots reinforce the analysis that the hot applied binders perform the best with the penetration grade showing superiority. A key observation in these plots is that the minimum and maximum values follow the same trend as the average. This indicates that although the range is fairly large, it is very similar across the different tiles.
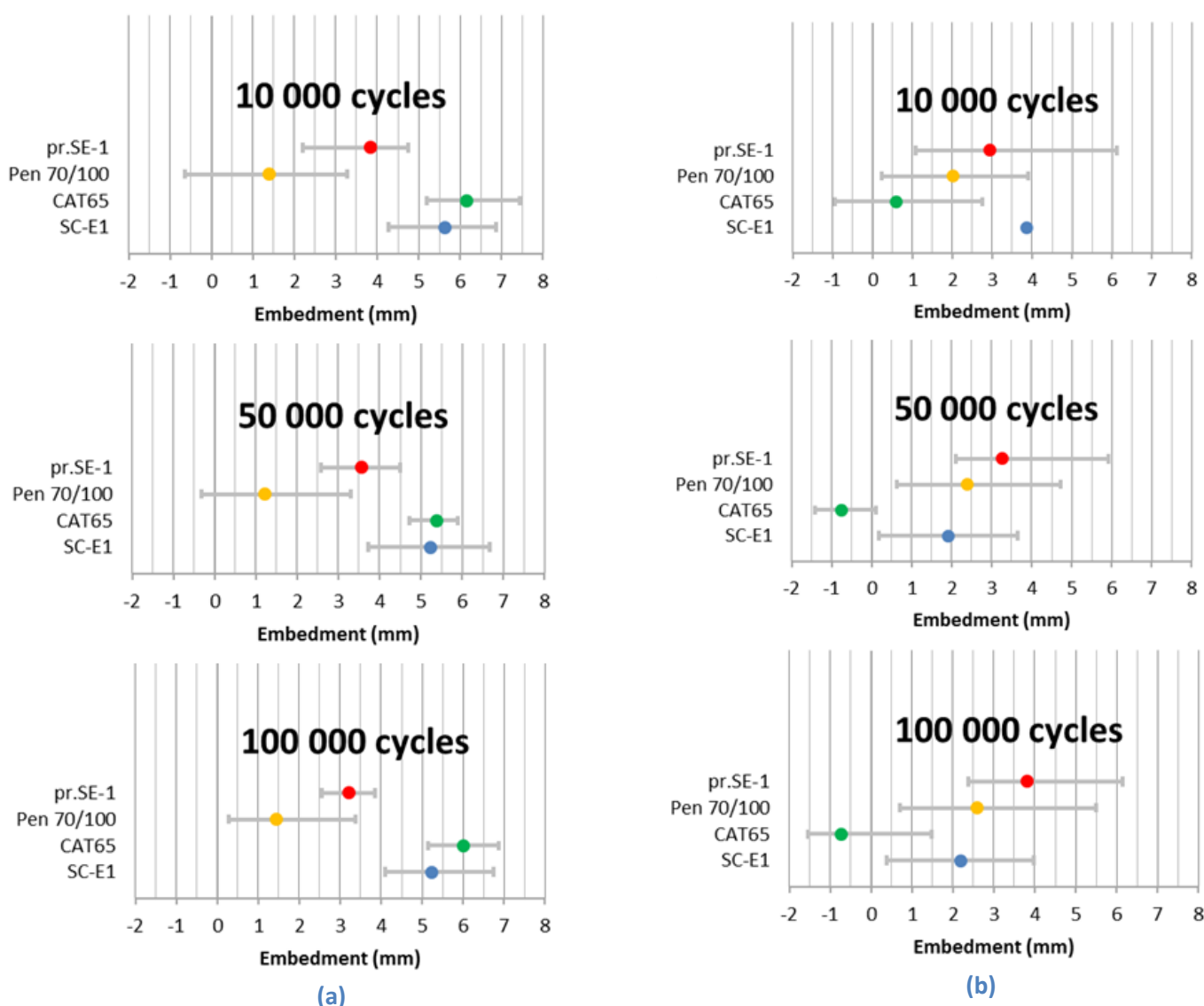

Figure 71: Aggregate loss on Tile 10

(a)

(b)

Figure 72: Average, minimum and maximum plots of the binder comparison embedment measurements (a) dense sh-sh, 19 mm (b) open sh-sh 13.2 mm
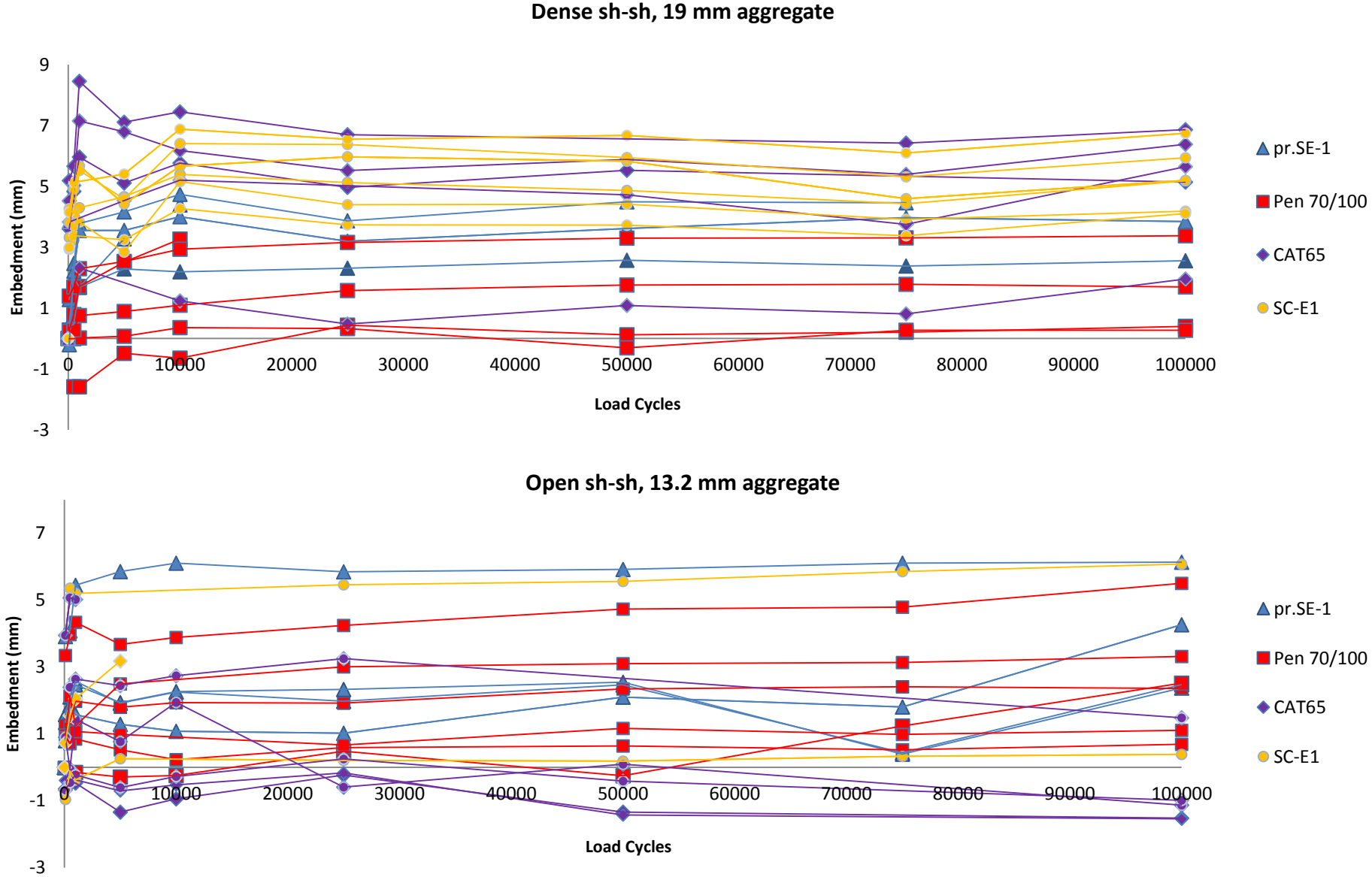
120

Dense sh-sh, 19 mm aggregate

Open sh-sh, 13.2 mm aggregate

Figure 73: Plots indicating the cumulative embedment for the four different binder types

121

6.2.5 Seal aggregate configuration

Figure 75 shows the plot of the two aggregate configurations for two different seal design parameter sets; CAT 65, 13.2 mm aggregate and SC-E1, 13.2 mm aggregate with the ranges summarised in *Table 16*. The performance of the seals from a configuration perspective is not easily discernable due to the lack of identified stones, with the few that were identifiable indicating a wide range of variance. The CAT 65, 13.2 mm tile also had aggregate loss as indicated previously (*Figure 71*) causing these measurements to be further distorted.

Table 16: Embedment ranges for aggregate configuration comparison

	Configuration	Range (mm)	Number of stones
Binder type: **CAT 65** **Aggregate size:** **13.2 mm**	Dense sh-sh	-0.9 – 2.3	5
	Open sh-sh	-1.5 – 1.5	6
Binder type: **SC-E1** **Aggregate size:** **13.2 mm**	Dense sh-sh	1.2 – 4.1	6
	Open sh-sh	0.4 – 4	2

The CAT 65, 13.2 mm tile had no aggregate loss in the dense sh-sh configuration tile indicating the regular gradual increase in embedment through the seal life period. The SC-E1, 13.2 mm tile showed no aggregate loss in the dense or open sh-sh configurations indicating this gradual increase in embedment consistently in all the stones measured. The ranges for the maximum degree of embedment are very similar in this case. It should however be noted that the open sh-sh configuration only had two stones measured through the entire load cycle spectrum not allowing much variation compared to the dense sh-sh configuration. It had been expected that the dense sh-sh configuration would indicate a higher total embedment and the open sh-sh configuration would allow for a greater amount of stone orientation due to the lower number of aggregate contact points and reduced aggregate interlock. These assumptions cannot however be confirmed based on these results.

Figure 74 provides a graphic representation of the average embedment measurements at three different load cycle phases during the seal life period for the two variable sets; (a) Cat65, 13.2 mm

(b) SC-E1, 13.2 mm. The graphs also indicate the maximum and minimum values providing an indication as to the range of the value. Of interest here is that the difference between the dense sh-sh and open sh-sh is generally quite high with the exception of the Cat 65, 13.2 mm tile and the changes in embedment are more pronounced in the open sh-sh configuration. This behaviour is most likely owing to the large difference in void content between the dense sh-sh configuration and open sh-sh configuration. Since the open sh-sh configuration has a larger amount of voids, it allows for more room for movement whereas the dense sh-sh configuration, with more contact points, shows a more gradual movement. The open sh-sh configuration also generally indicates a larger range when compared to the dense sh-sh configuration which is probably due to the same mechanism. The higher void content facilitates a greater allowance for reorientation and therefore a higher probability of drastic changes in embedment for each individual stone measured.

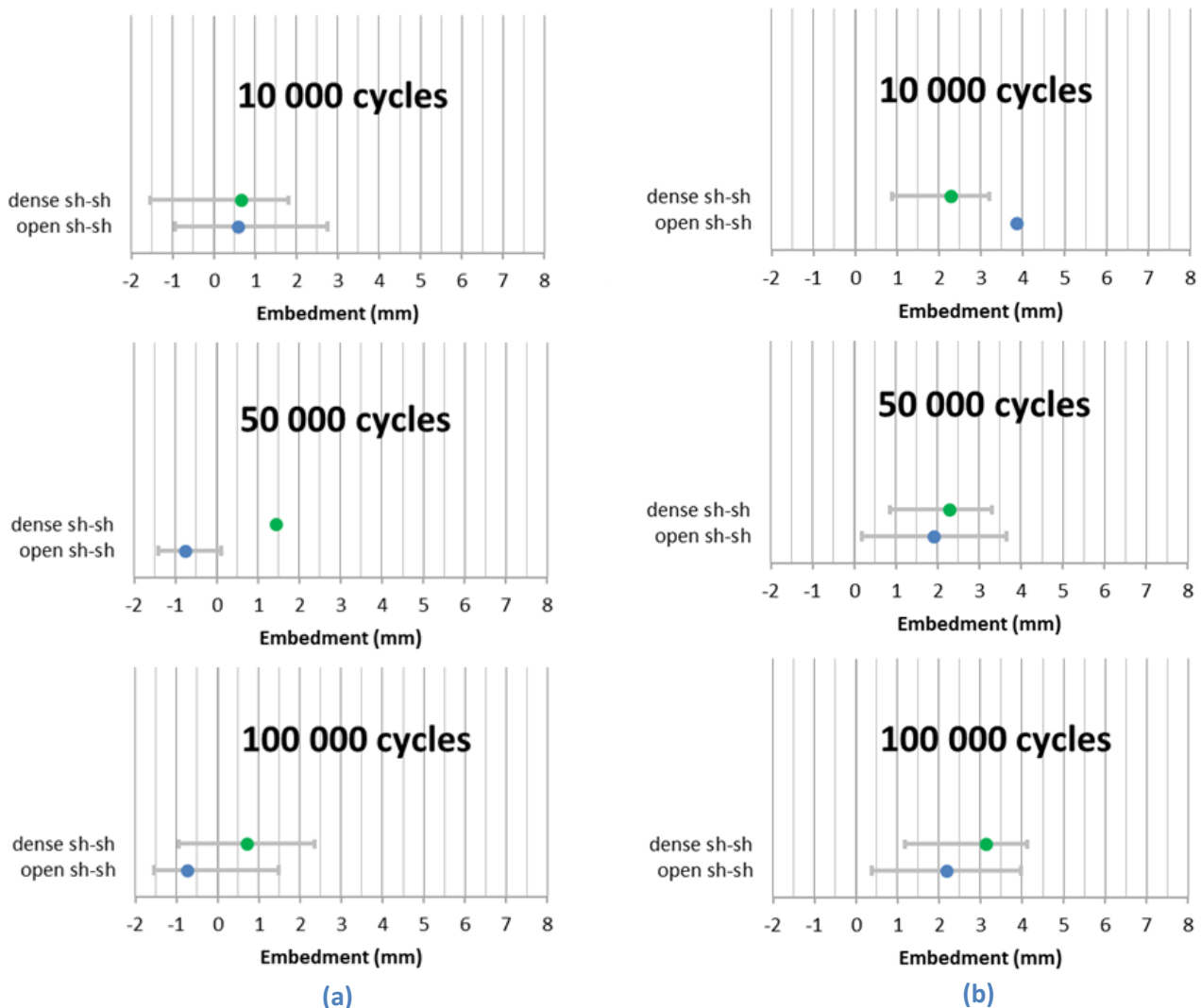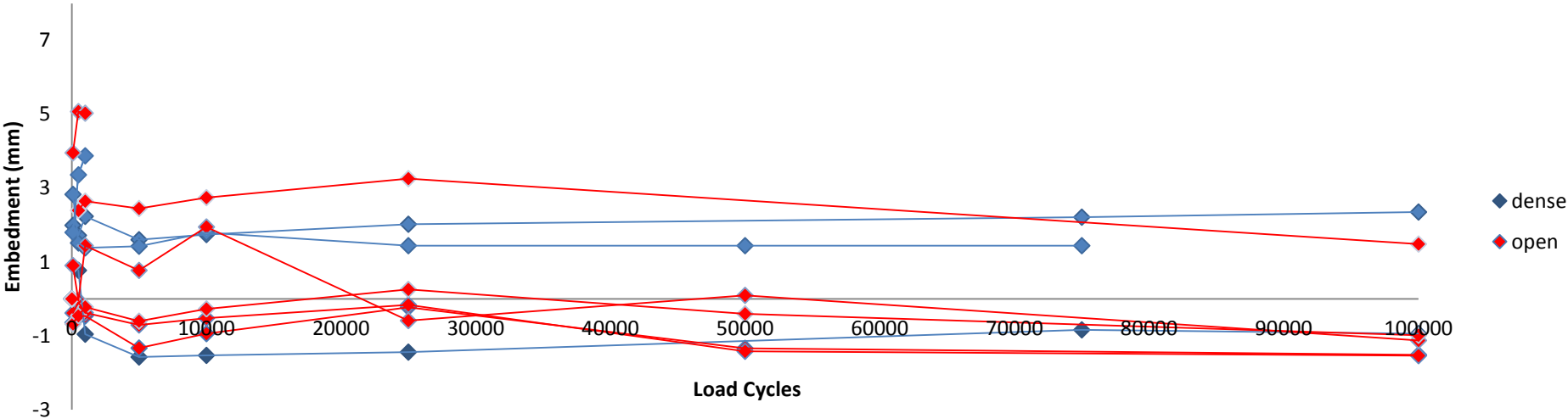(a)   (b)

Figure 74: Average, minimum and maximum plots of the aggregate configuration comparison embedment measurements (a) Cat65, 13.2 mm (b) SC-E1, 13.2 mm

123

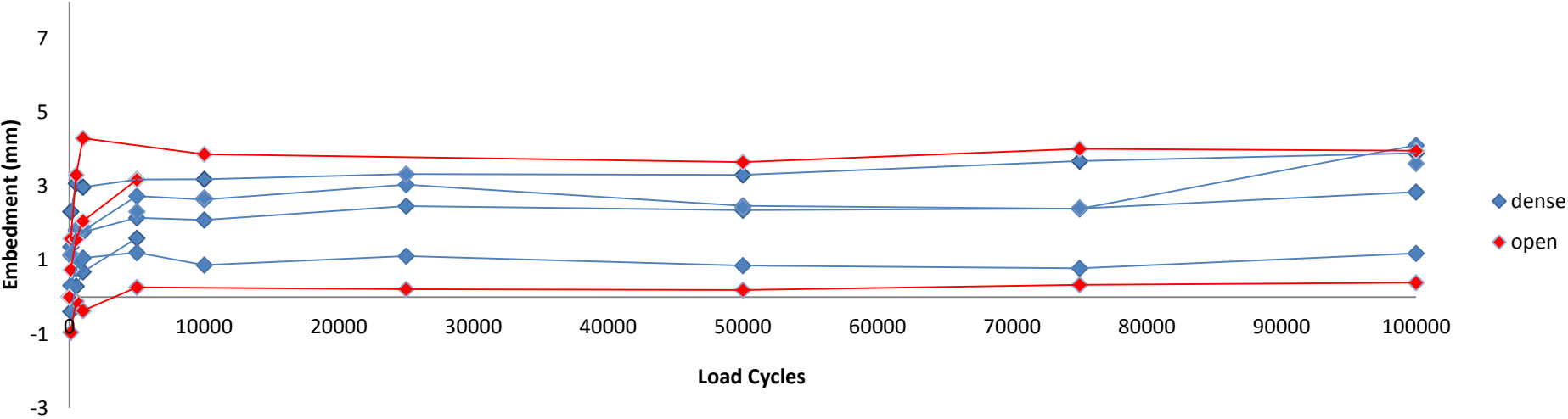# CAT65, 13.2 mm aggregate

SC-E1, 13.2 mm aggregate

Figure 75: Plots indicating the cumulative embedment for the two aggregate configurations

124

6.2.6 Seal aggregate size

Figure 77 shows the plot of the two stone sizes for two different seal design parameter sets; SC-E1 dense sh-sh, and CAT 65 dense sh-sh. In both sets, the 13.2 mm aggregate appears to outperform the 19 mm in terms of total embedment. *Table 17* that follows provides the final embedment ranges for the two stone sizes based on the various stones measured.

Table 17: Embedment ranges for aggregate size comparison

	Aggregate size	Range (mm)	Number of stones
Binder type: **SC-E1** **Configuration:** **Dense sh-sh**	13.2 mm	$0.4 - 4.0$	3
	19 mm	$4.1 - 6.7$	6
Binder type: **CAT 65** **Configuration:** **Dense sh-sh**	13.2 mm	-0.9 – 3.9	5
	19 mm	$1.9 - 6.8$	6

Figure 77 as well as the ranges shown above indicates clearly that the 13.2 mm aggregate performs better overall in terms of embedment. In both cases, the 13.2 mm seals reach stability earlier (around 5000 load cycles) and in both cases, the 19 mm stone shows a higher degree of total embedment. At around 50 000 load cycles the 19 mm seals appear to show orientation indicating a possible loss of adhesion, causing the embedment to subsequently increase. This is not seen in the 13.2 mm tiles where the degree of embedment climbs gradually throughout the seal life phase. Literature discussed in earlier chapters highlighted that larger aggregates would show a higher degree of initial embedment. This does not appear to be the case here. The 19 mm aggregate shows a higher degree of initial embedment as well as a higher degree of overall embedment relative to the smaller 13.2 mm aggregates. Of importance here could be the fact that the flakiness index for the 19 mm stone (21.9%) is considerably higher than that of the 13.2 mm stone (13.2%). The higher flakiness indicates that there is a larger percentage of flaky aggregate in the 19 mm seals. This could be the reason the initial embedment is higher, since more of the stones would tend to reorientate themselves onto their ALD causing an apparent jump in initial embedment. Despite this fact, the 13.2 mm stone has a more stable seal life period in terms of vertical displacement and this would be

125

counter intuitive from a flakiness perspective. The flakier aggregate should show a greater level of stability during the seal life, but this does not appear to be the case here.

Figure 76 below provides a graphic representation of the average embedment measurements at three different load cycle phases during the seal life period for the two variable sets; (a) SC-E1, dense sh-sh (b) Cat65, dense sh-sh. The graphs also indicate the maximum and minimum values providing an indication as to the range of the value. The plots clearly indicate the large difference in the embedment measurements between the 13.2 mm and 19 mm aggregates and this difference is maintained throughout the seal life. Although this large difference could be due to the large difference in initial embedment and orientation, both aggregate types appear to be similarly susceptible to reorientation at around 50 000 load cycles when emulsions are used. Whether or not this is the case with hot applied binders cannot be verified in this study.
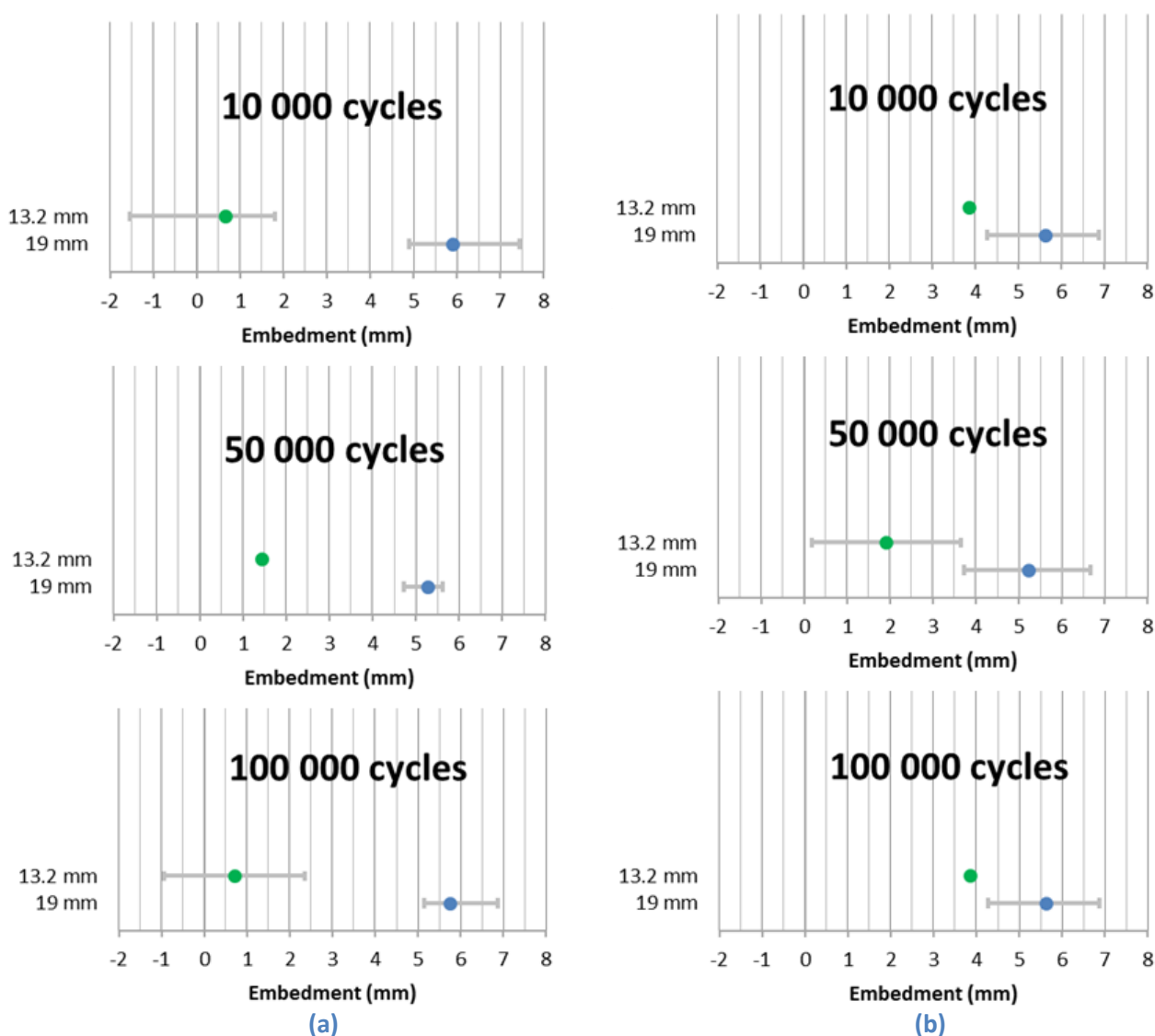

Figure 76: Average, minimum and maximum plots of the aggregate configuration comparison embedment measurements (a) Cat65, 13.2 mm (b) SC-E1, 13.2 mm

126
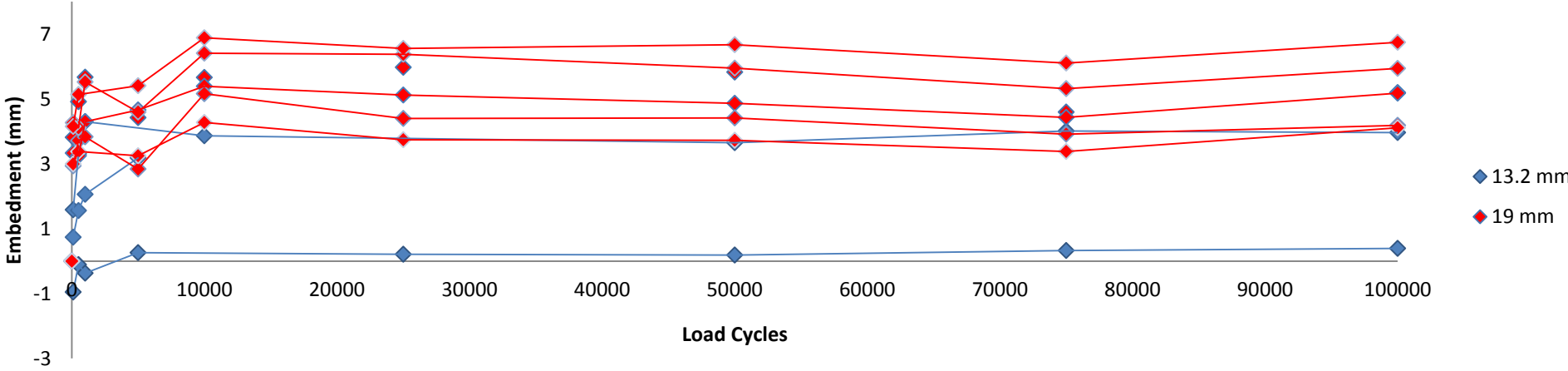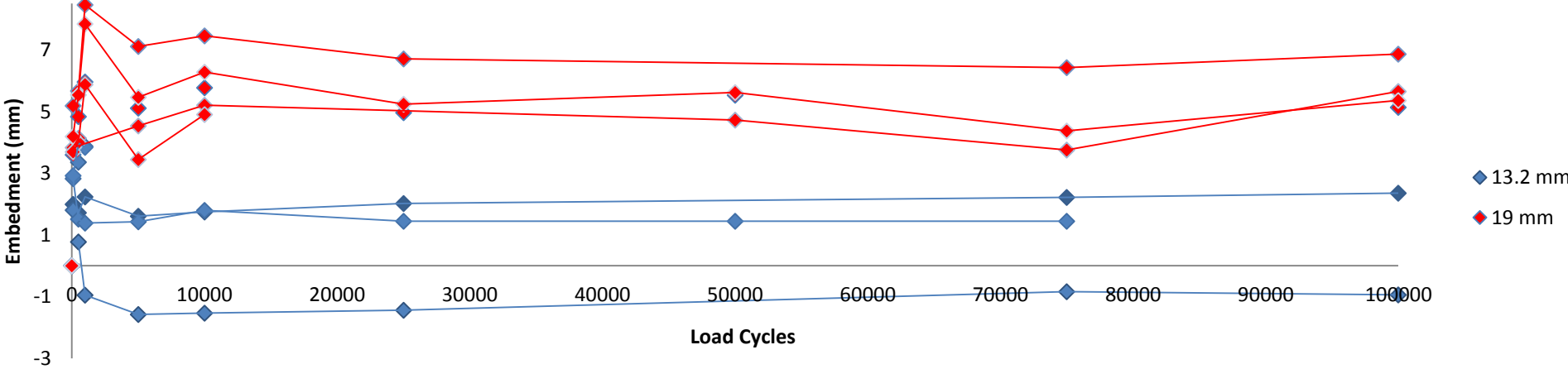
Figure 77: Plots indicating the cumulative embedment for the two aggregate sizes

6.2.7 Statistical analysis

The results that have been shown in *Section 6.2.3 – 6.2.6* and discussed will now be looked at from a statistical standpoint. The data that will be presented in this subsection will consolidate what has previously been shown using reducing the multiple stones that were measured to a single behaviour trend line governed by the 90th percentile. The aim of this analysis will be to analyse the data based on the general trend observed as opposed to the full collection. This section will be used to reinforce the observations made previously while also providing additional insight to comparatively assess the key variables that were tested.

6.2.7 (a) Traffic

Figure 78 shows the 90th percentile plot of all the stones measured in the centre of the wheel path. This plot validates the assumption used to divide the seal life into different phases as discussed in
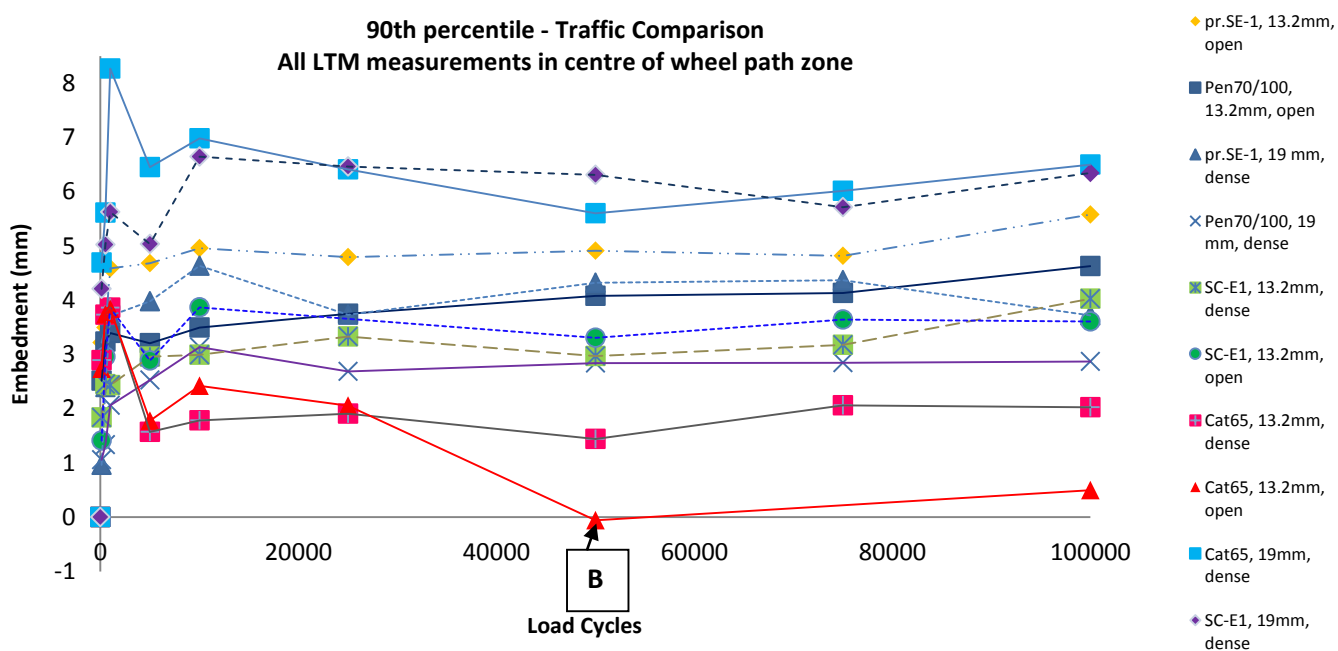
Figure 78: 90th percentile plot of all stones measured in centre of wheel path at different traffic cycle phases

Section 6.2.3. Statistically the point B in the seal life period could however be shifted to 50 000 load cycles (as shown in *Figure 78*) as opposed to 75 000 as stated in *Section 6.2.3.* The possible shift of this point in the seal life period still indicates that after a considerable number of load repetitions (whether 50 000 or 75 000 cycles) there could be adhesion issues and/or base stiffness loss. The assumption that 10 000 load cycles represent the initial embedment period appears to be echoed here. This initial embedment period plays a very critical role in the final embedment measured after 100 000 load cycles. *Table 18* shows the difference between the 90th percentile embedment at 10 000 and at 100 000 load cycles.

Table 18: Percentage difference in embedment at 10 000 and 100 000 load cycles (seal life period)

Difference between 90th percentile embedment at 10 000 and 100000 load cycles			
binder type	Aggregate Configuration	Aggregate size (mm)	Percentage Difference (%)
pr.SE-1	open sh-sh	13.2	11.1
Pen 70/100	open sh-sh	13.2	24.5
pr.SE-1	dense sh-sh	19	-24.7
Pen 70/100	dense sh-sh	19	-9.2
SC-E1	dense sh-sh	13.2	25.7
SC-E1	open sh-sh	13.2	-7.2
Cat65	dense sh-sh	13.2	11.8
Cat65	open sh-sh	13.2	-385.2
Cat65	dense sh-sh	19	-7.4
SC-E1	dense sh-sh	19	-4.7

The table clearly shows that with the exception of the Cat65, open sh-sh, 13.2 mm tile (which exhibited stone loss), the percentage difference between these two trafficking phases is no more than 25.7% indicating that more than 70% of the total embedment during the seal life occurs in the initial embedment phase. Furthermore, the average, maximum and minimum plots (*Figure 72, Figure 74 and Figure 76*) indicate that the embedment does not change dramatically during the seal life phase for any of the variables analysed (other than the Cat65, open sh-sh, 13.2 mm tile). This critical observation indicates that the embedment development over the seal life can essentially be predicted after the first 10 000 load cycles and the total embedment after 100 000 load cycles would be at most approximately 30 % greater.

What is also interesting from *Table 18* is that the 19 mm aggregate shows a greater likelihood of orientation during the seal life period which is identified by the negative percentage change (indicating that the stone had a negative final embedment relative to the measurement at 10 000 load cycles). The negative percentage change is observed at all the tiles using 19 mm aggregate as well as the two tiles constructed with emulsion and an open sh-sh configuration. The open sh-sh

configuration also has a greater likelihood of stone orientation during the seal life due to the lack of aggregate interlock but based on the statistics, it is only the emulsions that are susceptible to this behaviour.

6.2.7 (b) Tack coat binder type

Figure 79 (a) and *(b)* shows the 90th percentile plots of the binder comparison for the two different variable sets.

(a)

(b)
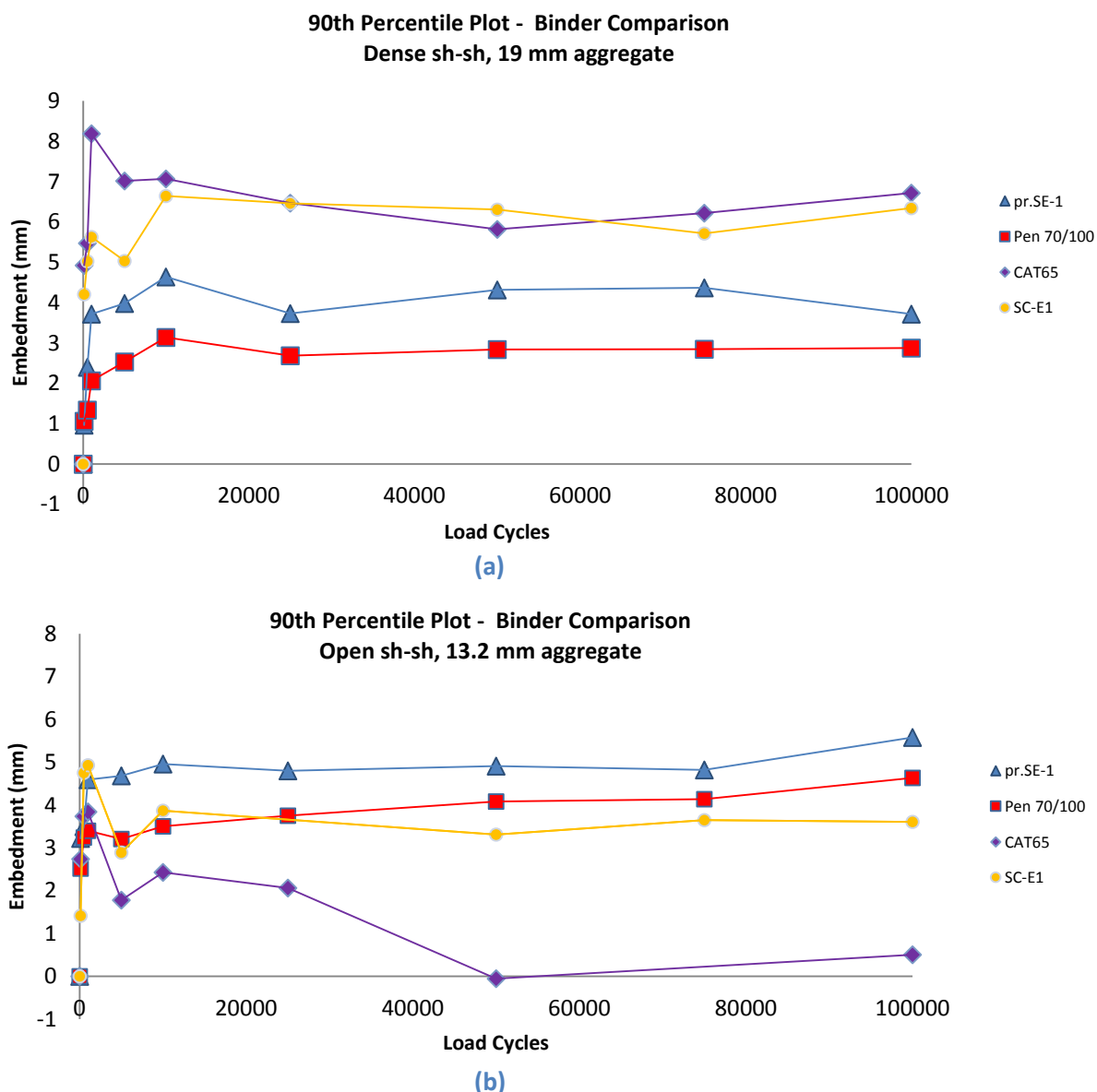
Figure 79: 90th percentile plots for the binder type comparison (a) Dense sh-sh, 19 mm aggregate (b) Open sh-sh, 13.2 mm aggregate

Based on the information in *Table 18* the emulsions in *Figure 79 (b)* most likely exhibit this lower final embedment due to the orientation and corresponding negative embedment which occurs during the seal life with the Cat65, 13.2 mm, open sh-sh tile showing stone loss resulting in an extreme case of negative embedment as shown in *Table 18* and *Figure 79 (b)* (the Cat 65 in *Figure 79*

(b) will therefore be omitted from any further comparative analysis). *Figure 79 (a)* typically depicts the behaviour that was noted in the previous analysis section with the hot applied binders showing a greater resistance to embedment compared to the emulsions. If the assumption that the embedment at 10 000 load cycles is representative of the total embedment that will be observed holds true, then the penetration grade bitumen outperforms all its competitors showing a lower embedment at the beginning of the seal life period (10 000 cycles) in both variable sets. The SC-E1 in *Figure 79 (b)* shows a lesser final embedment but this could be due to the orientation behaviour previously discussed.

Based on the initial embedment period the

6.2.7 (c) Seal aggregate configuration

Figure 80 (a) and *(b)* shows the shows the 90th percentile plots of the aggregate configuration comparison for the two different variable sets.

(a)

(b)

Figure 80: 90th percentile plots for the aggregate configuration comparison (a) Cat65, 13.2 mm aggregate (b) SC-E1, 13.2 mm aggregate

131

In both cases the dense sh-sh configuration appears to show a better embedment resistance during the initial embedment period and also during the seal life period. Of interest from these plots are the distinct similarities in behaviour between the two configurations in *Figure 80 (a)* during the initial embedment period. Statistically, the amount of orientation and embedment appears to be very similar between the two configurations in *(a)*. In *Figure 80 (b),* a somewhat similar trend is observed during the initial embedment period followed by a dip in embedment in the open sh-sh configuration most likely due to orientation, followed by a subsequent spike. It should however be noted that this behaviour is most likely skewed due to the lack of sufficient measurements as noted previously. Reliable observations can therefore not be made based on these results. Despite this, the dense sh-sh still appears to show a better overall performance based on the statistical information available as well as the observations made prior to this subsection.

6.2.7 (d): Seal aggregate size

Figure 81 (a) and *(b)* shows the shows the 90th percentile plots of the aggregate size comparison for the two different variable sets.
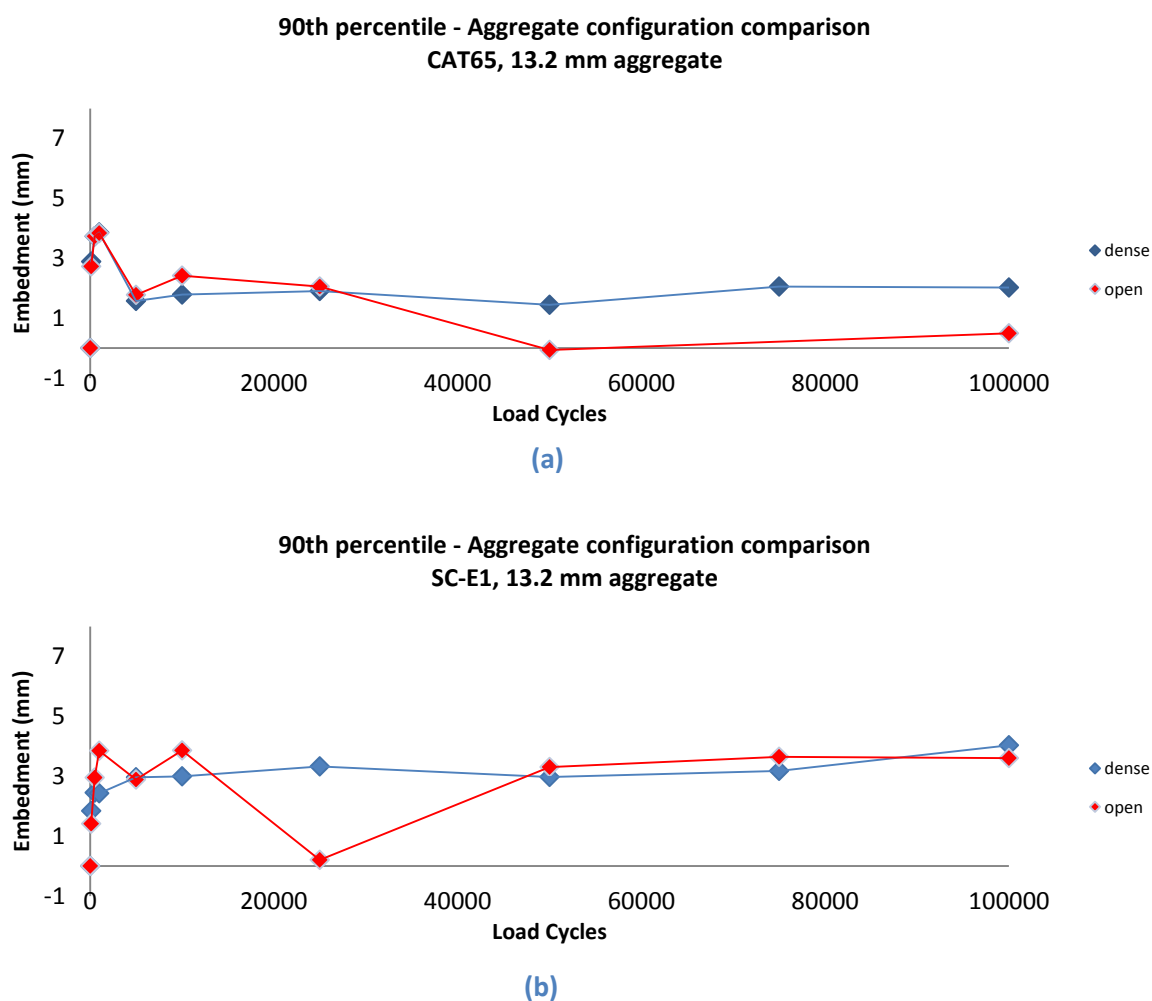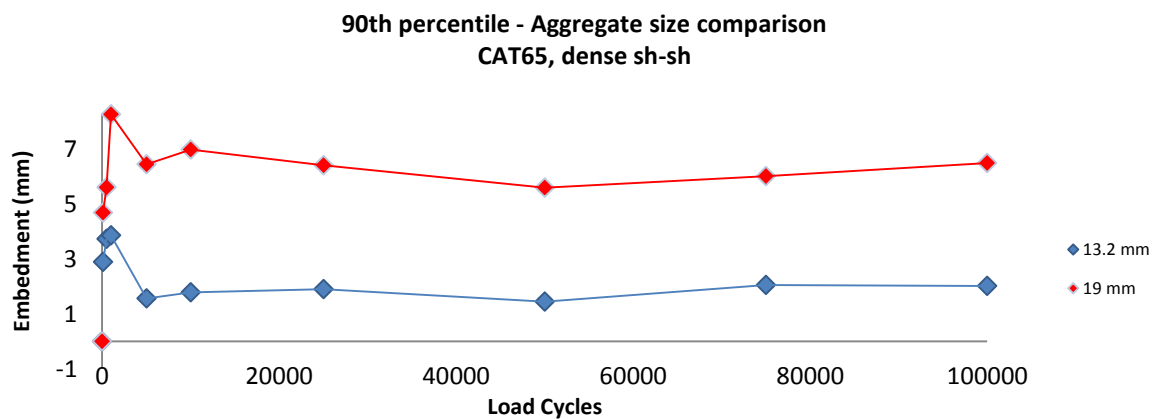

(a)
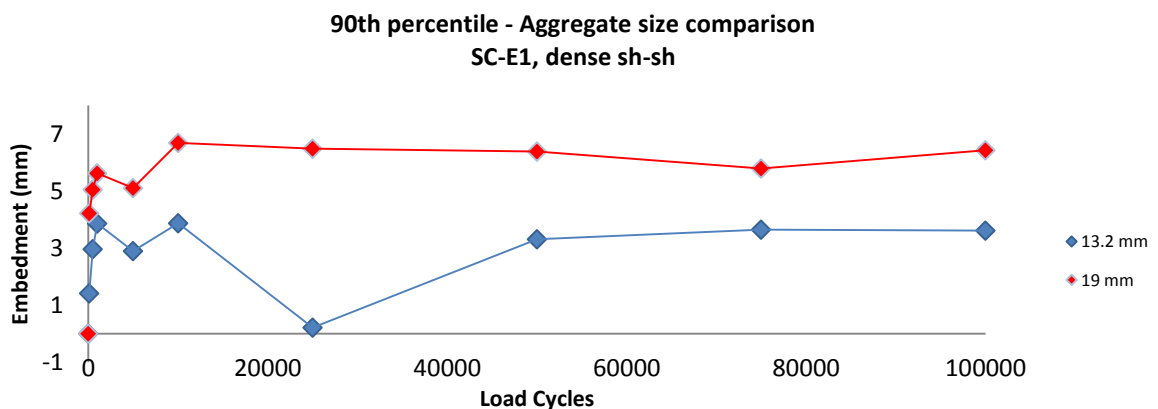
(b)

Figure 81: 90th percentile plots for the aggregate size comparison (a) Cat65, dense sh-sh (b) SC-E1, dense-sh-sh

During the initial embedment period the behaviour shows a very similar trend in both data sets with the 13.2 mm aggregate showing a significantly lower embedment compared to the 19 mm aggregate. This is then carried through the seal life period where the final embedment measurements reiterate that the 13.2 mm aggregate is superior over the 19 mm aggregate. Even in terms of the percentage of their ALD lost. The 19 mm stone lost 56% and 55% compared to the 24% and 43% lost in the case of the 13.2 mm stone for the cationic and modified emulsions respectively. This behaviour could be due to the lower void content in the 13.2 mm aggregate seals compared to the 19 mm seals or the higher flakiness index of the 19 mm aggregate or a combination thereof. The reason for the behaviour cannot be isolated but, statistically, the 13.2 mm aggregate outperforms the 19 mm aggregate in terms of embedment.

6.2.8 Summary

Based on the results and the analysis thereof, the behaviour of the seals, from an embedment perspective and based on the seal design parameters that were investigated can be summarised as follows:

In terms of traffic, the stones that were measured did not behave the same for the various parameters at the different traffic simulation phases. Although the behaviour varied, they all followed the same general pattern with distinct common trends observed in different seals at different stages of trafficking. These stages were then identified and used as part of the analysis when comparing the various seal design parameters. The stages were identified as the initial embedment period (0 to 10 000 load cycles), which could be related to the construction period of the seal in practice, and the seal life period (10 000 to 100 000 load cycles). Together, these two phases describe the total embedment experienced by the stones in the seal. The statistical analysis of data reinforced this and also showed that the degree of embedment during the initial embedment period would essentially govern the final embedment observed and that more than 70% of the total embedment takes place during this initial embedment period. If this initial embedment period is similar to the initial embedment that is observed in practice (i.e. the embedment induced through the construction of the seal), then the design assumption that 50% of the embedment potential (measured using the Ball Penetration Test) would be observed during construction may be inaccurate. Based on this study, it would seem that the Ball Penetration Test could dramatically underestimate the degree of embedment that could manifest in a seal given that the expected embedment based on the Ball Penetration Tests done estimated the initial embedment potential to be between 2.1mm and 2.5 mm. Initial embedment measurements were in excess of 6 mm in many cases and although this includes particle orientation, it still brings into

question the reliability of the Ball Penetration Test as an effective tool for measuring the embedment potential of a seal. The ball penetration test in principle uses a ball similar to a spherical particle, whereas most seal aggregates have some degree of angularity (refer to *Section 2.4.2 Figure 10*). This difference alone would see the types of forces at contact points between the seal and the base be significantly different.

The binder type has shown to be quite influential in the embedment performance of the seal. The hot applied binders appear to be superior to the emulsions and of the hot applied binders that were tested, the penetration grade bitumen seems to perform the best followed closely by the polymer modified SE-1. The emulsions were observed to have a relatively large total embedment and in some cases exhibited adhesion problems causing orientation of the stones during the seal life and in extreme cases stone loss (CAT 65, open sh-sh, 13.2 mm). These observations were reinforced through the statistical analysis

The aggregate configuration comparison was inconclusive. There were not sufficient measurements to confidently form observations regarding the effect of the configuration on the embedment performance. Looking at the statistical analysis along with the full data sets it can be noted that the likelihood of aggregate loss appears to be more pronounced in the open sh-sh configuration, especially when emulsions are used as the tack coat. This is seemingly intuitive since there is a lack of aggregate interlock when compared to the dense sh-sh configuration.

The seal aggregate size seems to also play an influential role in the embedment performance of the stones. What could add to this is the flakiness index of the aggregate which effectively describes the relative flatness of the aggregate used. The flakiness index would probably add to the amount of orientation the stones would undergo during the initial embedment period. Another influential factor would be the difference in void content between the two aggregate sizes with the 19 mm aggregate having a considerably higher void content. Statistically, the 19 mm stone showed a consistent negative embedment during the seal life period which is very likely due to the flakiness index and void content resulting in orientation. These factors could be the reason for the 13.2 mm aggregate outperforming the 19 mm aggregate in terms of resistance to embedment. The 13.2 mm aggregate is also observed to have better stability during the seal life period with the 19 mm stone showing signs of possible adhesion loss after the 50 000 load cycle trafficking phase while the 13.2 mm seal generally remain stable.

It has been statistically established that the degree of embedment could be predicted based on the embedment after 10 000 load cycles. Using this concept, *Plate 10* graphically describes the level of

influence of each of the variables investigated based on the maximum differences in 90th percentile measurements at 10 000 load cycles.
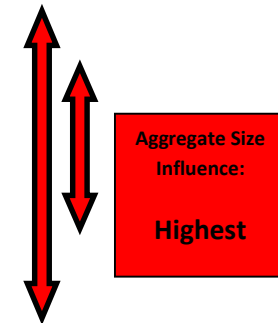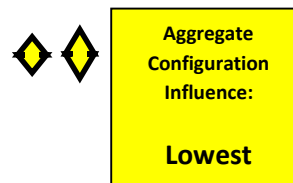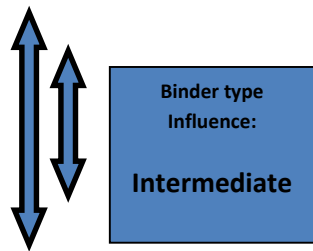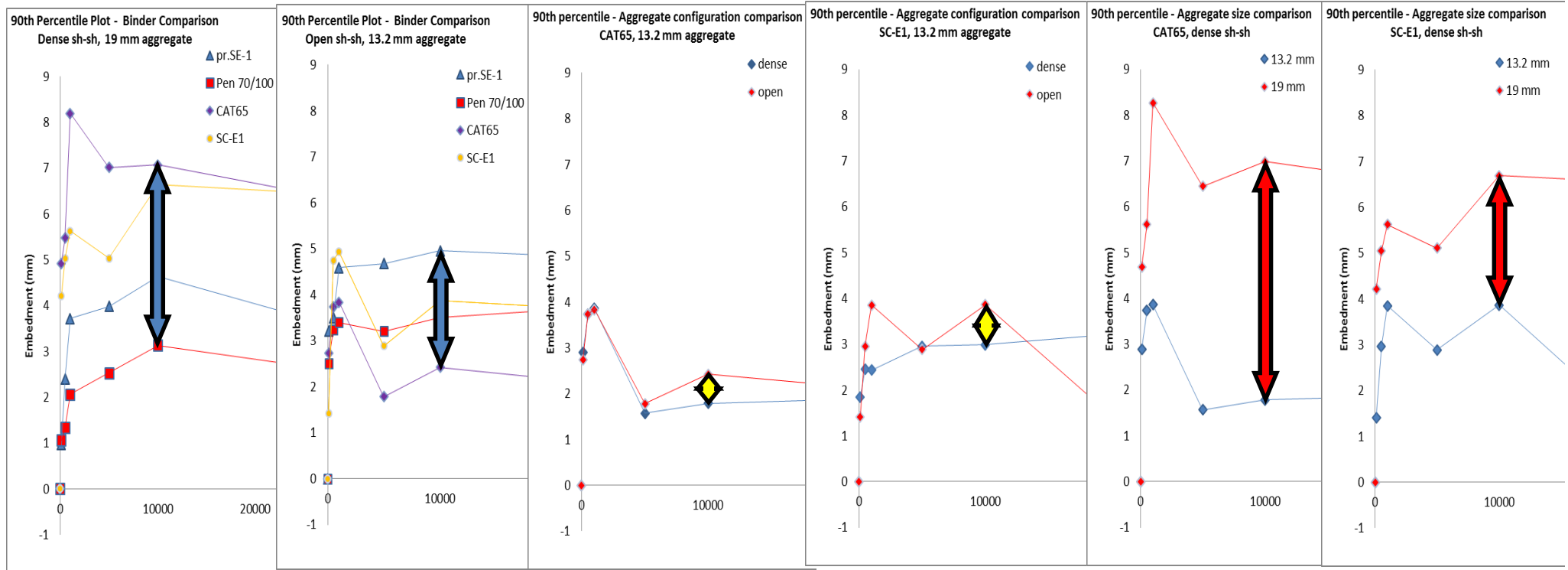
Plate 10: Establishing the level of influence of the variables investigates on embedment

7. CONCLUSIONS AND RECOMMENDATIONS

7.1 Conclusion

The primary aim of this study was to contribute towards the development of a standard test protocol by which key seal variables and their performance can be measured. The aim was then broken down into three distinct primary objectives.

The first was to investigate the failure mechanisms of surfacing seals. This was executed through an intensive literature study on seals which included an analysis of the factors which influence their performance, their failure mechanisms and how they manifest as well as a review of the past research that has been done using accelerated testing to evaluate the performance of seals. Additionally, the MMLS3 was investigated to identify its capabilities as an APT for use in seal testing. Milne's PhD (2004) investigated a performance related seal design method and used the MMLS3 as part of his study relating directly to this project and was thus used as a point of departure. Through this process, seal stone embedment was identified as the failure mechanism requiring improved testing and was also most suited to testing using the MMLS3.

Based on the knowledge attained through the literature study, the second primary objective could be addressed. Through the identification of critical performance parameters, the experimental matrix was designed to include key seal design variables which were thought to directly influence seal stone embedment. The key seal design variables selected for comparative analysis were:

- Tack coat binder type
- Aggregate spread rate configuration
- Aggregate size

The third and most challenging objective followed and was executed in two separate phases.

Phase one involved the design of the experimental testing setup. The method used to construct the seals in this study has been adapted for application in a laboratory environment. Although the construction of the seals may not be a precise replication of what is done in practice, an attempt was made to capture as much of the construction practice despite being in the confines of a laboratory without the machinery needed to recreate the process precisely. The process used in this study has been detailed fully and can be used as a starting point in future research and refined to better capture the essence of seal construction in practice. The second phase involved the use of computer aided software and the development of an efficient algorithm to process and collect the data

obtained using the LTM. Due to the limited capabilities of the LTM sensors, the degree of data processing required to obtain usable results was significant. The method and tools used to obtain the results used are therefore detailed fully as part of this report will be available for refinement and as a tool for future research requiring a similar type of data processing.

Based on this study, it is clear that there is much more work required before the successful development of a standard test protocol can be established. The large spectrum of variables involved in seal design as well as the environmental and loading conditions which all contribute to the large matrix of influences regarding seals. This study does however show that with an effective testing setup and an efficient analysis procedure, the application of the MMLS3 can successfully be used for evaluating the performance of surfacing seals.

It has been shown that the embedment performance could be predicted during the early stages of traffic simulation using the MMLS3. In terms of the variables that were tested, aggregate size appears to show the greatest influence on the degree of embedment, the binder type an intermediate influence while the aggregate configuration appears to show the lowest influence.

7.2 Recommendations for future research

The following key recommendations are made for future research towards the development of a standard test protocol for MMLS3 testing on seals:

- The inclusion of a larger scope of test variables including base hardness, tack application rates, aggregates with different material properties (e.g. flakiness index, ALD) etc.

- The addition and analysis of traffic related variables such the application of lateral wander, varying tyre pressures and axle loads and higher traffic volumes.

- The use of scanning instrumentation with a wider range of capabilities to enable the monitoring of stone orientation and thus allowing for the distinction between orientation and embedment.

- The refinement of the data processing tools which could improve the time taken to conduct and process the data obtained.

- The development of performance index models to quantify and rate seal design parameters. This is a key aspect required to successfully establish a standard test protocol. This could be achieved by correlating the physical measurements obtained through this type of research with

the work of Gerber (no date). Using the finite element based models from the research by Gerber (no date), the physical results from MMLS3 testing could be used to establish factors which could correlate the mathematical models to the physical measurements.

REFERENCES

Asphalt Academy, 2007. *Technical Guidelines: The use of modified Bituminous Binder in Road Construction. 2nd Ed.* Pretoria, SA: Asphalt Academy.

Caro, S., Masad, E., Bhasin, A. & Little, D.N. 2008. Moisture susceptibility of asphalt mixtures, part 1: Mechanisms. *International Journal of Pavement Engineering.*

Cilliers, J.A., 2006. *Towards a Rational Volumetric Cape Seal design method*, Thesis, (M Eng) University of Stellenbosch.

Committee for State Roads Authorities (CSRA). 1986. *Technical Methods for highways (TMH) 1.* Standard Methods of Testing road construction. Pretoria, SA: National Institute for transport and road research.

Committee for State Roads Authorities (CSRA). 1986. *Technical Methods for highways (TMH) 6.* Special Methods of Testing road construction. Pretoria, SA: National Institute for transport and road research.

Committee for State Roads Authorities (CSRA). 2007. *Technical Recommendations for highways (TRH) 3. Design and Construction of Surfacing Seals*. Pretoria, SA: National Institute for transport and road research.

Draft Protocol Guideline 1: Application of the MMLS3 for evaluating permanent deformation and moisture damage of asphalt. (First Draft Version 3 Rev1). 2008.

Gerber, J.A.K. Unpublished. *Numerical Modelling of performance and failure criteria for road seals.* Dissertation, (PhD). University of Stellenbosch.

Greyling, A.H. 2012. *Developement of a standard test method for determining emulsion bond strength using the bitumen bond strength (BBS) test - A South African perspective.* Stellenbosch, SA: University of Stellenbosch. (M Eng)

Herrington, P.P., Ball, G.F.A., Patrick, J.E., and Towler, J.I. 2012. *Aggregate breakdown as a cause of the Chip Seal flushing.* 25th ARRB Conference – Shaping the future: Linking policy, research and outcomes.

Hoffman, P. and Potgieter, C.J. 2007. *Bitumen Rubber Chip and Spray Seals in South Africa*. Randburg Waterfront: Potgieter Hattingh Inc.

Kane, M., Artamendi, I., and Scarpas, T. 2013. *Long term skid resistance of asphalt surfacing: Correlation between Wehner-Schulze friction values and the mineral logical composition if the aggregates* wear.

Kemp, M. 2006. *Concept to Reality – MLS10, Thesis, (B Eng)*. University of Stellenbosch.

Kim, Y., and Lee, J. 2006. *Performance Evaluation of Chip Seals with polymer-modified emulsions* North Carolina State University.

Kleyn, E. 2012. *Successful G1 Crushed Stone Basecourse construction.* 31st South African Transport Conference. Pretoria.

Lawson, W.D. & Senadheera, S. 2009. Chip seal maintenance: Solutions for bleeding and flushed pavement surfaces. *Transportation Research Record.*

Lawson, W.D., and Senadheera, S. 2009. Solutions for Bleeding and flushed pavement surfaces. *Chip seal Maintenance.*

Milne, T.I. 2004. *Towards a performance related seal design method for Bitumen and modified road seal binders*, Dissertation, (PhD). University of Stellenbosch.

Panagouli, O.K., and Kokkalis, A.G., 1997. *Skid resistance and Fractal Structure of pavement Surface.*

Read, J. & Whiteoak, D. 2003. *The shell bitumen handbook.* Thomas Telford Ltd

Robertson, R.E. 1991. *Chemical Properties f Asphalts and their relationship to prove performance.* Washington, DC: Strategic Highway Research Program.

Roelofse, C.B. 2014. *Influence of slushing on granular materials.* Thesis, (B Eng). University of Stellenbosch.

Sabita, 2006. *Interim Guidelines for primes and store precoating fluids.* South Africa: Sabita. Manuel 26.

Sabita, 2012. *Bituminous binders for road construction and maintenance.* 5th Ed. South Africa: Sabita. Manuel 2.

Shuler, S., and Lord, A. 2010. *Two New Methods to Measure Aggregate Embedment on Chip Seals during Construction*. Colorado: Colorado State University. Ft Collins.

South Africa National Roads Agency Ltd. CSRA (Auth). 2007. Design and Construction of surfacing seals. *Technical recommendations for highways (TRH3).*

South African National Roads Agency Ltd. 2014. South African pavement engineering manuel. 1st ed. South Africa: SANRAL.

South African National Standards (SANS) 4001-BT1. 2014. *Penetration grade Bitumens.* South Africa: South African Bureau of Standards (SABS)

Tarbuck, E. and Lutgens, F. 2008. *Earth: An introduction to physical geology 9th edition.* New Jersey, USA: Pearson Prentice Hall

Theyse, H.L. 2002. *Stiffness, Strength, and Performance of Unbound Aggregate Material: Application of South African HVS and Laboratory Results to California Flexible Pavements.* California: University of California. CSIR.

University of Stellenbosch. 2012. *Model Mobile Load Simulator testing Operators Manual.* University of Stellenbosch: Institute for Transport Technology.

van de Ven, M., de Fortier Smit, A., and Jenkins, K. 1998. *Traxial testing of Elasto-Plastic materials towards scaled down ATP.* 1998 Annual meeting of the transportation research board.

van Niekerk, A.A., 2002. *Mechanical Behaviour and Performance of granular bases and Sub-bases in Pavements.* Netherlands: Delft University Press.

Van Zyl, G. 2012. *Personal interview*. August, Stellenbosch

van Zyl, G. 2015. Construction of Surface treatments, Presentation. South Africa: University of Stellenbosch.

Wang, J., Jenkins, K., Molenaar, A., and Wu, S., 2011. *Evaluation of Resilient Modulus Modes for a high quality crushed stone*. 10th Conference on Asphalt Pavement for Southern Africa.

Woodward, W.D.H., Woodside, A.R., Yacoob, H., and Maquire, S.J. 2005. *Smaller store size surfacing dressing for high store surface mixes*. Northern Island: University of Ulster, Transportation and road Assessment Centre.

Appendix A: Binder application rate adjustments

A1: Adjustment for aggregate size (13.2mm vs. 19mm)

In order to adjust the binder application rate for the different aggregate sizes, the approximate percentage of wetted ALD is used. The application rate is reduced to an equivalent height, and the percentage of ALD is determined for the 13.2 mm aggregate. This percentage is then used to establish the increase in wetted height for the larger 19 mm aggregate.

13.2 mm ALD = 8.4mm

19 mm ALD = 11.8mm

280mm x 360 mm

mould
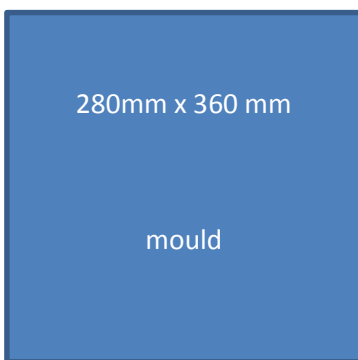
Area = 0.1008m^2

0.8 litre/ m^2 (low application rate)

Height approximation:

0.001 m^3/l x 0.8 l/m^2 = 8 x 10^{-4} m

= 0.8 mm

8.4mm
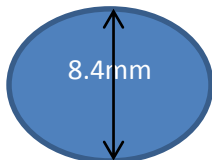
13.2 mm

0.8mm = **9.52%** of ALD
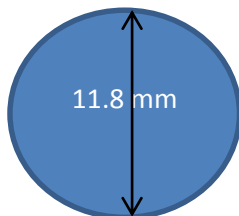
11.8 mm

19 mm

9.52 % of 11.8 mm (ALD)

1.123 mm

= 1.123 l/m^2

144

A2: **Adjustment for tack coat binder (dense sh-sh vs. open sh-sh)**

In order to adjust the tack coat binder amount used and to maintain a consistent "wetted height" of the aggregate, a volumetric approach is used. The required mass of aggregate to cover the seal tiles in the dense sh-sh configuration was used and scaled down to cover the area of the container shown. The same volume of binder applied (by area ratio) is then added to the container and the wetted height is observed. The mass of aggregate required to fill the same area in the open sh-sh configuration is then used and the additional water required to bring the water up to a similar wetted height is measured. This is used to estimate the percentage adjustment for additional tack coat on open sh-sh configuration compared to dense sh-sh configuration and maintaining a consistent wetted height.

280mm x 360mm

a = 0.1008 m²

with 80.64ml (volume binder sprayed to cover tile)

Figure A1

Diameter = 165 mm   r = 165/2 = 82.5

165mm

Area   = (0.8082.5)² π

= 0.0213825m²

=> 0.8213825   x 80.64

0.1008

= 17.106 ml required to cover this area
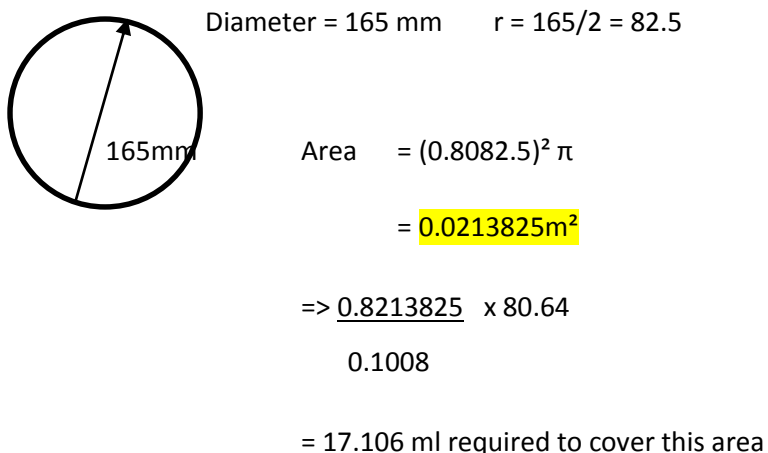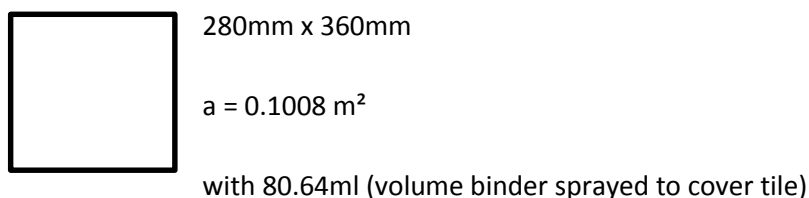
Sh/Sh: 1223g of stones over 0.1008 m²: 259.43 g (*Figure A1*) 0ver 0.0214 m²

Open 984g of stones over 0.1008 m²: n208.73 g over 0.0214 m ²

Since

242.4 g (with 2 x 17.106 ml)

Figure A2   145

9.2 g water brings level up to sh/sh (*Figure A2*)

∴ 9.2 ml of water

Thus for open sh-sh increase

Tack content by <u>9.2 ml</u> x <u> 1 </u> x 100

(Binder)   **2**   17.106ml

           Adjustment = **26.89 %** increase

Summary

The following application rates will thus be applicable :

13.2 mm aggregate, dense sh-sh configuration –   **0.8 l/m²**

13.2 mm aggregate, open sh-sh – 0.8 +(0.8 x 29.89%) =   **1.02 l/m²**

19 mm aggregate, dense sh-sh configuration –   **1.12 l/m²**

19 mm aggregate, open sh-sh – 1.123 +(1.123 x 29.89%) =   **1.46 l/m²**

Appendix B: Tests on base material and seal aggregates

B1: Optimum Moisture Content (OMC) Determination

Test Method A7 (TMH1, 1986)

The OMC was determined in accordance with the TMH1 Test Method A7.

$$Dry\ Density = \frac{(Mass\ of\ mould+sample)-(empty\ mould\ mass)}{100+MC(\%)} \times F$$

$$MC = \frac{wet-dry}{dry-empty} \times 100$$

Table B1 provides the measurements taken, *Figures B1* and *B2* provides the theoretical and measured MC vs. DD plots

With F = 42

MC – Moisture Content

DD – Dry Density

Table B1: OMC calculation measurements

7% =	490ml	mass (g)			
		empty	wet	dry	MC
mould y6		236	710.4	680	6.846847
DD=	2263	kg/m3			

5% =	350ml	mass (g)			
		empty	wet	dry	MC
mould 3b		185.9	689.6	659.6	6.333122
DD=	2347	kg/m3			

3% =	210ml	mass (g)			
		empty	wet	dry	MC
mould x4		236.6	805.4	785.9	3.549973
DD=	2224	kg/m3			

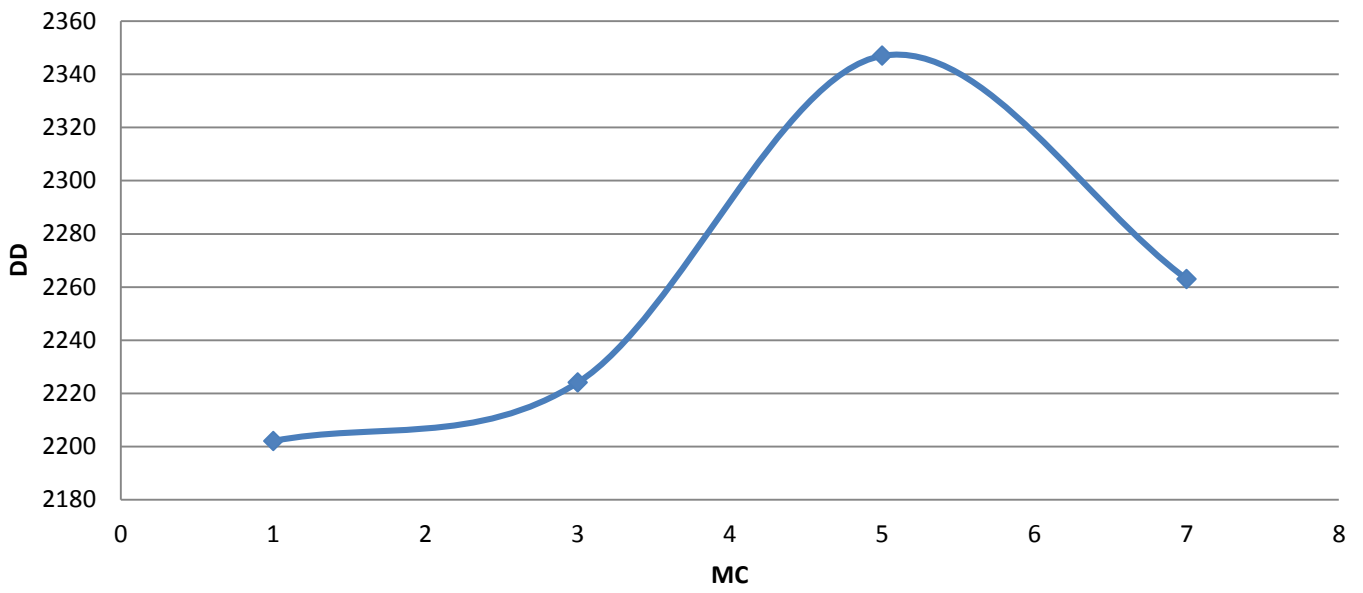| 1% =	70ml	mass (g)			
		empty	wet	dry	MC
mould TΛ		236.9	742.2	734.6	1.527024
DD=	2202	kg/m3			

148

Theoretical MC vs. DD

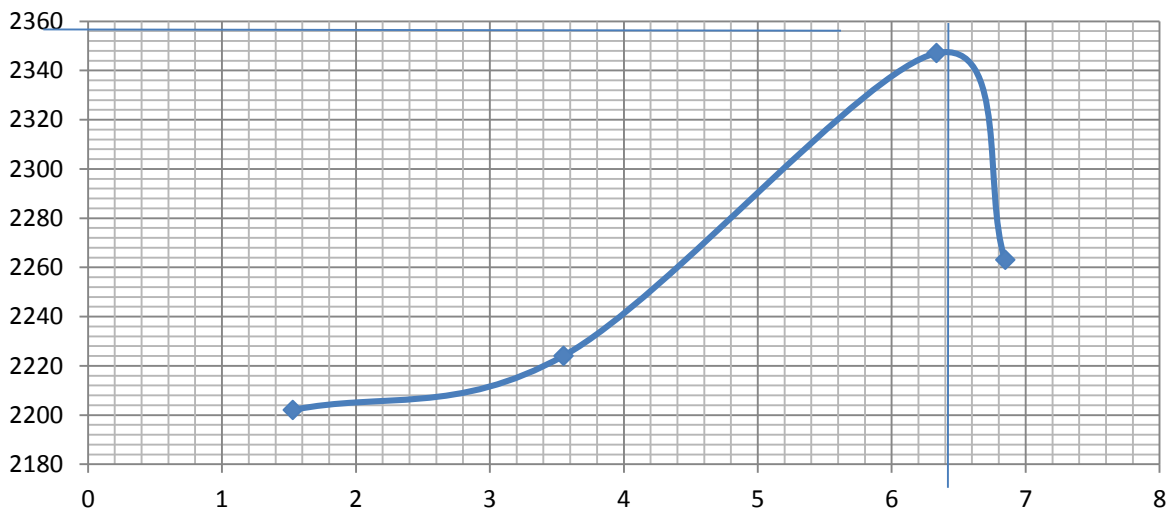**Figure B1: Theoretical MC vs. DD**

Measured MC vs. DD

Figure B2: Measured MC vs DD

The measured MC vs. DD plot is used to determine the OMC.

OMC = 6.4%

B2: Average Least Dimension (ALD)

Test Method B18(a) (TMH1, 1986)

The ALD was determined in accordance with the TMH1 Test Method B18(a).

Table B2.1: ALD measurements of 19 mm and 13.2 mm aggregate

#	19mm	13.2mm	#	19mm	13.2mm
stone number	ALD	ALD	stone number	ALD	ALD
1	14.4	6.1	51	10.2	10.4
2	9.5	7.5	52	11.2	11.1
3	13.9	11.3	53	5.6	7.3
4	7.7	6.9	54	13.2	7.99
5	12.21	10.3	55	7.5	12.1
6	15.3	9.3	56	10.6	7.9
7	11.8	9	57	12.07	12
8	19.9	7.2	58	8.8	10.9
9	18.53	6.6	59	14.9	10.4
10	11.52	10.6	60	13.6	8.2
11	14.32	9.5	61	12.8	10.3
12	13.9	11.3	62	13.6	8.11
13	15.27	12.3	63	18.5	10.7
14	8.9	8.9	64	11.7	6.4
15	16.1	8.2	65	12.2	10.2
16	13.1	9.8	66	13.7	6.2
17	9.6	6.8	67	14.4	10.7
18	12.9	10.2	68	7.2	7.4
19	9	9.3	69	9.6	8.03
20	7.9	8.8	70	13.5	10.1
21	14.1	6.3	71	15.9	10.1
22	9.1	9.6	72	9	6.9
23	11.5	10.8	73	6.9	3.9
24	10.2	10.9	74	12.7	8.01
25	12.7	7.3	75	10.1	6.8
26	7.9	7.3	76	15.3	7.1
27	13.1	9.03	77	13	8.4
28	14.3	7.6	78	13.9	5.4
29	11.1	5.8	79	13.5	7.9
30	15.6	4.03	80	9.7	3.9
31	12	8.9	81	15.3	9.9
32	13.2	9.8	82	5.5	7.7
33	14.7	4.3	83	16.1	10.2
34	8.3	4.7	84	12.5	6.97
35	14.2	8.5	85	16.7	8.1
36	11.2	8.6	86	14.8	8.6
37	9.9	4.6	87	16.5	6.7
38	8.9	6.2	88	12.8	11.6
39	11.2	7.3	89	9.2	7.4
40	9.4	9.5	90	11.9	8.6
41	11.5	8.9	91	11.8	11.6
42	8.9	11.8	92	14.1	13.4
43	5.7	12.9	93	14.02	9.1
44	16.2	8.6	94	9.3	5.7
45	18.3	8	95	6.7	10.7
46	11.8	6.4	96	7.9	6.1
47	12.5	8.6	97	7.5	6.3
48	8.3	5.03	98	11.5	9.3
49	9.7	6.7	99	7.7	12.5
50	13.02	8.3	100	12.7	7.6

Table B2.2: ALD measurements of 19 mm and 13.2 mm aggregate

#	19mm		13.2mm		#	19mm		13.2mm
stone number	ALD		ALD		stone number	ALD		ALD
101	9.8		5.5		151	7.6		8.1
102	7.2		7.2		152	6.5		7.1
103	14.3		7.2		153	10.9		7.6
104	9.8		9.5		154	13.01		9.1
105	13.6		9.1		155	7.7		5.1
106	13.3		10.1		156	17.3		6.3
107	12.9		11.2		157	10.4		6.8
108	10.8		9.8		158	10.7		9.7
109	5.3		13.1		159	8.2		7.9
110	11.5		7.3		160	7.3		9.2
111	12.3		11.8		161	7.8		10.3
112	12.2		8.6		162	8.3		8.1
113	7.8		9.5		163	16.2		10.6
114	14.5		9.8		164	10.3		9.2
115	16.6		11.1		165	13.1		5.8
116	18.5		10.2		166	10.4		6.2
117	8.1		8.8		167	14.4		7.2
118	15.7		11.2		168	15.7		3.8
119	14.7		12.2		169	13.7		9.8
120	18.3		7.03		170	13.8		10.8
121	12.7		8.5		171	12.6		5.9
122	14.9		11.4		172	13.1		9.2
123	12.2		8.96		173	13.5		6.9
124	7.3		9.6		174	14		6.3
125	17.1		9.01		175	8.6		8.4
126	17.4		8.3		176	8.5		10.6
127	14.6		9.3		177	10.9		5.7
128	10.6		11.5		178	12.03		7.2
129	8.8		7.4		179	8.6		9.4
130	14.3		6.8		180	12.8		7.04
131	10.7		10.4		181	11.01		8.6
132	6.7		9.6		182	8.5		9.9
133	12.6		6.3		183	6.2		8.5
134	7.3		10.1		184	13.7		4.8
135	18.1		8.3		185	12.8		5.6
136	13.1		4.7		186	8.4		10.3
137	15.7		4.5		187	11.6		5.2
138	16.2		6.97		188	11.6		4.3
139	12.4		9.4		189	11.5		6.7
140	9.4		5.5		190	11.7		7.9
141	11.5		10.3		191	11.7		9.5
142	11.5		5.7		192	10.2		10.96
143	19.8		9.2		193	9.7		9.1
144	7.8		7.1		194	8.6		6.7
145	9.8		10.1		195	9.7		6.95
146	11.5		4.7		196	8.8		9.01
147	11.3		10.2		197	4.3		8.4
148	12.8		5.2		198	7.9		8.2
149	7.3		6.65		199	10		10.1
150	16.5		8.2		200	12.5		9.6
					201	15.4		8.2

Measuring the ALD of at least 200 stones and calculating the average provides the ALD.

ALD$_{19mm}$ = 11.7 mm

ALD$_{13.2mm}$ = 8.4 mm

B3: Flakiness Index

Test Method B3 (TMH1, 1986)

The Flakiness Index was determined in accordance with the TMH1 Test Method B3.

Table B3: Flakiness Index determination

Stone size	Mass of material measured (g)	Mass passing slots (g)	Mass retained (g)	Flakiness Index (%)
19 mm	3500	766.7	2733.3	**21.9**
13.2 mm	2000	265.2	1734.8	**13.3**

Appendix C: Bitumen supplier product Sheets